AD-A160 280 HEAT PIPE SPACE NUCLEAR REACTOR DESIGN ASSESSMENT 1/2
VOLUME 2 FEASIBILITY ST..(U) NEW MEXICO UNIV
ALBUQUERQUE DEPT OF CHEMICAL AND NUCLEAR ENGI..
UNCLASSIFIED M S EL-GENK ET AL. AUG 85 F/G 10/9 NL

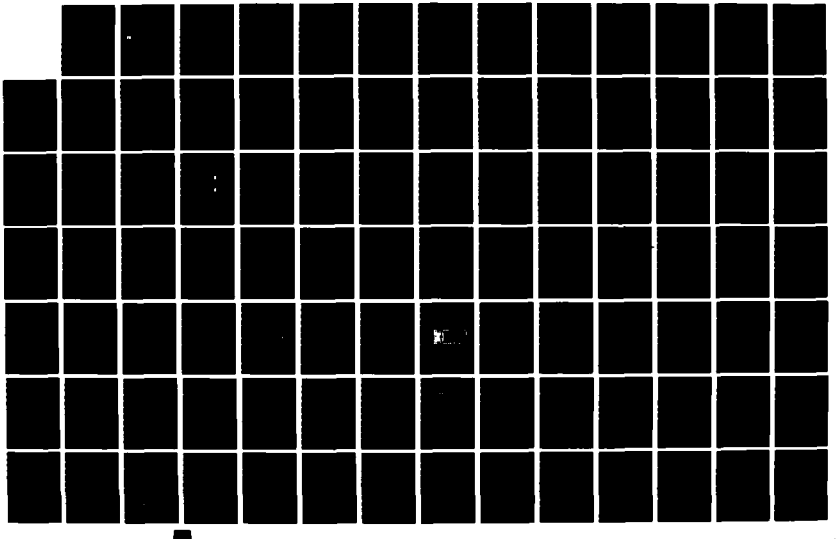

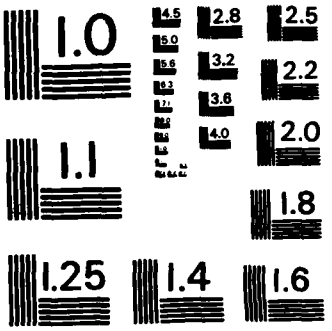

MICROCOPY RESOLUTION TEST CHART
NATIONAL BUREAU OF STANDARDS - 1963 - A

AFWL-TR-
84-126
Vol. II

(2)

AD-A160 280

HEAT PIPE SPACE NUCLEAR REACTOR DESIGN ASSESSMENT

Volume II of II
Feasibility Study of Upgrading the SP-100 Heat Pipe Space Nuclear Power System

Mohamed S. El-Genk
Jong-Tae Seo

University of New Mexico
Albuquerque, New Mexico 87131

August 1985

Final Report

AIR FORCE WEAPONS LABORATORY
Air Force Systems Command
Kirtland Air Force Base, NM 87117-6008

This final report was prepared by the University of New Mexico, Albuquerque, New Mexico under Contract F29601-82-K-0055, Job Order 57972302 with the Air Force Weapons Laboratory, Kirtland Air Force Base, New Mexico. Lieutenant David S. Ek (AWYS) was the Laboratory Project Officer-in-Charge.

This report has been reviewed by the Public Affairs Office and is releasable to the National Technical Information Services (NTIS). At NTIS, it will be available to the general public, including foreign nations.

If your address has changed, if you wish to be removed from our mailing list, or if your organization no longer employs the addressee, please notify AFWL/AWYS, Kirtland AFB, NM 87117-6008 to help us maintain a current mailing list.

This technical report has been reviewed and is approved for publication.

David Ek

DAVID S. EK
2nd Lt, USAF
Project Officer

FOR THE COMMANDER

Wayne T. Graybeal

WAYNE T. GRAYBEAL
Lt Col, USAF
Chief, Space Applications Branch

James H Head

JAMES H. HEAD
Lt Col, USAF
Chief, Applied Technology Division

DO NOT RETURN COPIES OF THIS REPORT UNLESS CONTRACTUAL OBLIGATIONS OR NOTICE ON A SPECIFIC DOCUMENT REQUIRES THAT IT BE RETURNED.

REPORT DOCUMENTATION PAGE

1a. REPORT SECURITY CLASSIFICATION UNCLASSIFIED	1b. RESTRICTIVE MARKINGS
2a. SECURITY CLASSIFICATION AUTHORITY	3. DISTRIBUTION/AVAILABILITY OF REPORT Approved for public release; distribution unlimited.
2b. DECLASSIFICATION/DOWNGRADING SCHEDULE	
4. PERFORMING ORGANIZATION REPORT NUMBER(S) NE-108 (85) AFWL-144-1	5. MONITORING ORGANIZATION REPORT NUMBER(S) AFWL-TR-84-126, Vol II of II
6a. NAME OF PERFORMING ORGANIZATION University of New Mexico, Dept of Chemical and Nuclear Engrg 6b. OFFICE SYMBOL (If applicable)	7a. NAME OF MONITORING ORGANIZATION Air Force Weapons Laboratory
6c. ADDRESS (City, State and ZIP Code) Albuquerque, New Mexico 87131	7b. ADDRESS (City, State and ZIP Code) Kirtland Air Force Base, NM 87117-6008
8a. NAME OF FUNDING/SPONSORING ORGANIZATION 8b. OFFICE SYMBOL (If applicable)	9. PROCUREMENT INSTRUMENT IDENTIFICATION NUMBER F29601-82-K-0055
8c. ADDRESS (City, State and ZIP Code)	10. SOURCE OF FUNDING NOS.

PROGRAM ELEMENT NO.	PROJECT NO.	TASK NO.	WORK UNIT NO.
62601F	5797	23	02

11 TITLE (Include Security Classification)
HEAT PIPE SPACE NUCLEAR REACTOR DESIGN ASSESSMENT (Vol II) Feasibility Study of (over)

12. PERSONAL AUTHOR(S)
Mohamed S. El-Genk and Jong-Tae Seo

13a. TYPE OF REPORT	13b. TIME COVERED	14. DATE OF REPORT (Yr., Mo., Day)	15. PAGE COUNT
Final	FROM 5May82 TO 27Mar85	1985 August	140

16. SUPPLEMENTARY NOTATION Note: This document reviews the heat pipe reactor, which was the SP-100 reactor design as of October 1982. Since current SP-100 designs include other concepts, SP-100 (whenever it appears in this report) should be interpreted as "heat (over)

17. COSATI CODES		
FIELD	GROUP	SUB. GR.
18	09	

18. SUBJECT TERMS (Continue on reverse if necessary and identify by block number)
Power upgrade, Heat rejection, Steady-state, Fuel swelling, Reactivity requirements, Fission gas, Energy conversion, Pulse-mode operation, release

19. ABSTRACT (Continue on reverse if necessary and identify by block number)
This report investigated the feasibility of upgrading the power of the Heat Pipe Space Nuclear Reactor (HPSNR) system design. The report has also discussed the four primary methods for power upgrading: Increasing the thermal power output to the reactor core, pulse-mode operation, improving the heat rejection, and improving the thermal-to-electric energy conversion.

20. DISTRIBUTION/AVAILABILITY OF ABSTRACT	21. ABSTRACT SECURITY CLASSIFICATION
UNCLASSIFIED/UNLIMITED ☒ SAME AS RPT. ☐ DTIC USERS ☐	UNCLASSIFIED

22a. NAME OF RESPONSIBLE INDIVIDUAL	22b. TELEPHONE NUMBER (Include Area Code)	22c. OFFICE SYMBOL
2nd Lt David S. Ek	(505) 844-1781	AWYS

DD FORM 1473, 83 APR EDITION OF 1 JAN 73 IS OBSOLETE.

11. TITLE (Contd)

Upgrading the SP-100 Heat Pipe Space Nuclear Power System

16. SUPPLEMENTARY NOTATION (Contd)

pipe reactor."

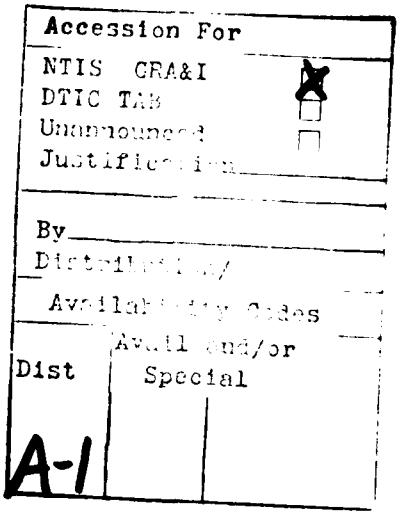

PREFACE

This report is the second of a two volume final report issued under contract with the Air Force Weapons Laboratory (AFWL). This contract's three objectives were to:

(1) Review the design status, as of October 1982, of the heat pipe space nuclear reactor (HPSNR) system developed at Los Alamos National Laboratory (LANL).

(2) Identify those technical areas requiring additional research as well as the development needed to support future system developments, and

(3) Investigate the feasibility of upgrading the HPSNR design to achieve high electrical power output (several hundred kilowatts to several megawatts).

Volume I reviewed the design status of the HPSNR and identified both the current design limitations as well as those systems, subsystems, and components requiring additional research (Ref. 1). Those areas deserving future development included: fabrication and testing of long heat pipes (up to 8 m), high emissivity and long-lived coating, fuel performance and irradiation behavior, criticality safety, high efficiency thermoelectric converters, and improved heat rejection concepts. Additional areas recommended for further research were: modeling of the transient behavior of heat pipes; modeling of fission gas and volatile release from the fuel and venting to space (Refs. 2,3); designing a system that allows adequate venting of fission gases; analyzing the thermal behavior and structure of the control drums and radiation shield; and analyzing the swelling and self-welding phenomena of the materials. These areas are common to other space nuclear power systems currently being developed under the Department of Defense (DOD)-Department of Energy (DOE)-National Aeronautics and Space Administration (NASA) SP-100 program.

Note: This document reviews the heat pipe reactor, which was the SP-100 reactor design as of October 1982. Since current SP-100 designs include other concepts, "SP-100" whenever it appears in this report should be interpreted as "heat pipe reactor."

CONTENTS

CONTENTS (Contd)

ILLUSTRATIONS

ILLUSTRATIONS (Contd)

TABLES

I. INTRODUCTION

This volume investigates the feasibility of upgrading the power of the HPSNR (heat pipe space nuclear reactor) system design and identifies those research areas considered most likely to expedite the upgrade to high power. Section II details the most promising options available for power upgrading: (1) linear system size increase, (2) improved heat rejection subsystem, (3) improved thermal-to-electric energy conversion efficiency, and (4) pulse mode operation.

Section III discusses in detail the linear size increase option. In this option, the HPSNR base line system was divided into five major subsystems, and the system's efficiency was calculated for both near term and future technological levels. The system mass, fuel swelling, and reactivity control were investigated as functions of electrical power output. Section IV discusses the feasibility of upgrading the power of the HPSNR with improved concepts for heat rejection. It focuses on the two major radiator concepts: the dust radiator concept and the liquid droplet radiator concept, currently being developed (Refs. 4,5) to improve the heat rejection capability by increasing the heat rejection area. (Appendix A gives details). Section V discusses the effects on the electrical power output of the HPSNR resulting from an improved thermal-to-electric energy conversion efficiency. Section V also discusses a total of six thermal-to-electric energy conversion systems and assesses some key design factors such as efficiency, mass and size, reliability, etc. for each system. Additionally, the suitability of any of these systems for space power generation is also investigated from the power upgrading point of view. A detailed description and analysis of various energy conversion systems is included in Appendix B.

Section VI discusses the fission gas and volatile release-venting model for space nuclear reactors. An interim report contained the results of a study that developed (Ref. 2) fission gas release and venting models for space nuclear reactors. Adequate venting of such materials into space is important for obtaining safe operation of the system during its 3-7 yr life time. Of course, adequate venting must be considered in the selection and design of the core and the fuel system of space nuclear reactors. Such a design must permit operation at both low (~100 kWe) and high electrical power (several hundreds of kilowatts to a few megawatts) for an extended

period of time. To assess the applicability of the developed models, they were applied to the HPSNR to investigate the effect on reactor operation of a partial or complete plugging of the venting system. Such plugging could cause overheating of the beryllium oxide (BeO) reflector and increase core can pressure. The accumulation of fission gases and volatile products (xenon, krypton, and cesium (Xe, Kr, and Cs)) in the core cavity could perhaps cause the core can to fail. The venting passages may become plugged from the continuous deposition of fission volatiles on the vents' cold walls. This analysis was performed as a function of the fuel operating temperature, fuel burnup, and the number of open vents, and was made using an intragranular fission gas release model coupled to a gas venting model. These models are described elsewhere along with the governing equations (Refs. 2,3).

The major conclusions of this feasibility study are presented in Section VII. However, it should be noted that the results presented here are not limited to a particular space nuclear power system design but may be more generally applied to other SP-100 class systems because of the close similarity of subsystems and design constraints. This material, therefore, should be useful to those who are currently working on the development of different designs of space nuclear power systems.

II. OPTIONS FOR POWER UPGRADING OF SPACE NUCLEAR POWER SYSTEM

In general, space nuclear power systems can be designed to operate in two modes: steady state operation and pulse-mode operation. For steady-state operation, for example, three possible methods of power upgrading are to increase linearly the size of the system, to improve heat rejection, and to improve thermal-to-electric energy conversion efficiency. Pulse mode operation may also be used to upgrade the system electrical power output. The methods for either operation mode used to upgrade the power of space nuclear power systems in general and the HPSNR baseline system in particular are fully discussed.

Figure 1 shows a flow chart of the different methods that can be used for upgrading the power of space nuclear power systems. The applicability of some or all of these methods to the HPSNR will be explored in the following subsections.

1. BASE-LINE SYSTEM

The base-line design of the HPSNR system (Refs. 1,6-8) was developed to generate 100 kWe of continuous power for ~3-7 yr lifetime while keeping the system total mass below 3000 kg. In this design, the reactor core has 120 heat pipe fuel modules arranged in five concentric rings around a central plug region. The central plug consisting of boron or boron carbide (B_4C) enriched in boron-10 (B^{10}) can maintain the core's safe subcritical state in case of accidental water immersion. The fuel modules have a central heat pipe with integral fins and the fuel wafers, composed of 93.1 percent enriched uranium dioxide (UO_2) are placed in between the fins. Without the reflector, the cylindrical core is 33.1 cm high by 33.1 cm in diameter. A beryllium reflector region containing 12 rotating control drums is located outside the core. One-third of each control drum cylinder is B_4C. The remaining two-thirds of each control drum, except for the drive shaft, is beryllium. Another beryllium reflector is located at one end of the core; the other end has a reflector of beryllium oxide spheres, packed around the heat pipes outside the core.

After exiting the core, the heat pipes bend around the radiation shield on their way to the thermoelectric (TE) converter-radiator systems. The heat transferred by the heat pipe is then radiatively transferred from the

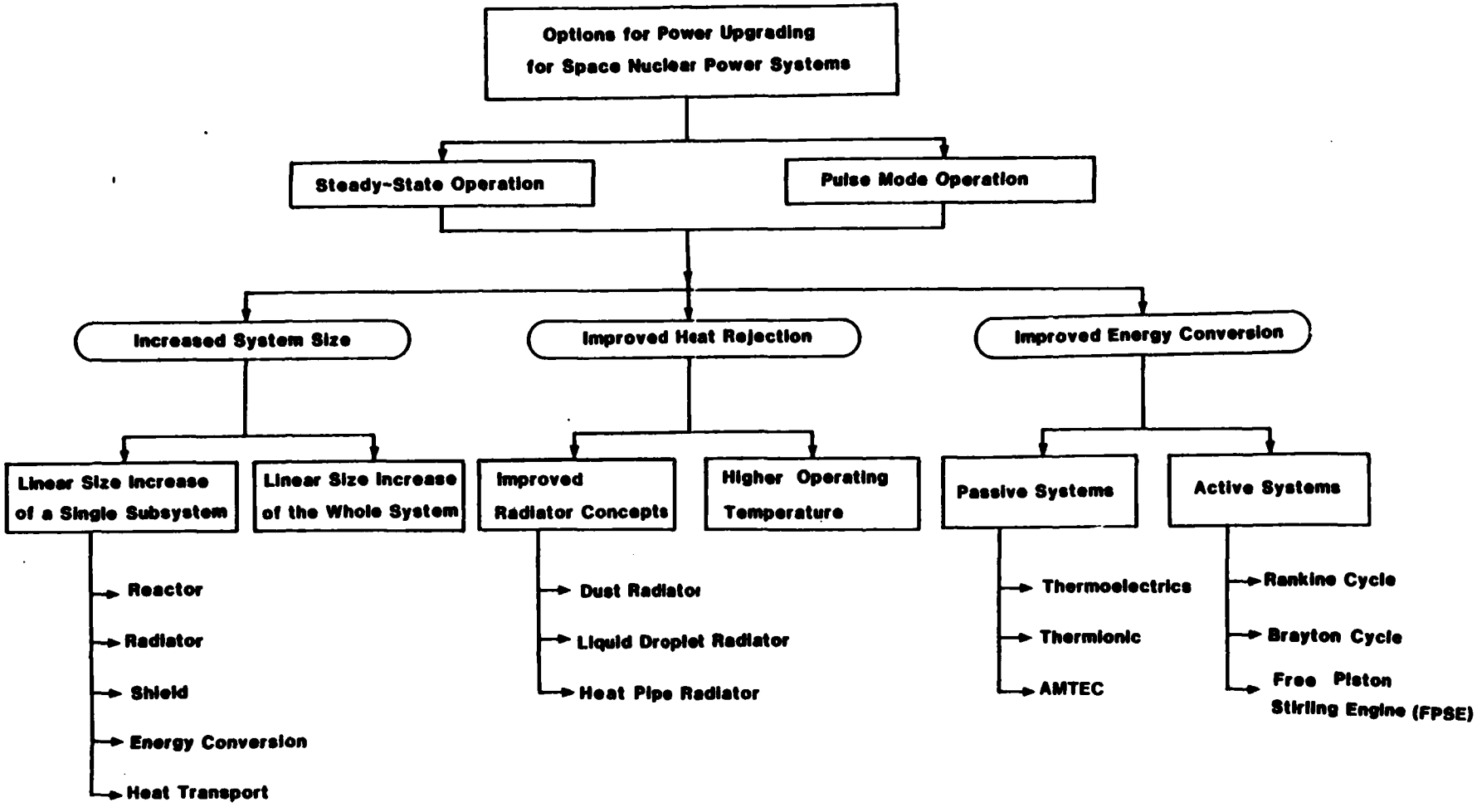

Figure 1. Options for power upgrading for space nuclear power systems.

heat pipes to the hot side of the TE converters located in the radiator panels. This thermal energy is partially converted into electricity, and the rest of the heat is radiated from the cold side of the TE converters into space.

The radiation shield is composed of a thin tungsten (W) layer to attenuate the gamma radiation and a relatively thick lithium hydride (LiH) layer to attenuate the neutrons emitted from the core. The mechanical strength of the shield is provided by a stainless steel matrix that runs radially in the shield. More details on the conceptual design of the HPSNR system can be found in References 6-8.

2. LINEAR SYSTEM SIZE INCREASE

More thermal energy can be produced by simply increasing the size of the nuclear reactor core. However, this option has numerous constraints that must be considered, such as fuel swelling, reactivity control, and the overall system mass. For example, increasing the size of the reactor core will cause the size of subsystems, such as the primary heat transport subsystem, the energy conversion subsystem, the heat rejection subsystem, and the radiation shield subsystem to increase also. The effects of such an increase in reactor thermal power output on each of these subsystems as well as on the mass of the whole system are discussed in Section III.

3. IMPROVED HEAT REJECTION

The heat rejection for a space nuclear power system is a linear function of converter efficiency (Eq. 1) and an inverse fourth power function of temperature (Eq. 2). The electrical power output and the waste heat rejected through the radiator are closely related:

$$P_{rej} = \frac{1 - \eta}{\eta} P_e \qquad (1)$$

where P_{rej} is the heat rejection power, P_e is the electrical power output, and η is the overall conversion efficiency of the system. For a given system efficiency, when P_e increases, P_{rej} increases. Therefore, if the electrical power output is to be increased, the amount of the rejected heat must be proportionally increased.

The heat rejection (as shown in Eq. 2) depends on the emissivity, ϵ, the radiator surface area, A, and the surface temperature, T_{rad}.

$$P_{rej} = \sigma \epsilon A F T_{rad}^4 \tag{2}$$

where σ is Stefan-Boltzmann constant, and F is the radiation shape factor. The radiation shape factor for the space nuclear power system radiator is slightly less than 1 because of the effects of the earth, the sun, and the moon. In Equation 2, P_{rej} can be increased significantly by increasing T_{rad} due to the fourth power effect. The radiator temperature, however, is limited by the reactor core operating condition.

Another method for increasing P_{rej} is to increase the radiator emissivity. Although the maximum theoretical material emissivity $\epsilon = 1$ is practically unachievable, the HPSNR base line design has proposed a carbon composite radiator surface which has a theoretical emissivity of 0.85.

The final factor affecting the heat rejection is the radiator surface area, A. For the panel type radiator, as in the HPSNR base line design, increasing the radiator area will linearly increase the radiator mass. To avoid such a penalty, other, more efficient, high-rejection systems must be developed such as the liquid droplet radiator or the metallic dust radiator. Each of these concepts, more fully discussed in Appendix A, uses the high surface-to-volume ratio capability of small spheres.

4. IMPROVED ENERGY CONVERSION

Another commonly used method to increase the electrical power output is to use an energy conversion system with improved conversion efficiency. The method is based on the premise that the electrical power output is directly proportional to the thermal-to-electric energy conversion efficiency, i.e., that

$$P_e = \eta P_{th} \tag{3}$$

where P_{th} is thermal power. Equation 3 shows that increasing the system efficiency not only increases the electrical power output, but also decreases the heat rejection load of the radiator. This, subsequently, reduces the radiator size and the overall mass of the system.

The efficiency of thermal-to-electrical energy conversion varies widely with the system being used. A total of six different thermal-to-electric energy conversion systems can be employed in space nuclear power systems (Ref. 9). Three are static converters: the Alkali Metal Thermoelectric Converter (AMTEC), the Thermionic fuel design, and the Thermoelectrics. The other three energy conversion systems are basically heat engines which utilize dynamic components: the Brayton cycle; the Rankine cycle; and the free piston stirling engine (FPSE). These thermal-to-electric energy conversion systems are discussed in Appendix B.

Unlike dynamic systems, the static converters have no moving parts and, therefore, do not require regular maintenance. However, their conversion efficiencies (5-12%) are much less than those of the dynamic systems (up to 34 percent). Figure 2 shows estimates of the total system efficiencies for both near term and future technology levels for each of the six conversion systems (Ref. 9). Although the static systems may be more advantageous than the dynamic systems because of the relatively lower weight penalty for electrical power outputs of several hundred kilowatts, the dynamic systems could be more favorable in the multimegawatt system from the weight penalty point of view.

5. PULSE-MODE OPERATION

Pulse mode operation is another approach that may be used to upgrade the power of an operating reactor designed to operate at certain power level continuously for 3-7 yr. Pulsing the power of the system to higher power for short periods (few milliseconds) may be accomplished without having to increase the maximum steady-state power output of the system. The peak power of the pulse depends on the steady-state power prior to pulsing as well as on the transient response of the different subsystems such as the nuclear reactor core, heat pipes, fuel system, TE converters, and radiators. The first three may impose the most constraints on the system during the pulse mode of operation. For example, depending on the initial operating power before pulsing, the peak power and the pulse duration could be limited by either the operating limits of the heat pipes or the ability of the radiator to handle the increased heat load during the pulse.

However, to operate the reactor core in both steady-state and pulse-mode, major design modifications must be introduced into the core control

system as well as into the overall core and shielding design. Additionally, an overall system analysis should be performed to determine the effect of different pulses on the safety and the operation of various subsystems.

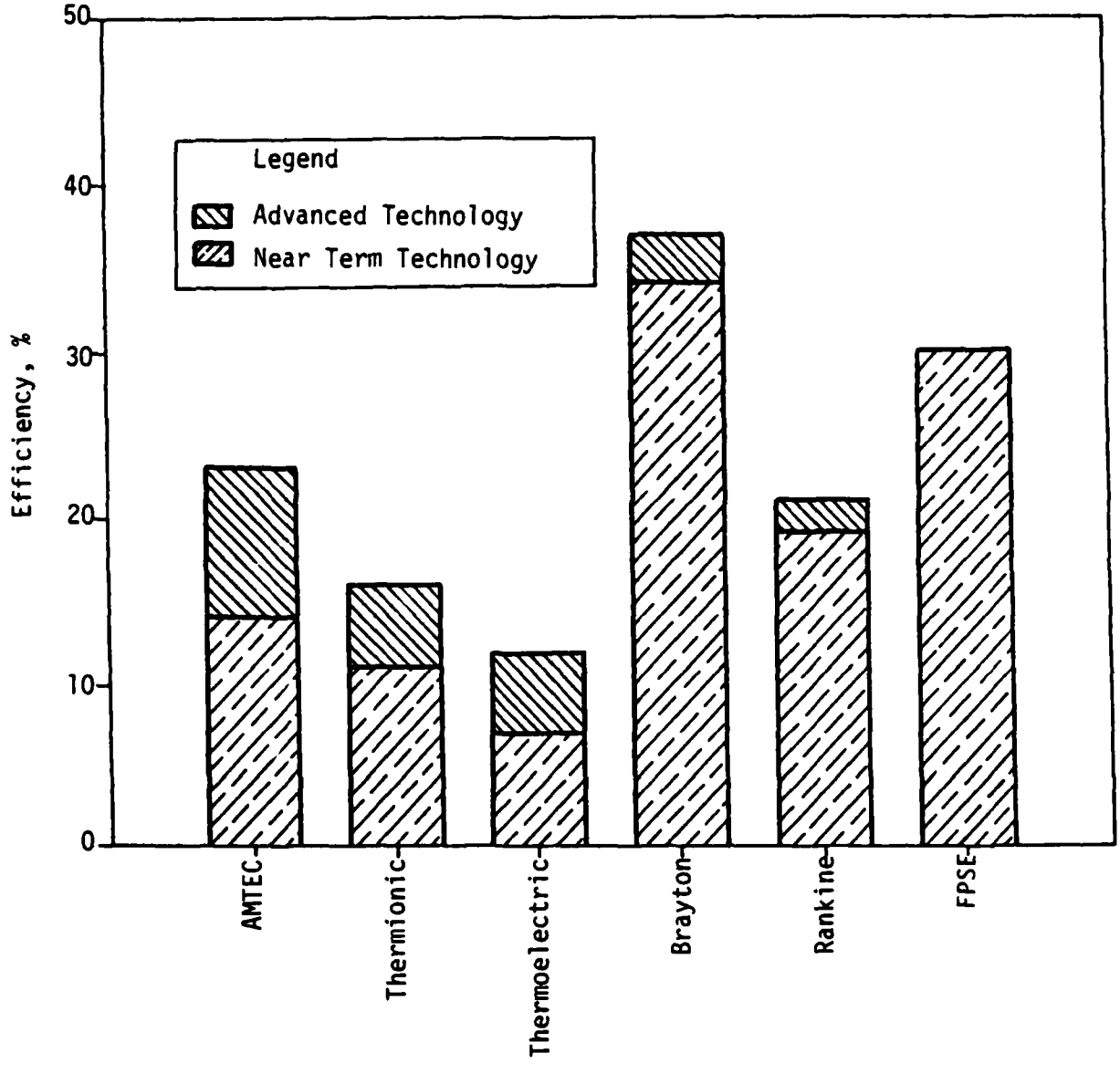

Figure 2. Energy conversion system efficiencies.

III. POWER UPGRADE OF THE HPSNR BY LINEAR SIZE INCREASE

A large space nuclear power system capable of continuously producing several hundred kilowatts to a few megawatts of electricity may not be possible without first increasing the size of the current HPSNR baseline design. In this section, the linear size increase of the HPSNR baseline design necessary to achieve higher power and the possible methods for upgrading the design are discussed, as well as some of the design limitations.

In order to determine the physical size of the HPSNR power system for an electrical power output higher than the 100 kWe established for the baseline design, the following design assumptions were introduced:

(1) The reactor core is a right-circular cylinder with a length to diameter ratio that is the same as the baseline design.

(2) The same fuel material and fuel density as used for the baseline design is used.

(3) The same heat transport device (heat pipes) as used for the baseline design is used.

(4) The same fuel operating temperature (1500 K) as used for the baseline design is used.

(5) The same energy conversion system (thermoelectrics) as used for the baseline design is used.

(6) A 7-yr lifetime is to be used.

These assumptions were then applied to the HPSNR power system. This system is divided into five major subsystems: (1) reactor, (2) shield, (3) energy conversion system, (4) radiator, (5) heat transport and structure. The physical size and the operating conditions of the system significantly depend on the overall system efficiency. Therefore, the total system efficiency should be determined first for both near term and future, more advanced, technological levels. In order to determine the total system efficiency, first, the efficiency of thermoelectric energy converters is plotted in Figure 3 as a function of the figure-of-merit, Z, and the temperature of the TE hot side.

As the plot in Figure 3 indicates, the efficiency of thermoelectric converters increases as the figure-of-merit, z, and/or the hot side temperature, T_h, increases. Additionally, the TE cold side temperature, T_c, should be kept as low as possible to increase the thermoelectric efficiency.

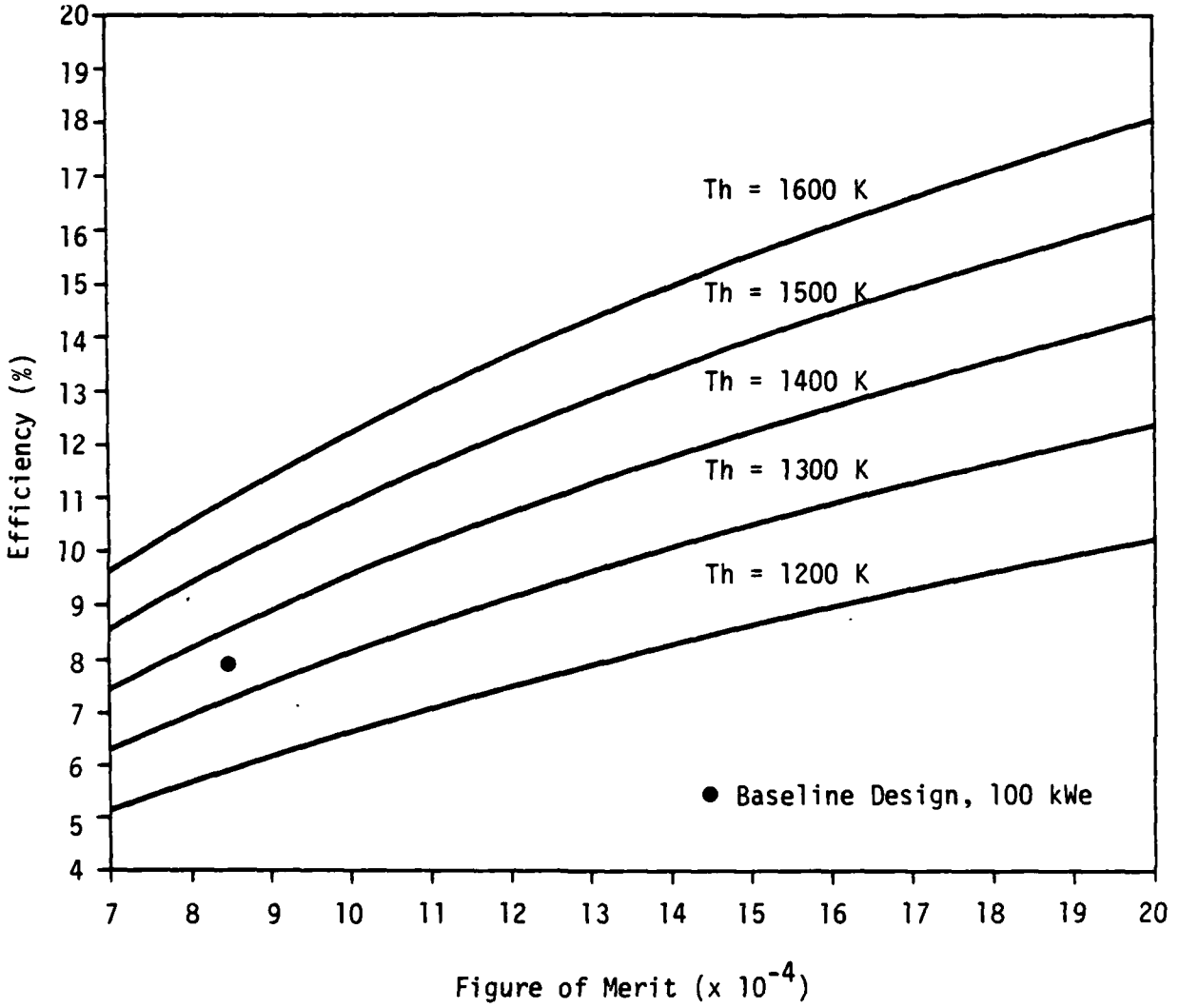

Figure 3. Thermoelectric efficiency with T_c = 800 K.

This temperature, however, is limited by the radiator operating temperature, because the lower the T_c, the larger the radiator size. The hot side temperature, T_h, is also limited by the reactor operating temperature. A high reactor operating temperature, although improving the heat rejection process to space, will cause high fuel swelling and may shorten the lifetime of the mission.

The present HPSNR baseline design and perhaps the more advanced designs anticipated in the future use 1350 K for the TE hot side temperature and 800 K for cold side temperature. For such temperatures, the state-of-the-art thermoelectric figure-of-merit is 0.7×10^{-3}. The baseline design now uses 0.85×10^{-3}; but for the more advanced system design in the future, the thermoelectric figure-of-merit was proposed as 2.0×10^{-3} (Ref. 10). Table 1 lists the figure-of-merit, the corresponding TE conversion efficiency, and the overall system efficiency. By the year 1990, shown in the table, the highest anticipated value for the TE conversion efficiency is 13.334 percent (Ref. 10). However, based on the available technology at present, this value should be much lower (about 6.884 percent).

TABLE 1. THERMOELECTRICS AND OVERALL SYSTEM EFFICIENCIES

	Current Technology	HPSNR Baseline Design	Future Technology	
Figure of merit	0.7×10^{-3}	0.85×10^{-3}	1.0×10^{-3}	2.0×10^{-3}
TE efficiency (%)[a]	6.884	7.905	8.827	13.334
System efficiency[b]	6.196	7.115	7.944	12.001

[a] TE efficiency was calculated with Tc = 800 K, Th = 1350 K.

[b] System efficiency was calculated assuming 10 percent loss of total power in the electrical interconnections, power conditioning, and thermal bypass losses in the system.

1. NUCLEAR REACTOR CORE

The nuclear reactor discussed in the previous section is the most important component of the system. This subsection analyzes the effects on

various core components of upgrading the reactor core power by increasing the core size linearly.

a. Mass of the reactor--Figure 4 plots the reactor mass as a function of electrical power output and the overall system efficiency (Ref. 11). In addition to the mass of the reactor core, this mass includes the reflector, control drums, actuators, and support structures up to the reactor-shield interface.

As shown in Figure 4, the reactor mass is nonlinear with the electrical power output. It increases rapidly below 500 kWe and slows down above 500 kWe. For the baseline design, the reactor mass is 490 kg. Such mass, however, will be 1275 kg, 1180 kg, and 977 kg for 1.0 MWe power with a system conversion efficiency of 6.2, 7.1, and 12 percent, respectively.

b. Fuel swelling--Fuel swelling is an important factor for determining the reactor core operating temperature as well as the mission lifetime. UO_2 fuel swelling (percent of volume increase) versus electrical power output for various operating temperatures is given in Figure 5 (Ref. 11). These swelling values taken from the existing data on the irradiation of unrestrained UO_2 are considered quite conservative.

The fuel swelling limit in the HPSNR baseline design was set at 10 percent by volume. Thus, based on fuel swelling alone, a reactor cannot be built that would generate more than 240 kWe with a system efficiency of 12 percent and 1500 K operating temperature. However, the fuel swelling limitation can be overcome by: (1) increasing system efficiency, (2) reducing the operating temperature of the fuel, and/or using uranium nitride (UN) fuel.

(1) Increasing system efficiency--For an energy conversion system with an efficiency of around 25 percent, the electrical power output would exceed 500 kWe without violating the 10 percent fuel swelling limit. With such high conversion efficiency, the fuel swelling at 1 MWe power will be approximately 12-13 percent. Therefore, with improved energy conversion systems, the fuel swelling may not be a major limitation.

(2) Reducing the operating temperature of the fuel--As shown in Figure 5, the HPSNR system can generate over 600 kWe with 1300 K operating temperature without violating the 10 percent fuel swelling limit. However, the reduced operating temperature will cause the radiator size and, hence, the system mass to increase, and the conversion efficiency of the thermo-

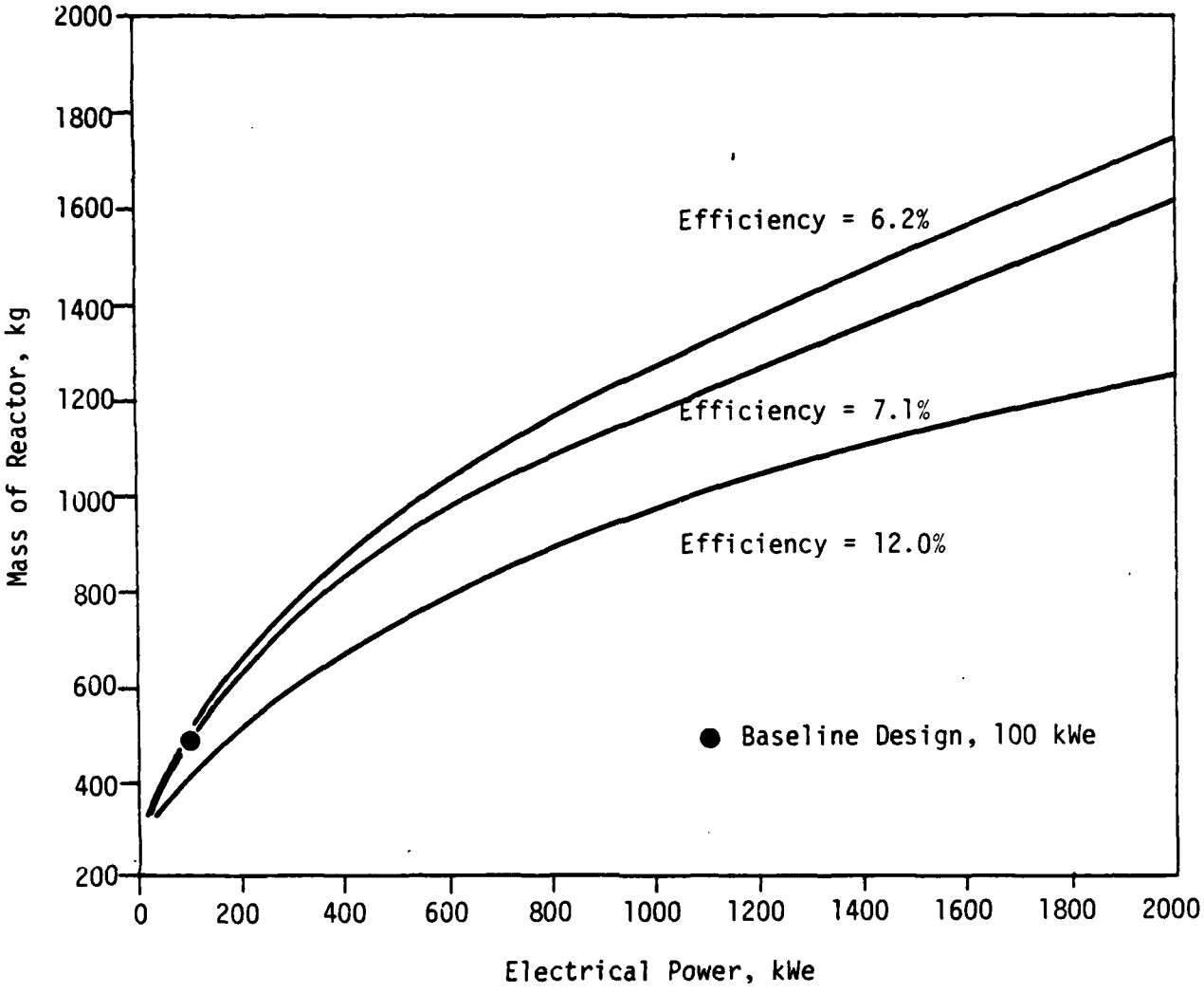

Figure 4. Mass of the heat pipe reactor as a function of electrical power and system efficiency.

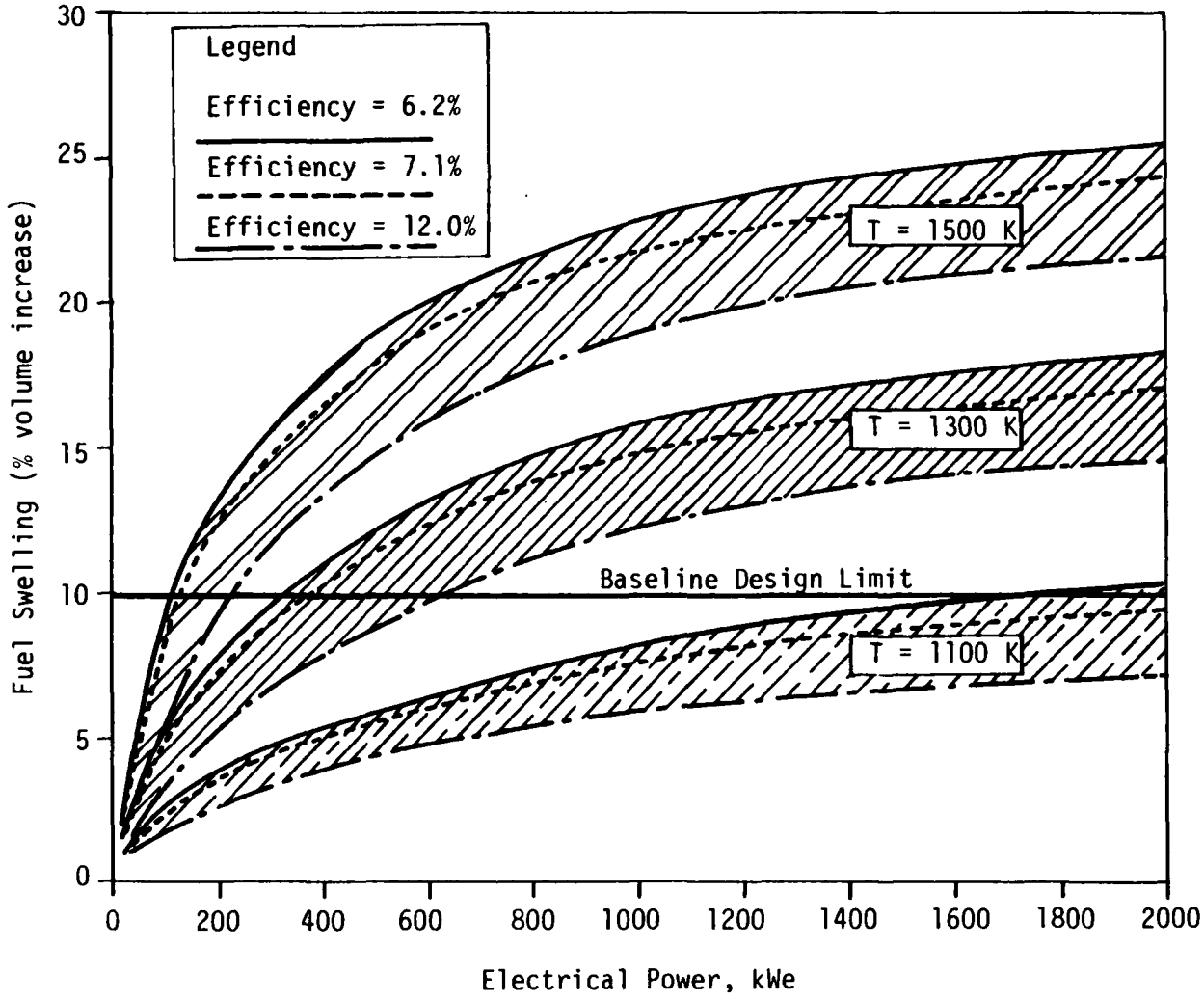

Figure 5. UO_2 swelling at the end of 7-yr operation with full power.

electric converters to decrease. Nevertheless, the option may be valid by using the free piston stirling engine, which can operate at relatively low temperatures, while keeping the system thermal-to-electric energy conversion efficiency quite high (~20-25 percent).

c. Fuel system--Figure 6 compares the fuel swelling of UO_2, UN, and UC (uranium carbide) fuel at 1 atom percent burnup (Ref. 12). Comparable high burnup data were not available for UN and UC. Swelling of UN fuel may become slightly higher than that for UO_2 at higher burnup, and UC would show significantly greater swelling at high burnup.

Calculations were performed based on the comparisons shown in Figure 6. These calculations assumed that all fuel systems have cylindrical fuel elements with the same dimensions and that they are all operated to the same burnup (1 atom percent), at the same power output and operating time, and with the same linear power and fuel surface temperature. The same fuel surface temperature means that the systems have the same operating temperature as well as the same TE conversion efficiency. The calculations show that the maximum fuel temperature for fuel system 1 and 2 can be given, respectively, as:

$$(T_{m1} - T_s) = \frac{q'}{4\pi k_1} \tag{4}$$

$$(T_{m2} - T_s) = \frac{q'}{4\pi k_2} \tag{5}$$

and the average fuel temperatures as:

$$T_{av1} = \frac{T_{m1} + T_s}{2} \tag{6}$$

$$T_{av2} = \frac{T_{m2} + T_s}{2} \tag{7}$$

where

T_m = maximum fuel center temperature,

T_s = fuel surface temperature,

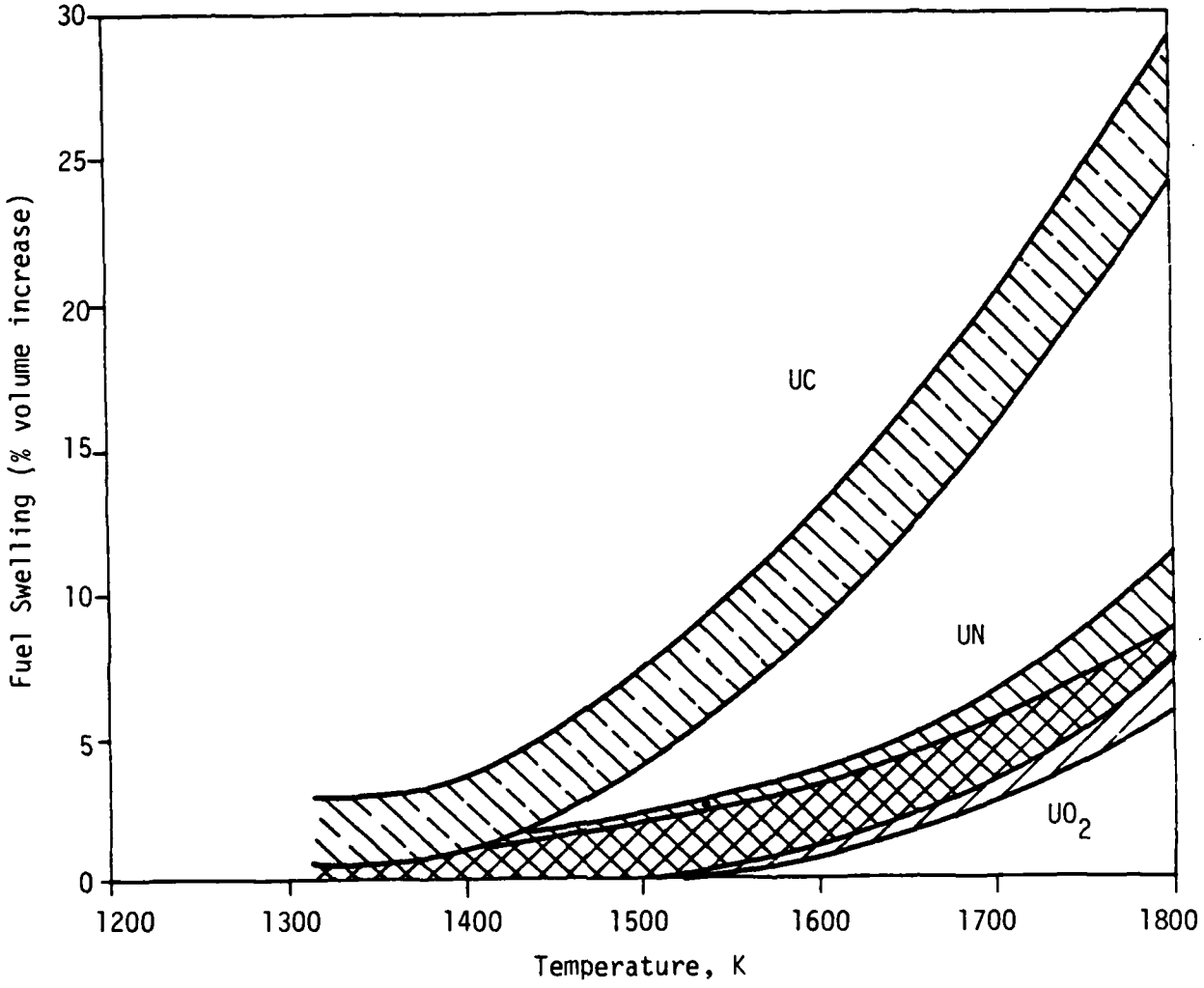

Figure 6. Fuel swelling at 1 atom percent burnup.

T_{av} = average fuel temperature.

Equations 8 and 9 are then obtained from Equations 4 through 7:

$$\frac{T_{m1} - T_s}{T_{m2} - T_s} = \frac{k_2}{k_1} \tag{8}$$

and

$$\frac{T_{av1} - T_s}{T_{av2} - T_s} = \frac{k_2}{k_1} \tag{9}$$

Therefore, the ratio of the temperature differences for two different fuel systems is inversely proportional to their thermal conductivity ratio. If 1700 K is chosen as the UO_2 fuel maximum temperature, then the corresponding temperatures for other fuel systems can be calculated as shown in Table 2. The Table 2 results show that for the same fuel surface temperature and burnup, the volume increase is 6.3 percent for UC fuel, 2.1 percent for UO_2, and 1.3 percent for UN. Although the average temperature of the UC fuel is much less (87 K) than that of the UO_2 fuel, the fuel swelling of the UC fuel is three times as much as that of the UO_2 fuel. These results indicate that UN fuel could be a better alternative for UO_2 fuel because of its comparable swelling rate and high thermal properties. However, additional research is needed to develop a data base and to understand the irradiation behavior of UN fuel as an advanced fuel system for a future generation of space nuclear reactors.

TABLE 2. FUEL SWELLING FOR DIFFERENT FUEL MATERIALS WITH THE SAME SURFACE TEMPERATURE (1500 K) AND BURNUP (1 atom %)

Physical Parameters	Fuel Material UO_2	UC	UN
Thermal conductivity (W/cm K)	2.5	20	26
Maximum temperature (K)	1700	1525	1519
Average temperature (K)	1600	1513	1510
Volume increase (%)[a]	2.1	6.3	1.3

[a]Obtained from Figure 6.

TABLE 3. FUEL TEMPERATURE FOR DIFFERENT FUEL MATERIALS WITH THE SAME FUEL SWELLING (3% volume increase) AND BURNUP (1 atom %)

Physical Parameter	Fuel Material UO_2	UC	UN
Average Temperature (K)[a]	1645	1425	1620
Surface Temperature (K)	1500	1407	1606
Maximum Temperature (K)	1790	1443	1634
TE Hot Side Temperature (K)[b]	1350	1266	1445
TE Conversion Efficiency	7.905	6.809	11.780
Relative Radiator Size	1.000	1.175	0.643

[a]Obtained from Figure 6.

[b]Assumed 10 percent temperature drop from the surface temperature.

The results shown in Table 3 also reveal that the fuel operating temperatures that induce the same fuel swelling of 3 percent at 1 atom percent burnup differ significantly with the fuel system. If a 10 percent temperature drop between fuel surface and the TE converter is assumed, the temperature of the hot side of the TE converters would be 1445 K with UN fuel, 1350 K with UO_2 fuel, and 1266 K with UC fuel. Such variations of TE hot side temperatures indicate variable requirements for heat rejection surface area and radiator size as well as different TE conversion efficiency. With the radiator size for UO_2 fuel system normalized to unity, the radiator size for UC and UN fuel system is 1.175 (17.5 percent increase in surface area) and 0.643 (35.7 percent reduction in surface area), respectively.

In summary, the UN fuel system showed the lowest fuel swelling (1.3 percent versus 6.3 percent for UC) and the least requirement for radiator size (35.7 percent less than the UO_2 system) among the three fuel systems considered (UO_2, UC, and UN). Therefore, with an appropriate fuel design capable of accommodating the over pressurization caused by nitrogen (Ref. 13), the UN fuel could be the best fuel candidate for space nuclear reactors. The second best is UO_2 fuel which enjoys a large data base for irradiation

behavior from the experience with commercial light water reactors (LWRs) and liquid metal fast breeder reactors (LMFBRs).

d. Reactivity control system--The reactivity control requirements (Ref. 14) for space nuclear power reactors are shown in Figure 7. For the 100 kWe system, the total available $\Delta k/k$ of 7.1 percent provides for a 2 percent shutdown margin; 0.7 percent for thermal expansion; 2.4 percent for fuel burnup over 7-yr lifetime, including both fuel depletion and fission product poisoning effect; and a 2 percent contingency margin. For the 1 MWe system, a total $\Delta k/k$ of 12.7 percent is required to compensate for an approximately 8 percent $\Delta k/k$ for fuel burnup.

The amount of reactivity control available for the HPSNR is shown in Figure 8 (Ref. 11). As the surface-to-volume ratio of the core decreases with increasing core diameter, the neutron leakage becomes relatively less important. As a result, the reactivity worth of a fixed number of control drums would decrease as the core diameter increased (Fig. 8). However, if the number of control drums were proportional to the core diameter, the reactivity worth of the control drums will increase slightly as the core diameter increases. In this case, for example, the control margin provided by the control drums would be around 12 percent $\Delta k/k$, which is slightly less than the required reactivity margin for a 1 MWe reactor core (Fig. 7).

Figure 8 compares the reactivity requirement curve with the reactivity availability curves for two design concepts. In the first concept (lower case), the number of control drums is kept the same as in the HPSNR baseline design (12 drums). In the second concept, the number of control drums was increased proportionally with the core diameter (upper curve). For a proper design of the reactor control system, the reactivity availability curve should always be kept above the reactivity requirement curve in Figure 8. The maximum core size, therefore, would be limited by the reactivity control system used. If the number of control drums increased with the core diameter, the maximum core diameter attainable would be about 61 cm, resulting in a maximum electrical power output of about 920 kWe. This core diameter is approximately 20 percent larger and the electrical power output is approximately 50 percent larger than the maximum core diameter and the maximum power available with the other control system design (i.e., 12 control drums).

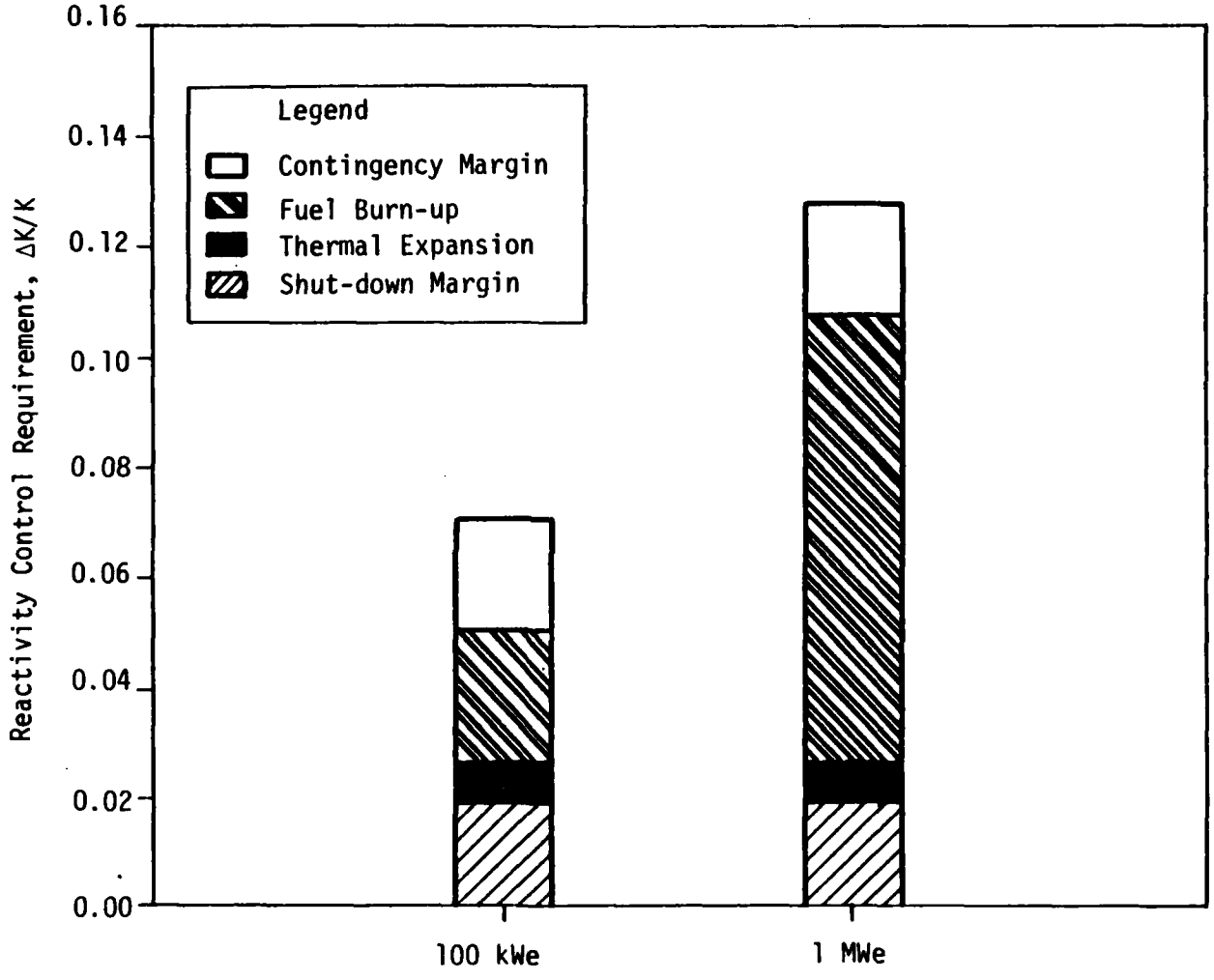

Figure 7. Control swing requirement.

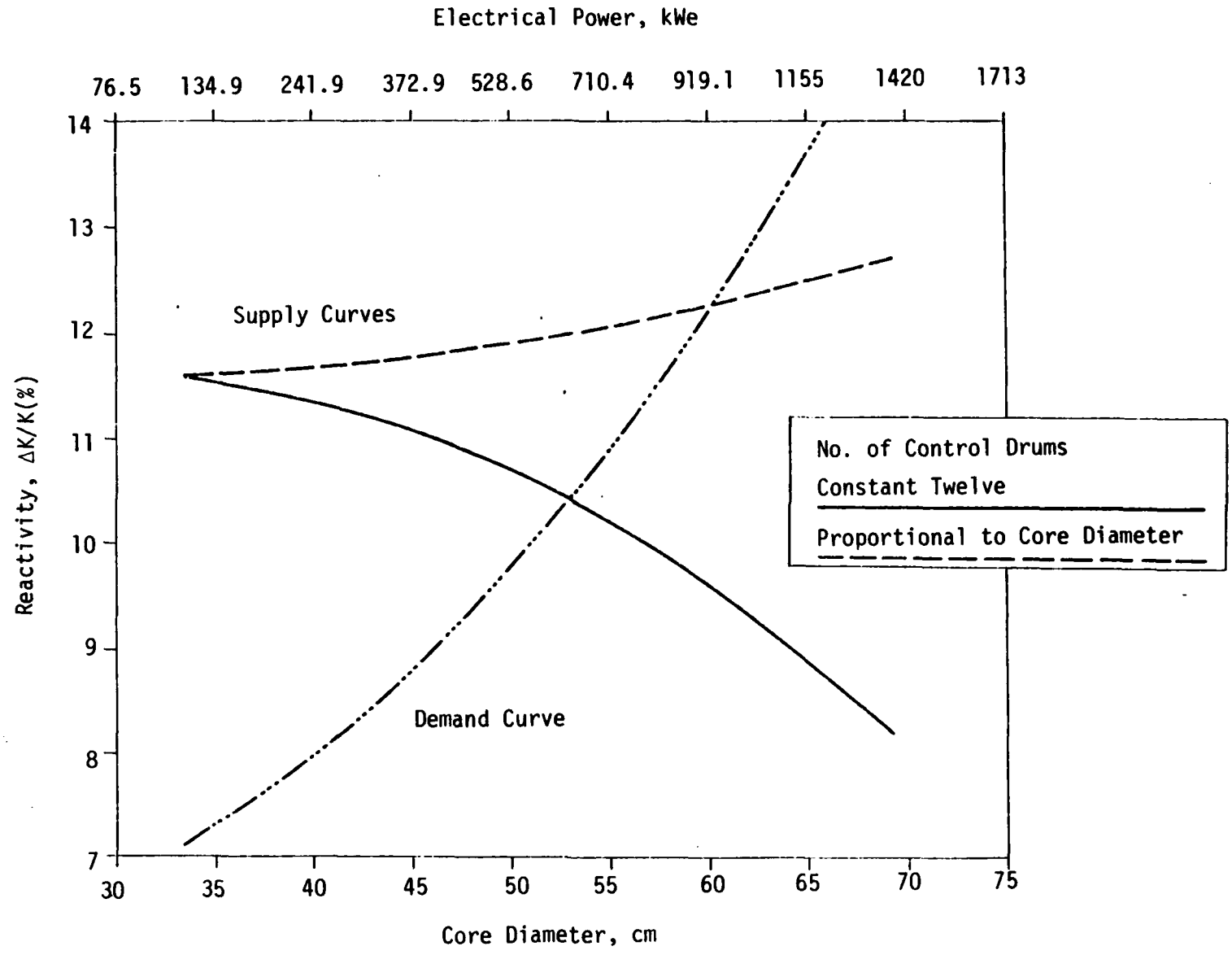

Figure 8. Reactivity control available and required for HPSNR upgraded design.

In conclusion, designing the reactivity control system where the number of control drums is proportional to the core diameter would be advantageous for upgrading the power of the HPSNR system. Such a design would allow increasing the core size from the present 31.1 cm to about 61 cm without requiring an additional reactivity control system.

2. RADIATOR SUBSYSTEM

The main constraints in increasing the radiator size comes from the overall system size required to fit within one third of the shuttle cargo bay. Figure 9 shows the radiator area as a function of the electrical power output and the overall system efficiency. The area of the radiator, A, as a function of the electrical power output, P_e, can be given as

$$A = P_e \left(\frac{1 - \eta}{\eta}\right) \Big/ \left[\varepsilon F \sigma (T_{rad}^4 - T_s^4)\right] \qquad (10)$$

where η is the thermal-to-electric energy conversion efficiency, ε is the surface emissivity of the radiator, F is a shape factor, and σ is Stefan-Boltzman constant [5.669×10^{-8} w/m^{2}K^4]. T_{rad} is the radiator surface temperture and T_s is the ambient temperature. For calculations delineataed in Figure 9, the values of these parameters were taken as

$$T_{rad} = 800 \text{ K} \qquad T_s = 200 \text{ K}$$
$$\varepsilon = 0.85 \qquad F = 0.95$$

The radiator is assumed to have a specific mass-to-surface area of 5 kg/m^2 (Ref. 9). For a 1 MWe power level and system efficiencies of 6.2, 7.1, and 12 percent, the radiator areas are 810, 700, and 395 kg, respectively. In Figure 10, the radiator mass is plotted as a function of electrical power output and system efficiency. As Figures 9 and 10 show, the electrical power output for the HPSNR baseline design could be doubled (~200 kWe) without any increase in the radiator size or mass if the system efficiency could be raised from 6.2 to 12 percent.

3. RADIATION SHIELD SUBSYSTEM

The mass of the radiation shield in the HPSNR is the largest of any subsystem. The radiation shield chosen for the HPSNR baseline design

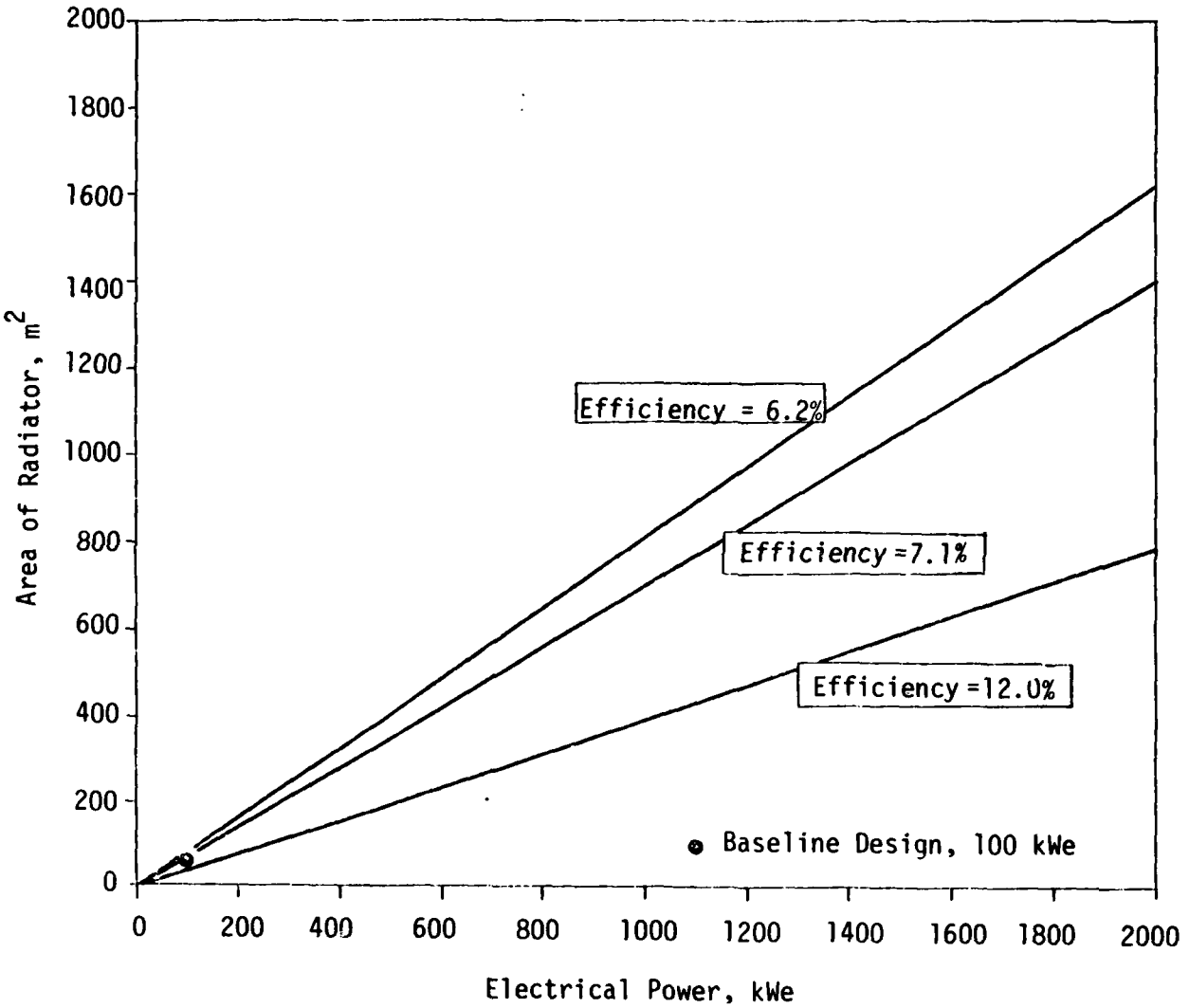

Figure 9. Area of the radiator as a function of electrical power and system efficiency.

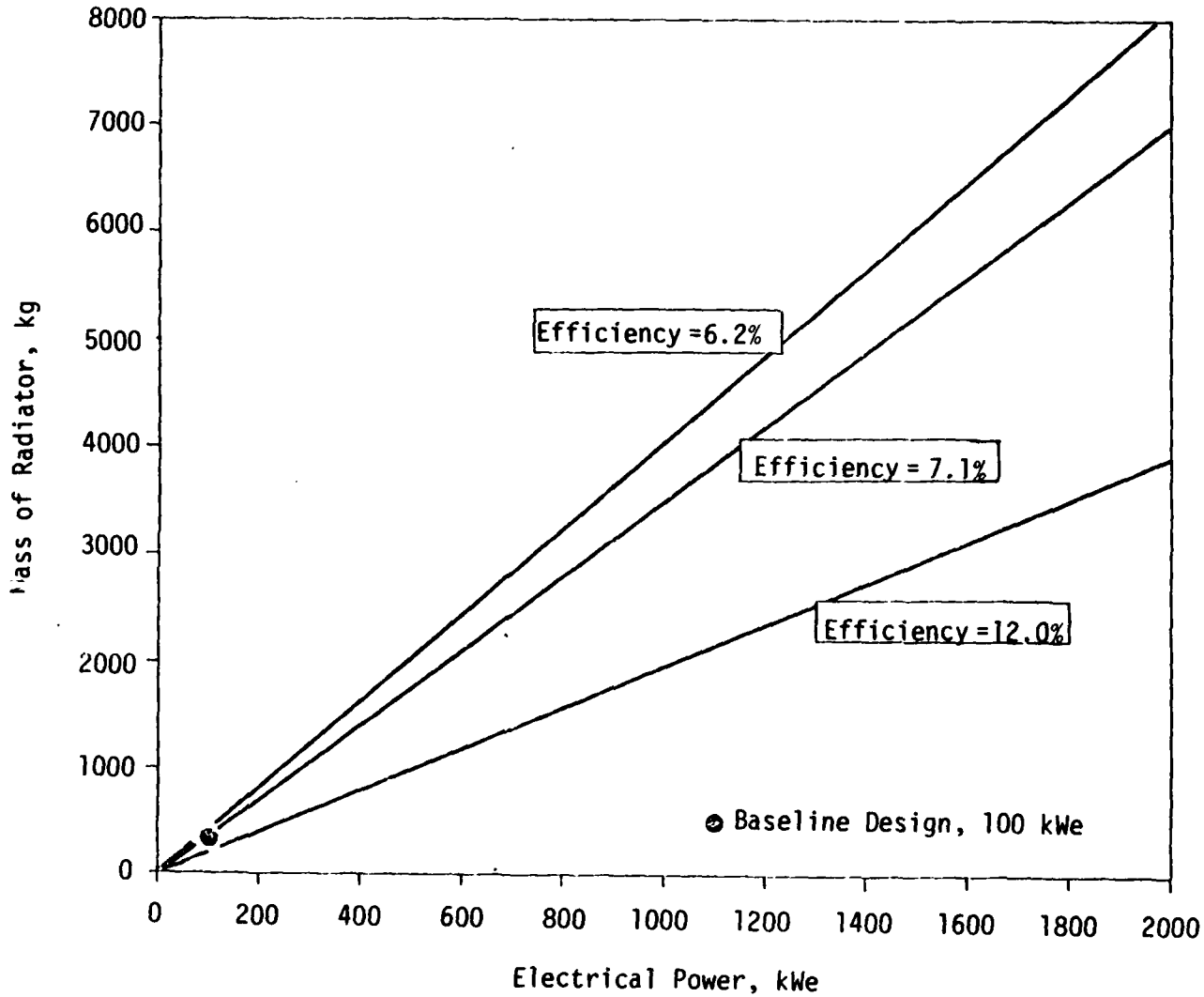

Figure 10. Mass of the radiator as a function of electrical power and system efficiency.

ensures that over 7 yr of continuous operation, the radiation exposure at the dose plane would not exceed 10^6 rd for gamma photons and 10^{12} nvt (neutron fluence) for fast neutrons at a distance of 25 m and within a 15-deg cone half-angle (Ref. 7). Figure 11 shows the shield mass versus electrical power output for various system efficiencies (Ref. 13). It also shows that at the 1 MWe power level, the shield mass is 5100, 3800, and 2300 kg for system efficiencies of 6.2, 7.1, and 12 percent, respectively.

However, because of the large mass and amount of energy deposition in the shield at high power level, extensive thermal and stress analyses must be made of the shield structure before this approach can be used (Ref. 15). Additionally, cooling requirements of the shield at upgraded power levels must also be addressed because these requirements could increase the specific mass of the shield (kg/kWe).

4. ENERGY CONVERSION SUBSYSTEM

In the present HPSNR design, the specific mass of the thermoelectrics was assumed to be 200 kg/MW_{th} (Ref. 9). The specific mass would be 3.23, 2.82, and 1.67 kg/kWe for overall system efficiencies of 6.2, 7.1, 12 percent, respectively. In Figure 12, the thermoelectric system mass is plotted as a function of electrical power output and system efficiency and shows that by increasing either the system efficiency or the electric power output, the specific mass of the TE converters subsystem would decrease, thus, resulting in a significant reduction of the total mass of the system.

5. HEAT TRANSPORT AND STRUCTURE SUBSYSTEM

The specific mass of heat transport subsystem (heat pipe) in the HPSNR is 300 kg/MW_{th} (Ref. 9). For system efficiencies of 6.2, 7.1, and 12 percent, respectively, the specific mass would be 4.84, 4.23, and 2.50 kg/kWe. The heat transport subsystem (heat pipe) mass is plotted in Figure 13 as a function of electrical power output and system efficiency. Like the specific mass in the TE converters, the specific mass of the heat pipes would decrease as either the system efficiency or electric power increased. The structural material mass was assumed to be 10 percent of the total system mass except for the structure itself (Ref. 14).

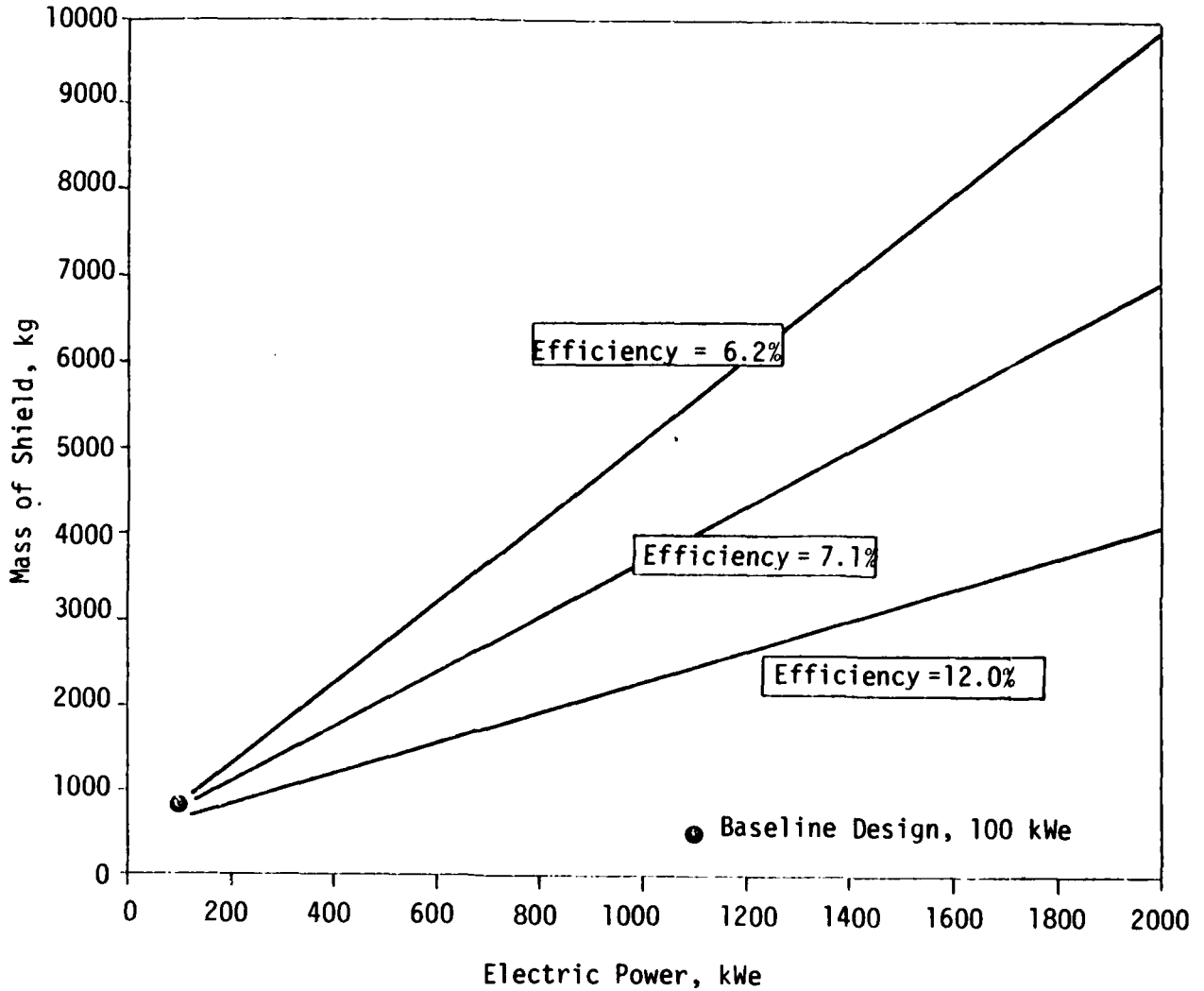

Figure 11. Mass of the shield as a function of electrical power and system efficiency.

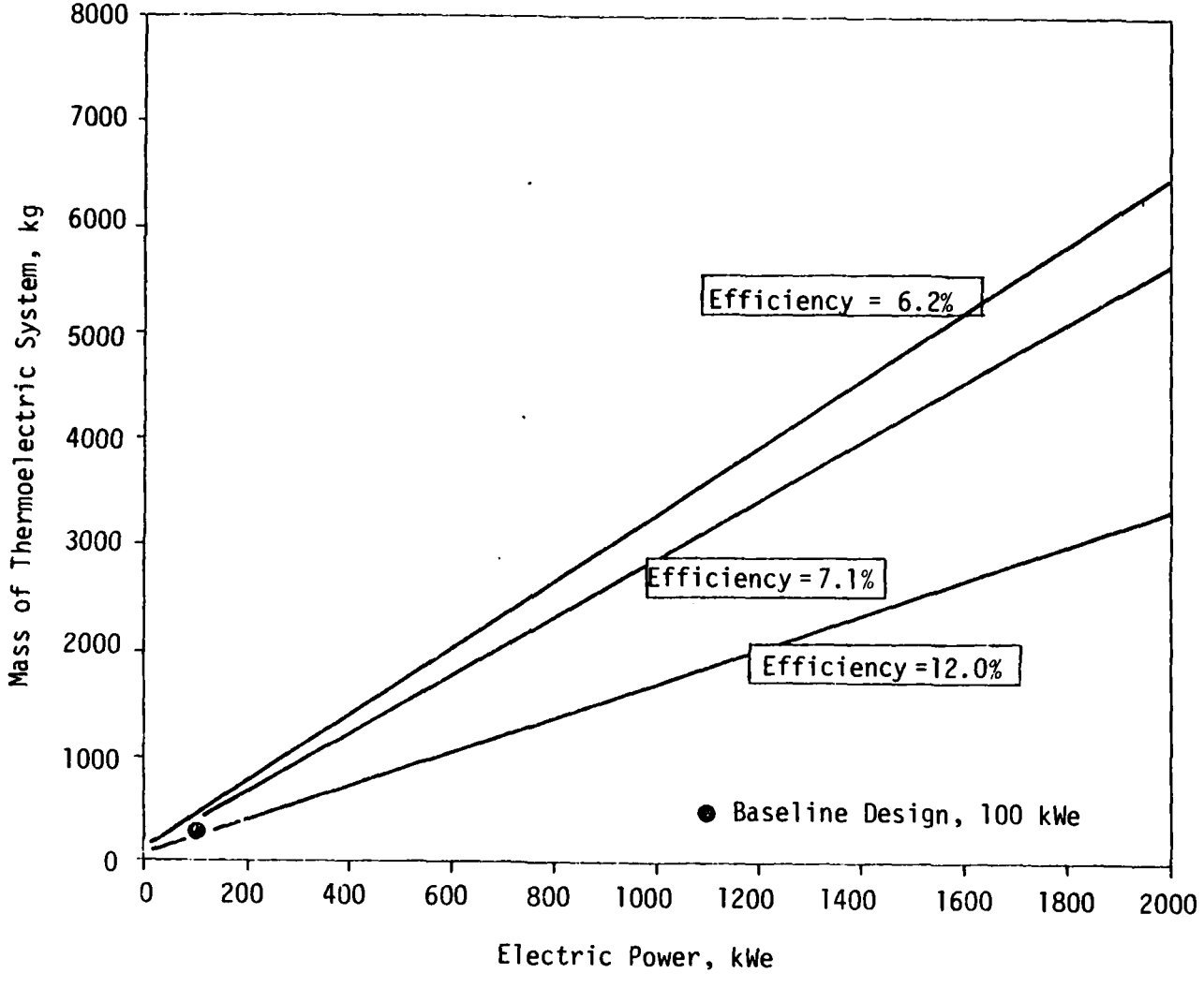

Figure 12. Mass of the thermoelectric system as a function of electrical power and system efficiency.

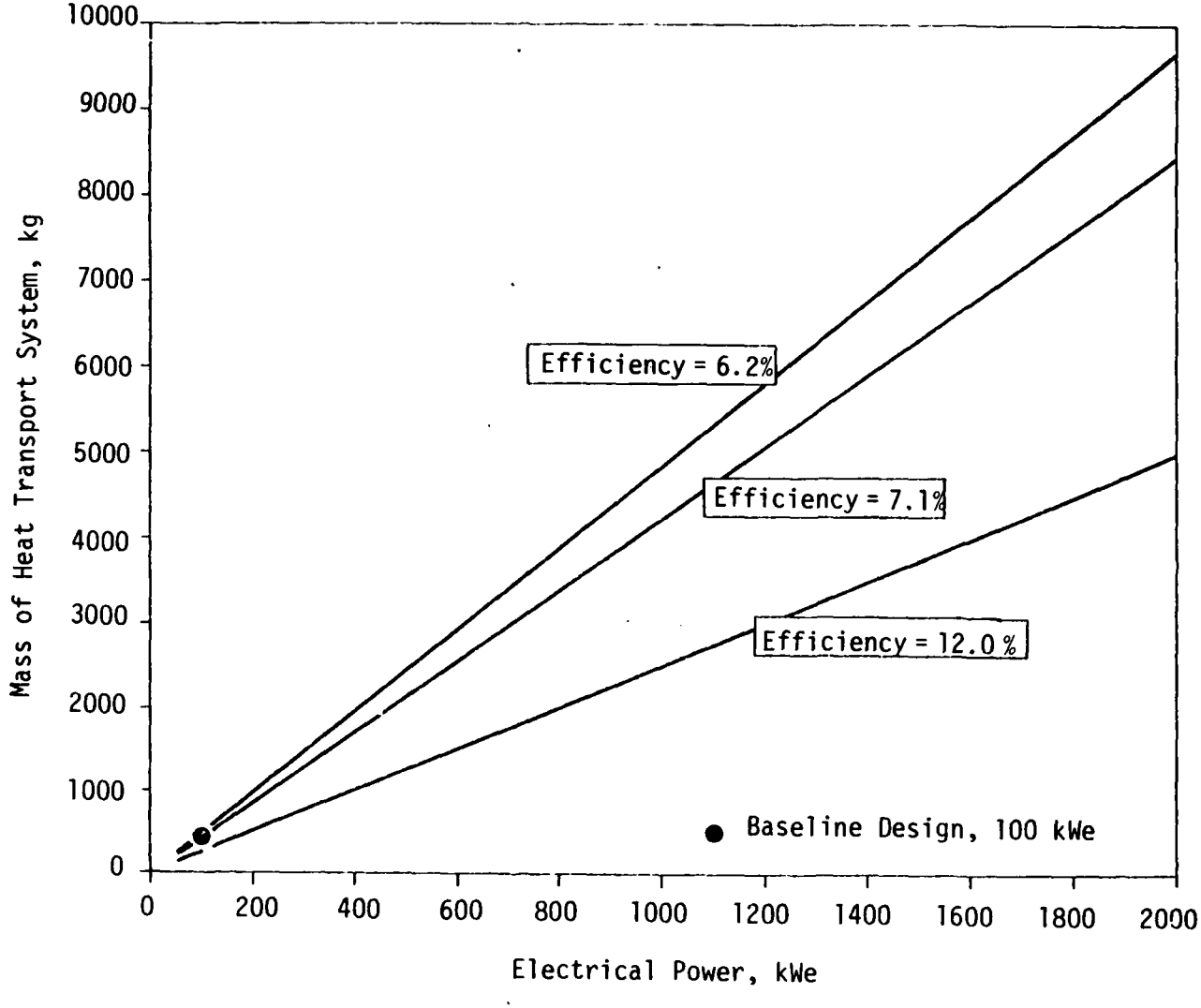

Figure 13. Mass of heat transport system as a function of electric power and system efficiency.

6. TOTAL MASS OF THE WHOLE SYSTEM

The total mass of the HPSNR system for various system efficiencies is plotted in Figures 14, 15, and 16 as a function of electrical power output. For example, for 100 kWe (baseline design), the reactor mass is 22.4 percent of the total system mass and is only 9.5 percent for 1 MWe when the system efficiency is 12 percent. The mass fraction of various subsystems are summarized in Table 4 and plotted in Figures 17, 18, and 19 for various system efficiencies and electrical power outputs.

As this table clearly shows, for a given system efficiency, the reactor and shield mass fractions decrease as the electrical power output increases. The mass fractions of the radiator, thermoelectric conversion subsystem, and heat transport subsystem increase with the electrical power output, while the mass fraction of the structure remains constant. For a given electrical power output, the mass fraction of the reactor increases as the system efficiency increases, while the mass fraction of the radiator decreases. The mass fractions of the other subsystems, however, are not a strong function of the system efficiency.

TABLE 4. MASS FRACTION OF THE HPSNR SUBSYSTEMS

Power Output	System Efficiency (%)	Percent of the Total System Mass					
		Reactor	Radiator	TE	Shield	HT[a]	Structure
100 kWe	6.2	18.22	13.22	11.54	29.73	17.29	10
	7.1	18.98	12.52	11.03	30.09	16.55	10
	12.0	22.42	9.56	8.92	35.75	13.35	10
500 kWe	6.2	9.02	17.39	15.18	25.66	22.75	10
	7.1	10.15	17.76	15.65	22.97	23.47	10
	12.0	12.96	15.78	14.72	24.50	22.04	10
1 MWe	6.2	6.32	18.34	16.02	25.33	23.99	10
	7.1	7.02	19.04	16.77	22.01	25.16	10
	12.0	9.53	17.46	16.29	22.33	24.39	10
2 MWe	6.2	4.48	18.94	16.53	25.27	24.76	10
	7.1	5.02	19.81	17.46	21.52	26.19	10
	12.0	6.46	18.66	17.41	21.41	26.06	10

[a]Heat Transport Subsystem

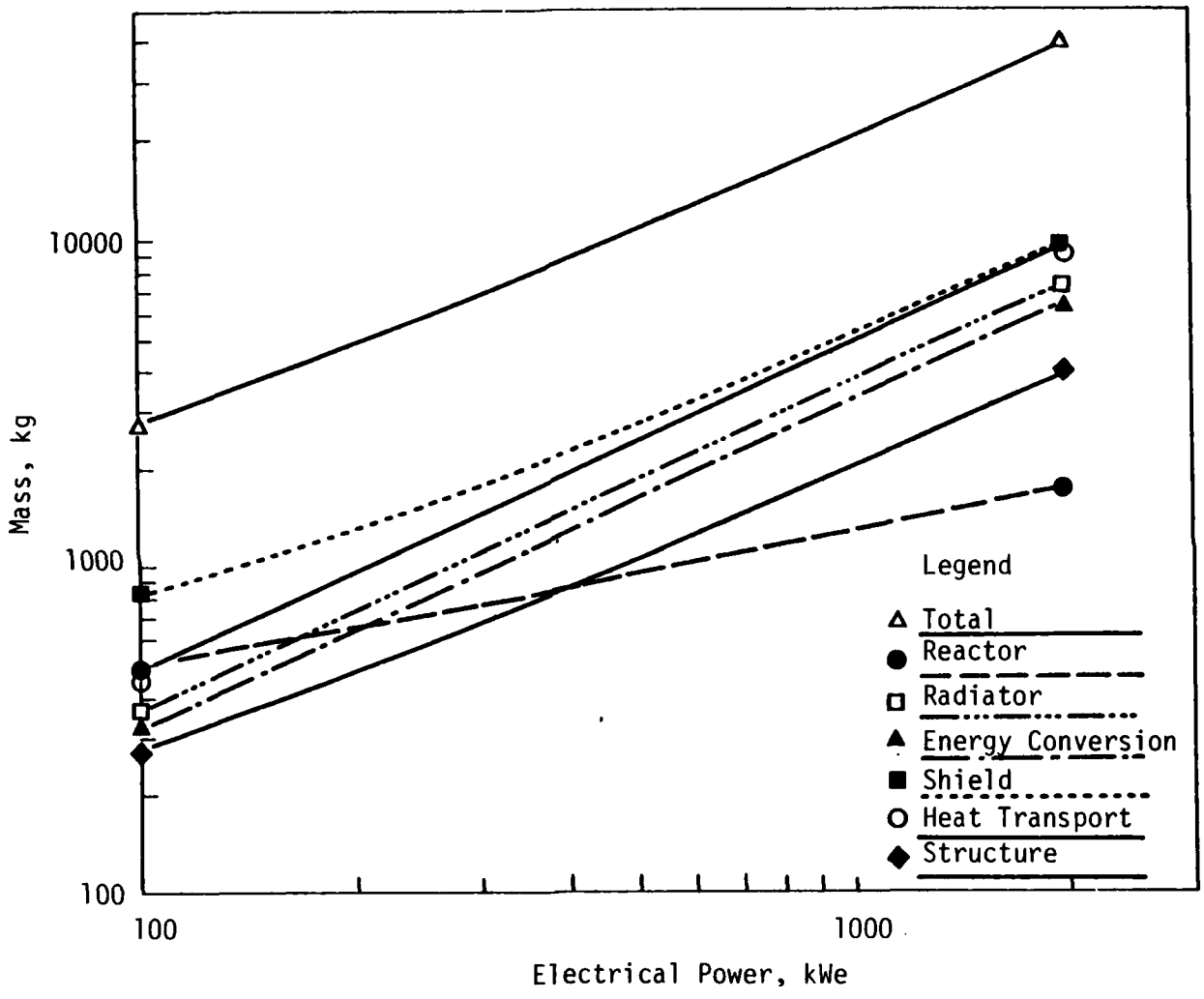

Figure 14. Total system mass and subsystem mass (with system efficiency 6.2 percent).

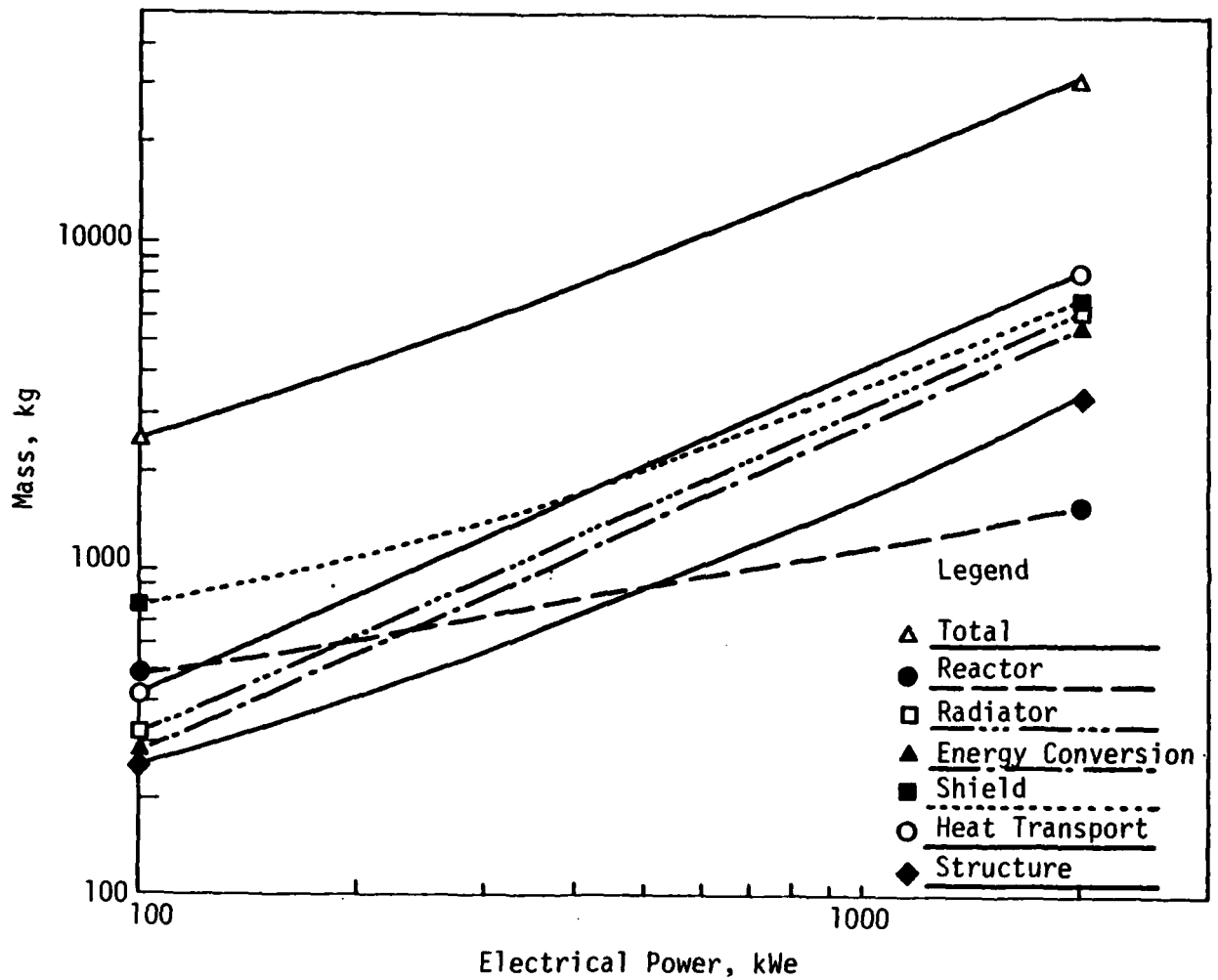

Figure 15. Total system mass and subsystem mass (with system efficiency 7.1 percent).

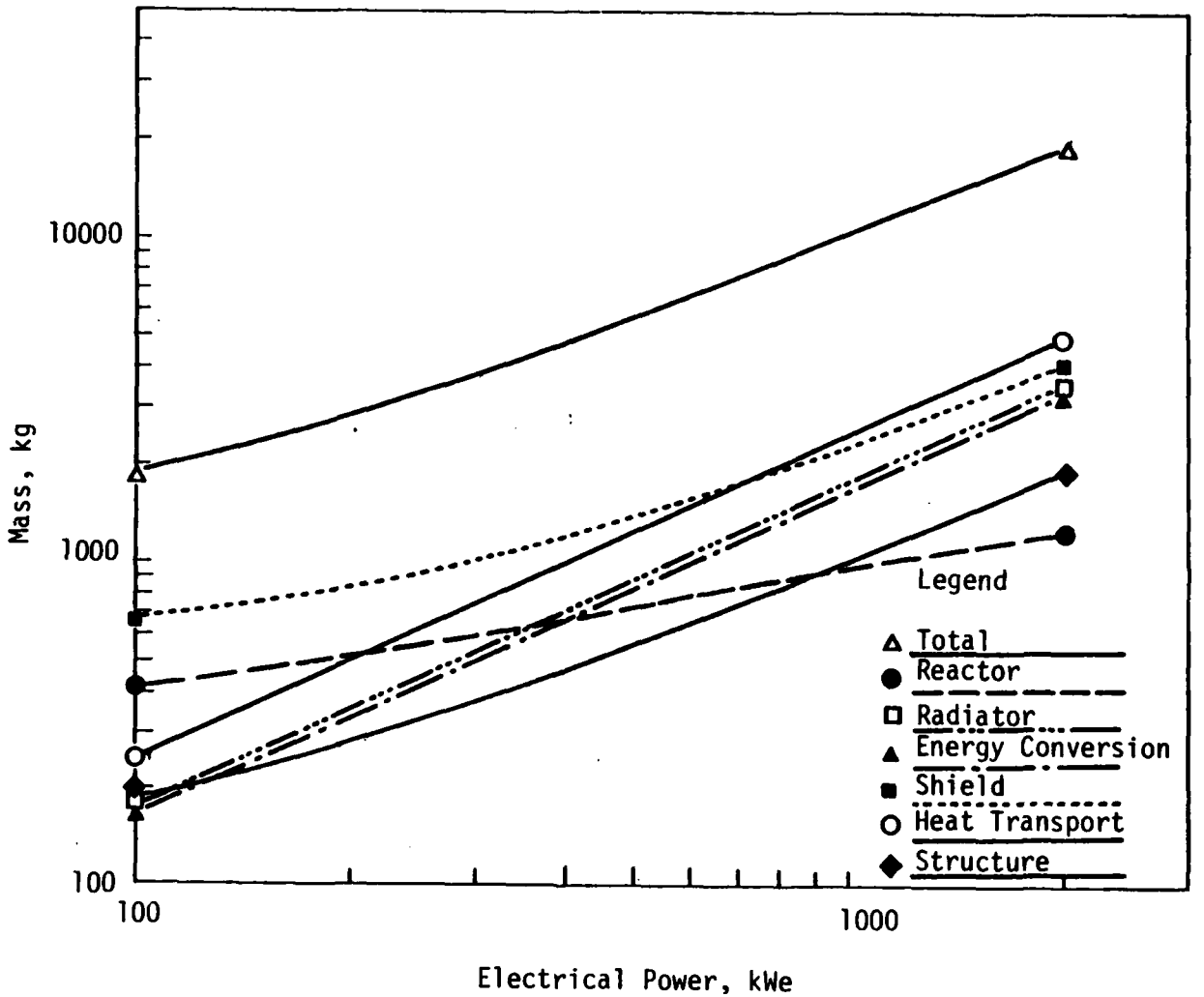

Figure 16. Total system mass and subsystem mass (with system efficiency 12.0 percent).

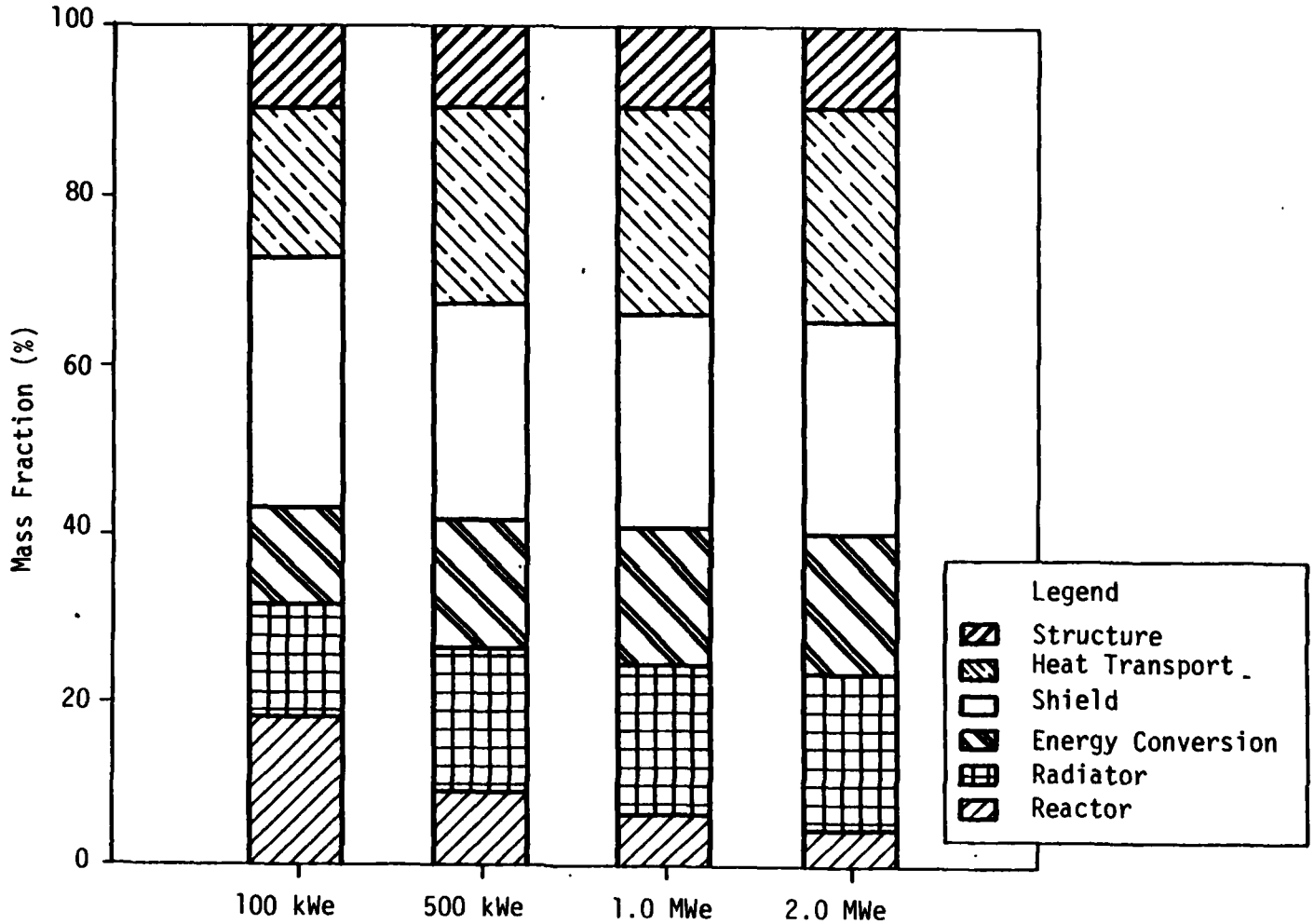

Figure 17. Mass fraction of subsystems (with system efficiency 6.2 percent).

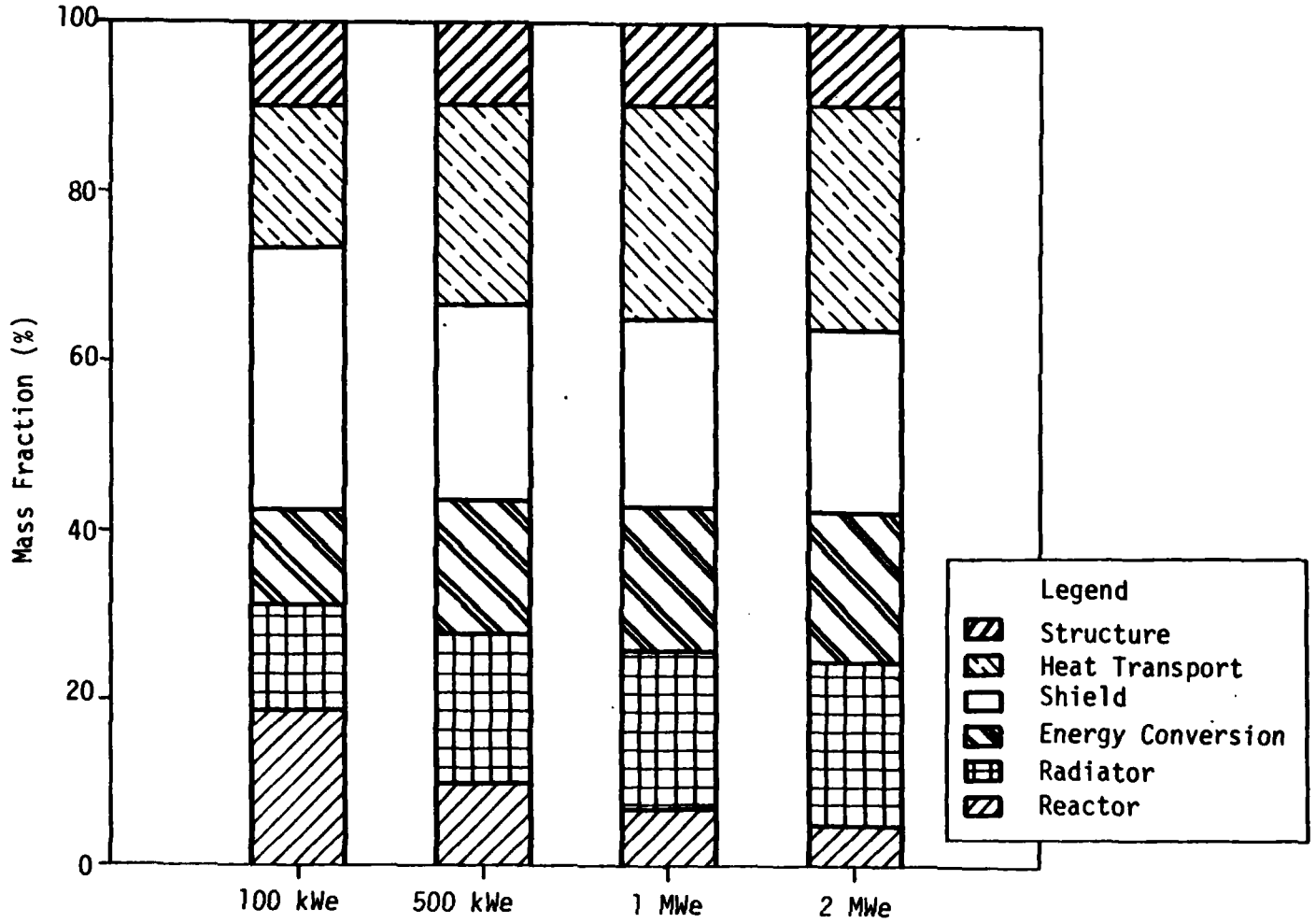

Figure 18. Mass fraction of subsystems (with system efficiency 7.1 percent).

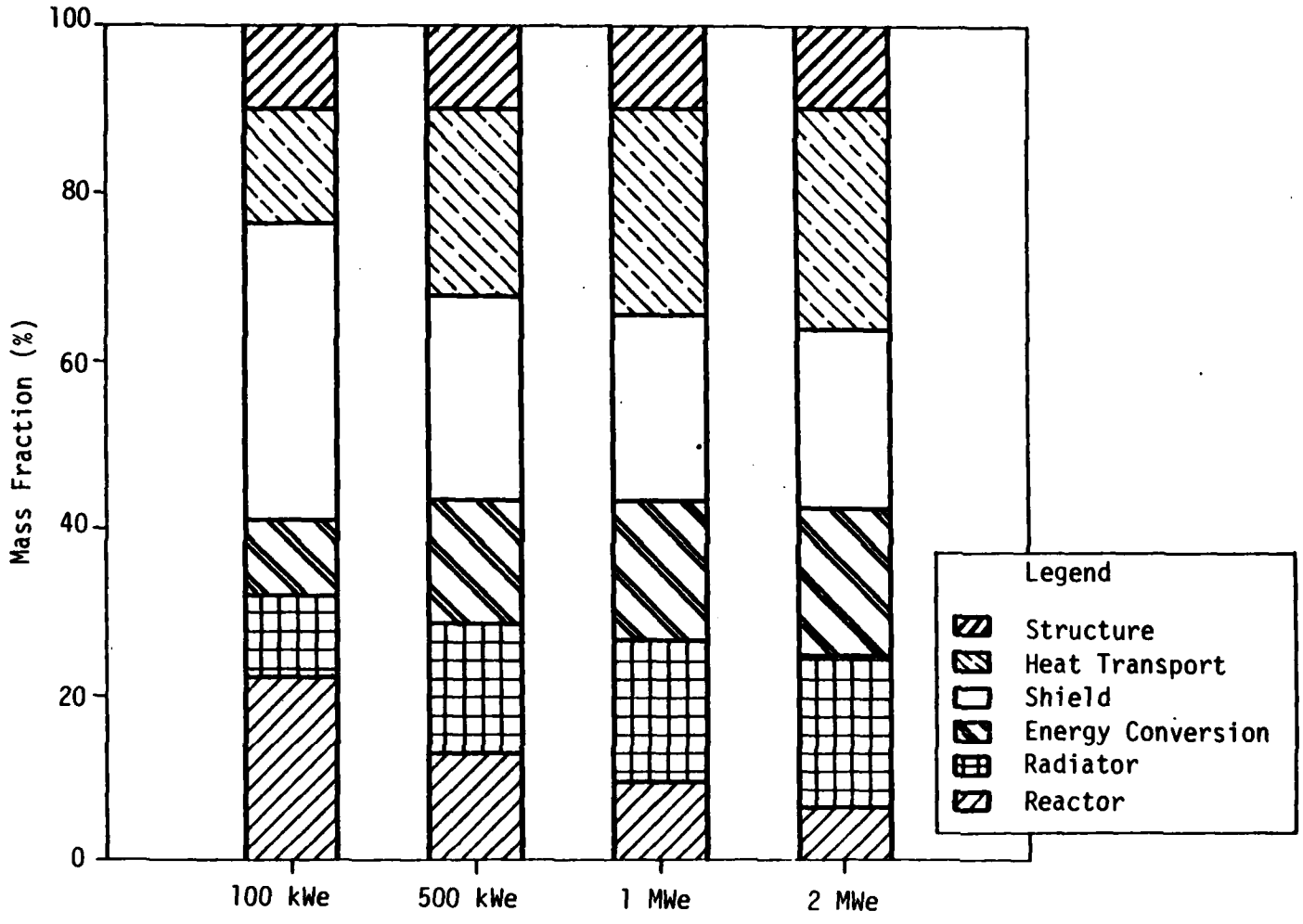

Figure 19. Mass fraction of subsystems (with system efficiency 12.0 percent).

The specific power of the system is plotted in Figure 20 as a function of electrical power output and the system efficiency. The increase in the specific power is significant in the 100 to 500 kWe region, and relatively slows at higher power. The specific mass, however, plotted in Figure 21, decreases rapidly with power in the 100 to 500 kWe power range, then it remains relatively constant with power.

7. SUMMARY AND CONCLUSIONS

As the calculations show, the linear size increase option for upgrading the power of the HPSNR baseline design would have numerous limitations:

(1) System mass is too large to be launched by a single space transportation system. Even if the system efficiency increases to 0.12, the total system mass will be more than 10,000 kg to generate 1 MW of electrical power.

(2) The UO_2 swelling during 7 yr of operation at 1500 K operating temperature and 1 MW of electrical power would be 22 to 16 percent with the system efficiencies of 6.2 and 12 percent, respectively. Even though this swelling could be reduced by constraining the pellet by cladding, the reduction would not be sufficient.

(3) The maximum core size would be limited by the reactivity available compared with the reactivity demand. Even in the case where the number of control drums increased proportionally to the core diameter, the maximum reactivity available would be less than the control requirement if the core diameter exceeds 60 cm.

The maximum power achievable without violating the system requirements are plotted in Figure 22. As this figure shows, the UO_2 swelling is the principal limiting factor for upgrading the power of the HPSNR system. Without violating the UO_2 fuel swelling limit (10 percent volume increase), the maximum achievable electrical power output is only 142 and 240 kWe for system efficiencies of 7.1 and 12 percent, respectively. However, by having the number of control drums proportionate to the core diameter, the power of the HPSNR system can be increased up to 920 kWe for a system efficiency of 7.1 percent. With a system efficiency of 12 percent the maximum power will be 1555 kWe. With a 3000 kg system mass limit the electrical power output cannot be increased by more than 122 and 216 kWe for system efficiencies of

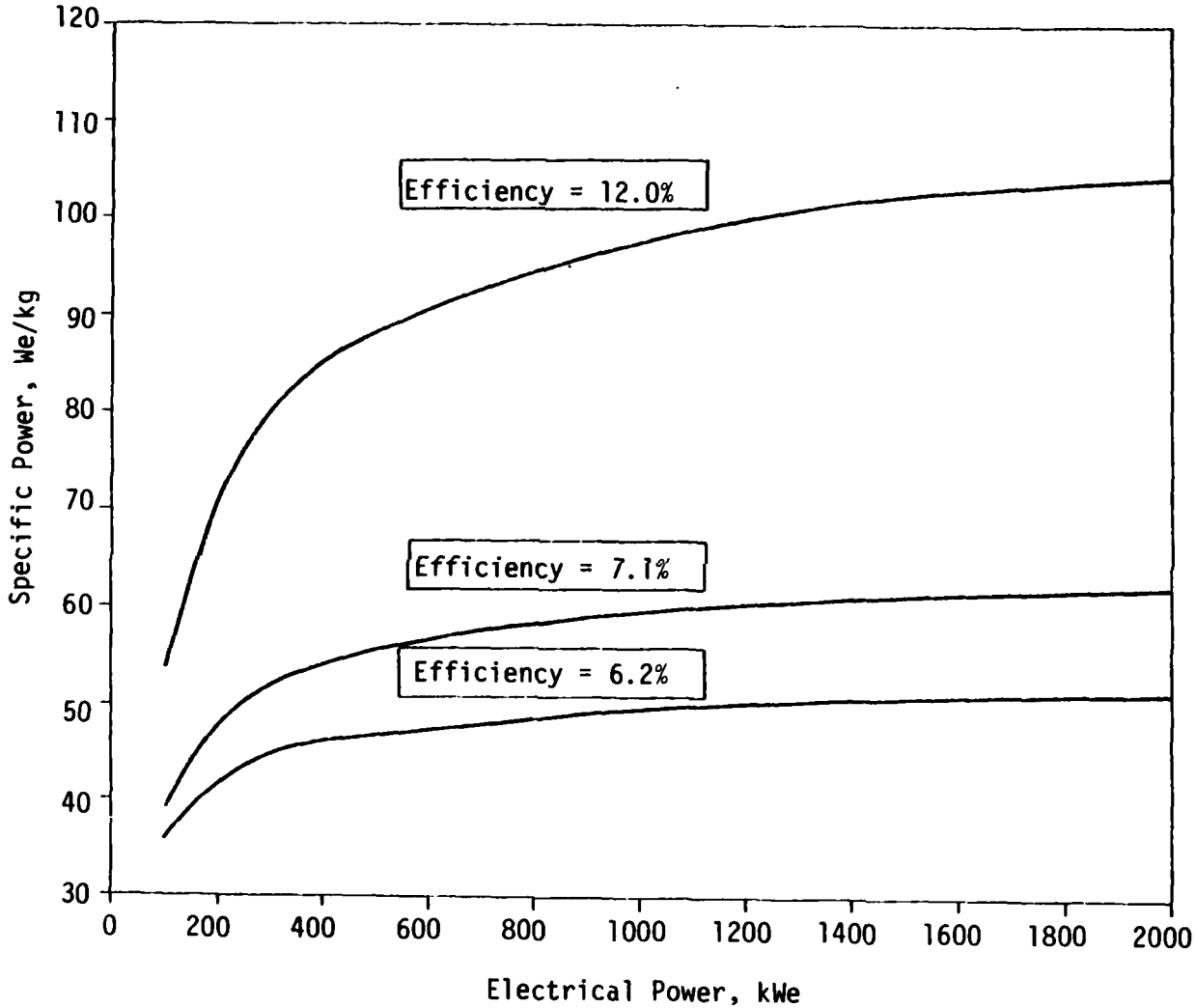

Figure 20. Specific power as a function of electrical power and system efficiency.

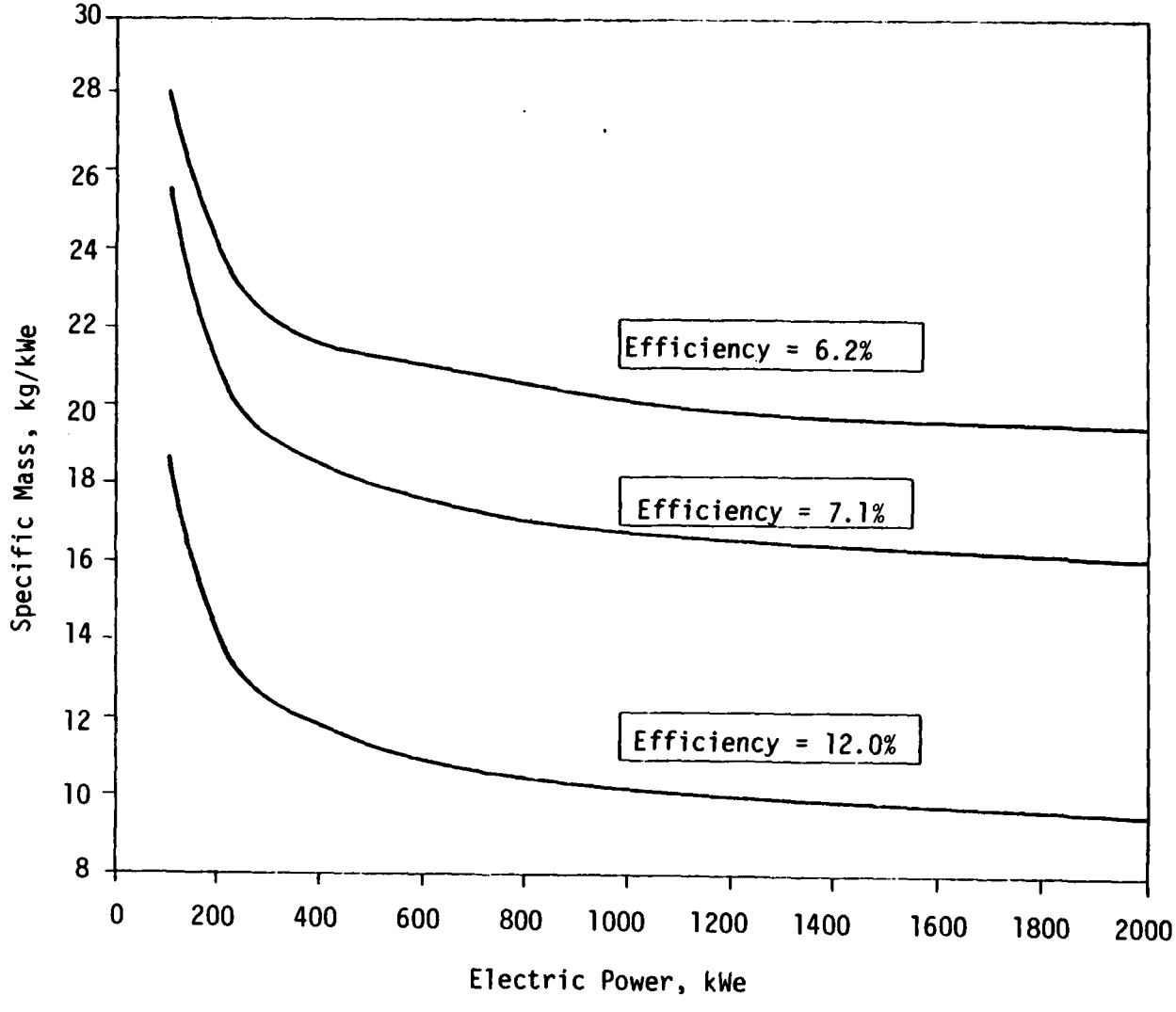

Figure 21. Specific mass as a function of electrical power and system efficiency.

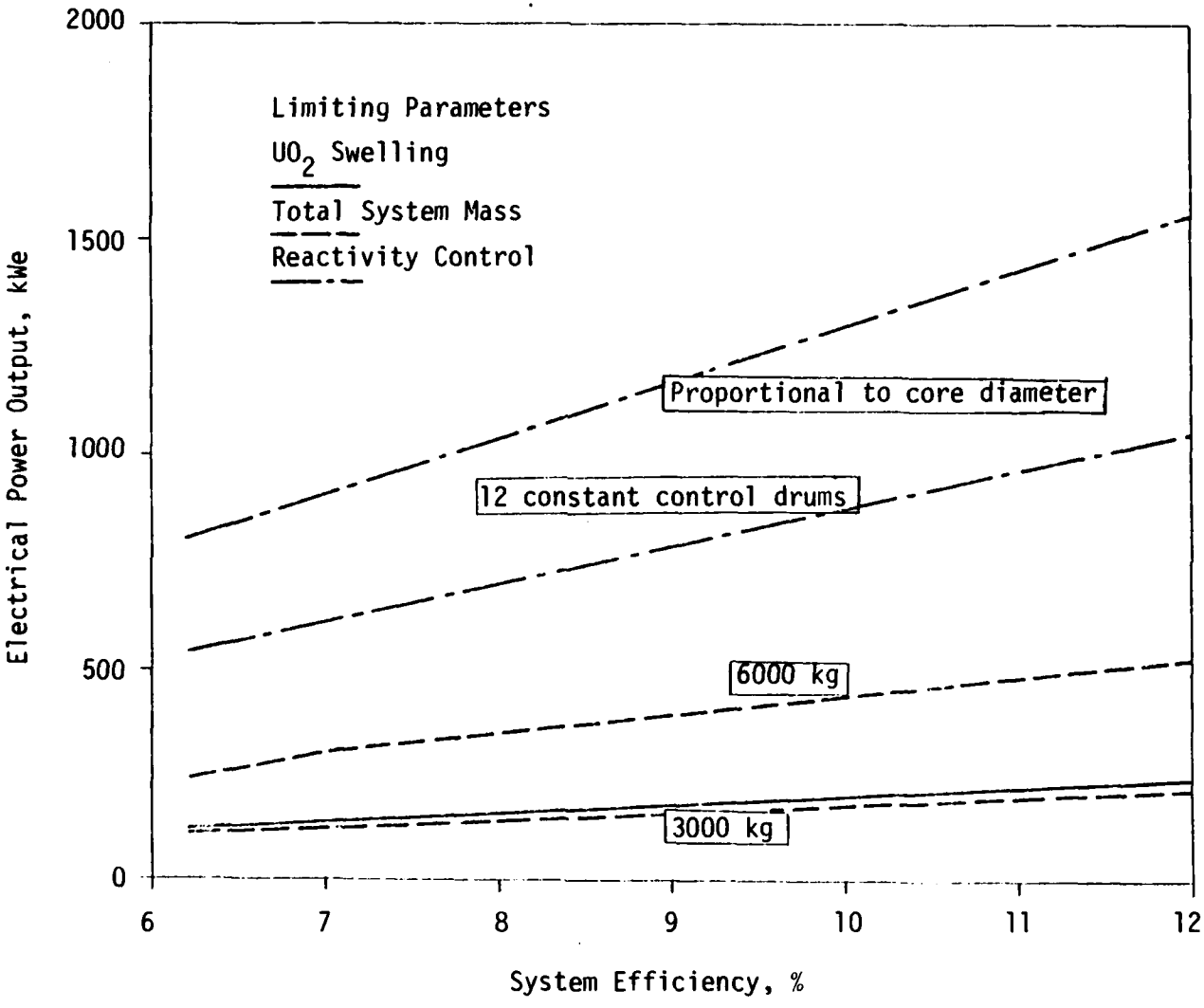

Figure 22. The maximum electrical power achievable.

7.1 and 12 percent, respectively. However, for a 6000 kg mass limit (twice as much as the baseline system mass limit), the electrical power output can be increased up to 313 and 524 kWe for system conversion efficiencies of 7.1 and 12 percent, respectively.

In conclusion, the power upgrade of the HPSNR system (several hundred kilowatts to a few megawatts) by increasing the size of the HPSNR baseline design is limited by several design factors. Other methods, however, can be used to overcome some of these limitations at higher power, for example;

(1) Use thermoelectric converters with improved efficiencies. This will subsequently reduce the problem of system overall mass and fuel swelling. By the year 1990, the highest TE conversion efficiency achievable will be about 13 percent with a figure-of-merit of 2.0×10^{-3}, a hot side temperature of 1350 K, and cold side temperature of 800 K.

(2) Use more efficient radiator concepts, such as dust and liquid droplet radiators, to reduce the radiator mass and size, and hence reduce the whole system mass and size.

(3) Use an energy conversion system concept with low specific mass, such as the free piston stirling engine and the Brayton cycle. This would increase system efficiency, reduce the mass of the energy conversion system, and reduce system overall mass and fuel swelling.

(4) Use a fuel system with low swelling. The UN fuel could be the best candidate fuel if the problem of nitrogen overpressurization can be overcome.

(5) Use an energy conversion system that is efficient at lower temperature (e.g. FPSE) to reduce fuel swelling.

(6) Use burnable poison or breeding concepts to provide a sufficient reactivity control margin in the reactor core.

IV. POWER UPGRADE BY IMPROVED HEAT REJECTION

As discussed in Section III, an improved heat rejection concept could increase the electrical power output and/or decrease the system size and mass. The heat rejection capability of a space nuclear power system can generally be improved either by raising the radiator temperature or increasing its surface area for heat rejection to space. These techniques would also help reduce the size and mass not only of the radiator but also of the whole space nuclear power system. However, the maximum radiator temperature is limited by: (1) the maximum fuel swelling during the life of the mission (~10 percent for 7-yr mission) which increases as the fuel operating temperature increases and (2) the figure-of-merit for the TE converters which depend on the temperature of the hot side as well as the temperature difference between the cold and hot side of the TE converters. Therefore, the actual temperature of the radiator would be constrained by these two design limitations.

Two radiator concepts currently being developed to improve the heat rejection capability of the radiator by increasing the heat rejection area are the dust radiator concept, and the liquid droplet radiator concept. However, although these concepts are theoretically possible, further development is required before they can be considered for space application. These two concepts are reviewed in the following two subsections.

1. DUST RADIATOR CONCEPT

The dust radiator uses small spherical particles (~240 μm in diameter) to carry the rejected heat from the energy conversion system and then radiate it to space. Small particles have a higher surface area-to-volume ratio than large particles. The dust particles (steel spheres) are heated in a container and projected into a stream that would be caught by another container. Then, the dust particles are recycled for reheating. The process is repeated to reject heat into space by the large surface area of the dust during its flight between the emitter and the collector. The required traveling distance of the particles in space must be short in order to minimize the material used. Figure 23 shows a conceptual design of a dust radiator that is being proposed for use in a space nuclear power system (Ref. 4).

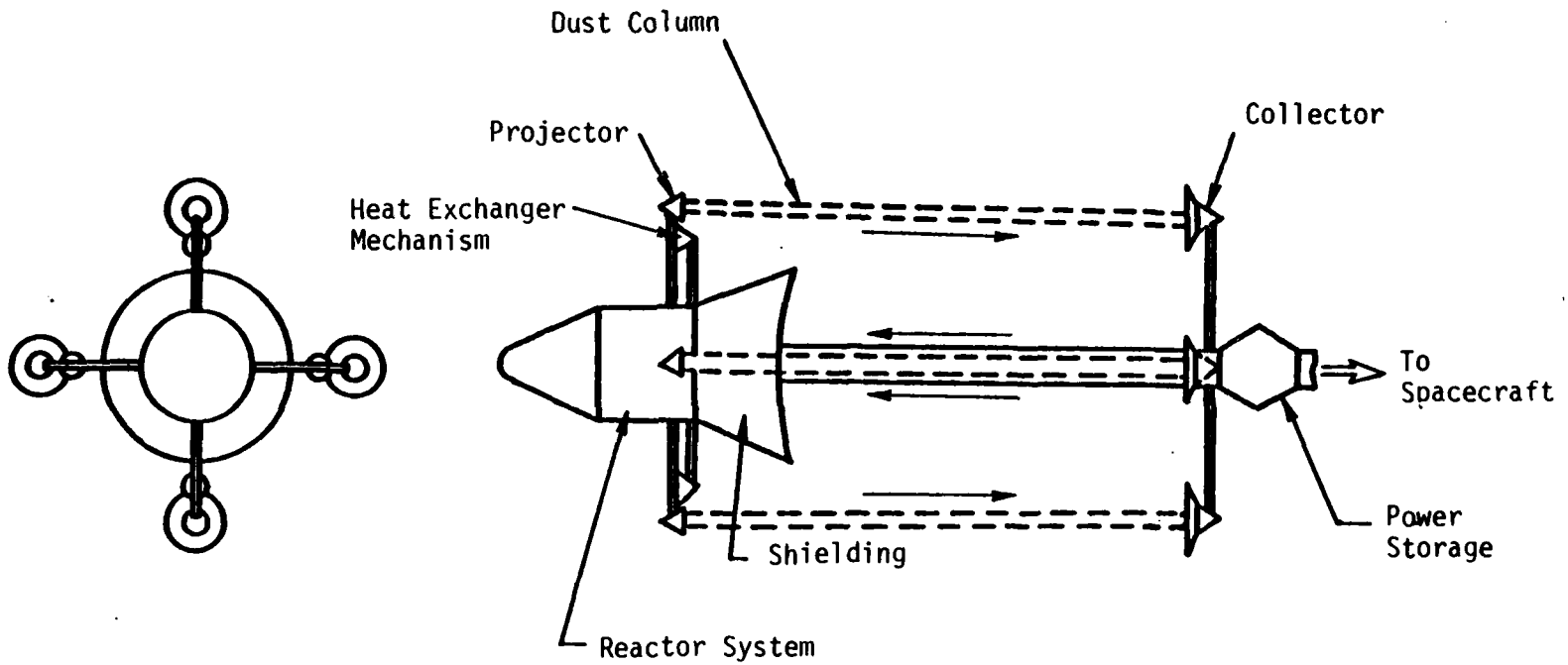

Figure 23. Schematic of a typical dust radiator for a space nuclear reactor system.

Based on an analysis done by Hedgepeth (Ref. 4), a 10 MW_{rj} radiated power dust radiator would require a 270-m long stream, 3.2-mm particle spacing, 2.5-mm particle diameter, and would have a specific mass of 64 kg/MW thermal rejected. Because of its relatively small mass penalty, the dust radiator offers significant advantage over the panel type radiator used in the HPSNR baseline design. As shown in the Figure 10, the panel type radiator mass at 10 MW_t of rejection power (which corresponds 0.76 MWe electrical power output with the system efficiency of 7.1 percent) would be ~2400 kg which is about four times the mass of an equivalent dust radiator.

Although the dust radiator concept seems technologically possible and offers a great advantage over the panel type radiator, there are still many heat transfer and engineering problems remaining, for example: how to recoat the particles in the container, how to keep particles from dispersing in the stream, and how to capture the stream in the next chamber. These problems must be solved before this concept can be incorporated successfully in future space nuclear power systems.

2. LIQUID DROPLET RADIATOR CONCEPT

The liquid droplet radiator uses liquid which absorbs the rejected heat from the energy conversion system. The hot liquid is then projected into space by the droplet generator in such a way that a thin conversing sheet or small droplets (~50 μm in diameter) flies toward the collector module (Ref. 5). During the flight between the droplet generator and the collector module, the liquid droplet radiates the heat into space. The droplet collector module is a rotating drum which forms a droplet stream into a continuous liquid by centrifugal acceleration. Pumps, spaced symmetrically around the periphery of the drum, pressurize the liquid to overcome the centrifugal force and provide the back pressure for the main heat exchanger pump. Figure 24 shows a conceptual design of a liquid droplet radiator for a space nuclear power system.

The liquid droplet radiator has advantages that are similar to those of the dust radiator. However, in addition to allowing heat transfer by conduction, the liquid droplet radiator is also easy to manipulate. The specific mass of the droplet system is 0.11 kg/m^2 while that of the panel type radiator is 5 kg/m^2 and the operating temperature (550-1000 K) is suitable for a high temperature rejection system (Ref. 5). An important problem

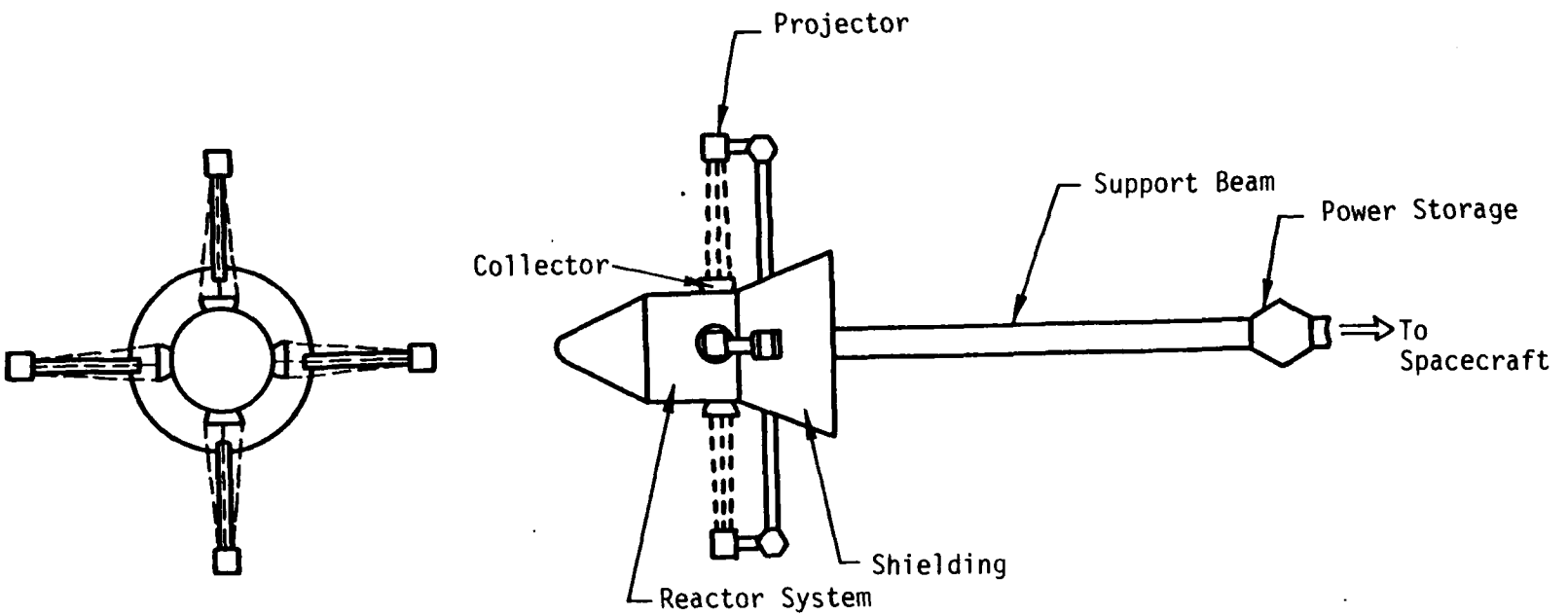

Figure 24. Schematic of a typical liquid droplet radiator for a space nuclear reactor system.

with the liquid droplet radiator concept is the evaporation losses of the working fluid while projecting the droplets into space. This would require extra liquid in the system to replace the quantity of liquid lost through evaporation. Other problems are the freezing of the liquid droplets during the flight in space and the increasingly low intrinsic emissivity of liquid metal.

3. SUMMARY AND CONCLUSIONS

Both the dust radiator and the liquid droplet radiator offer significantly low specific masses. However, both still have many technological problems with heat transfer, engineering, and material losses. Technological problems for the dust radiator concept involve transferring heat from the source to the dust and shortening the traveling distance of the solid particles in space to reduce the need for excess dust particles. One suggestion is to use a reverse concept of the Cyclone nuclear reactor for transferring heat from the primary fluid to the particles in a centrifugal force generator. Another suggestion is to use particles that can be magnetized. In this concept, when the particles are directed into space, after some traveling distance they will be attracted by a magnet on the spacecraft, forcing the particles to travel in a loop configuration.

Technological problems with the liquid droplet radiator concept involve preventing or reducing the evaporation losses of the liquid, preventing the freezing of liquid droplets, and increasing the emissivity of the liquid droplet. One suggestion is to allow the liquid droplet to freeze. For a given droplet initial temperature and heat rejection, the mean radiation temperature would be lower for nonfreezing than for freezing droplets. Thus, a shorter flight length would be needed for freezing droplets. To remelt these frozen droplets, however, a large inventory of liquid may be needed, which would increase the radiator specific mass when compared with the radiator mass used for nonfreezing droplets.

One suggestion for increasing the emissivity of the liquid droplet is to use a sheet configuration for the droplet stream. The sheet configuration can minimize the solar radiation absorbed by the stream by correct orientation. Another possibility for increasing the emissivity of a droplet sheet is to add a high emissivity powder to the surface of the droplet in order to increase the overall emissivity. The problem associated with this

technique is to make sure that the powder would remain on the periphery of the droplet and separate out upon collection.

Both the dust and the liquid droplet radiator concepts are promising for high power rejection systems because both can utilize the large surface area-to-volume ratio of small particles to reject waste heat.

V. POWER UPGRADE BY IMPROVED ENERGY CONVERSION

A total of six different thermal-to-electric energy conversion systems might be employed in space nuclear power applications. These systems can be categorized as follows:

(1) Passive systems, which include thermoelectric converters, thermionic conversion, and alkali metal thermoelectric converters and

(2) Active systems, which include the Rankine cycle, the Brayton cycle, and the free piston stirling engine.

To determine the suitability of any of these systems for space power generation, some key design factors should be taken into account, such as conversion efficiency, mass, size, reliability, operating temperature, lifetime, compatibility with other subsystems, and technology development. In the following subsections, these design factors for the various conversion systems are analyzed. The potential of each system for upgrading the power of the HPSNR system design is also discussed. A description of various energy conversion systems can be found in Appendix B.

1. PASSIVE SYSTEMS

The passive thermal-to-electric energy conversion systems are characterized by the electricity produced by atomic processes. Usually these systems have low conversion efficiencies. For applications in space, particularly for long life missions (3-7 yr), the passive conversion systems have major advantages because of their technology readiness and high redundancy characteristics. Lack of moving parts makes these systems highly redundant. In the following subsections, the passive systems (TE, in-core TI, and AMTEC conversion systems) are discussed.

a. Thermoelectric conversion system--The operation of a thermoelectric converter depends mainly on the Seebeck effect. A potential is produced in a circuit of two dissimilar materials if the two junctions are maintained at different temperatures. Therefore, the conversion efficiency (η) of the thermoelectric conversion system is a function of the operating temperature difference between the hot and cold sides, and the material properties (figure-of-merit) as shown in Equation 11.

$$\eta = \frac{T_h - T_c}{T_h} \left\{ \frac{\sqrt{1 + z\,T_{av}} - 1}{\sqrt{1 + z\,T_{av}} + \frac{T_c}{T_h}} \right\} \qquad (11)$$

where,

T_h = hot side temperature

T_c = cold side temperature

T_{av} = average temperature

z = figure-of-merit

The TE conversion system is extremely simple. A nuclear reactor core could be cooled either by heat pipes or by a liquid metal coolant system. The heat is transferred to the energy conversion system and then to the radiator where it is rejected to space. The TE modules are situated between the hot side of the radiator (the reactor side) and the cold side (space side) of the radiator. Figure 25 shows the TE converters in the HPSNR with a brief description of the system components.

The TE conversion system is well developed and holds much promise as a near term candidate for space energy conversion. The prime advantage of the TE system is its lack of moving parts. Additionally, the system's flight experience has proven that it is reliable for continuous operation for up to 10 yr (Ref. 13). However, this flight experience has been restricted to the radioisotope thermoelectric generators (RTGs) which have used telluride as a base TE material. For the high temperatures (~1500-1700 K) desired in a nuclear reactor power system. Silicon-germanium could be used since it does not sublimate at higher temperatures as does telluride. Figure 26 shows the variation of figure-of-merit with temperatures for various TE materials. Compared to other conversion systems, TE conversion has an average specific weight (35 kg/kWe) and an above average specific area (0.93 m^2/kWe) (Ref. 10). These factors make the TE system an attractive choice for space applications.

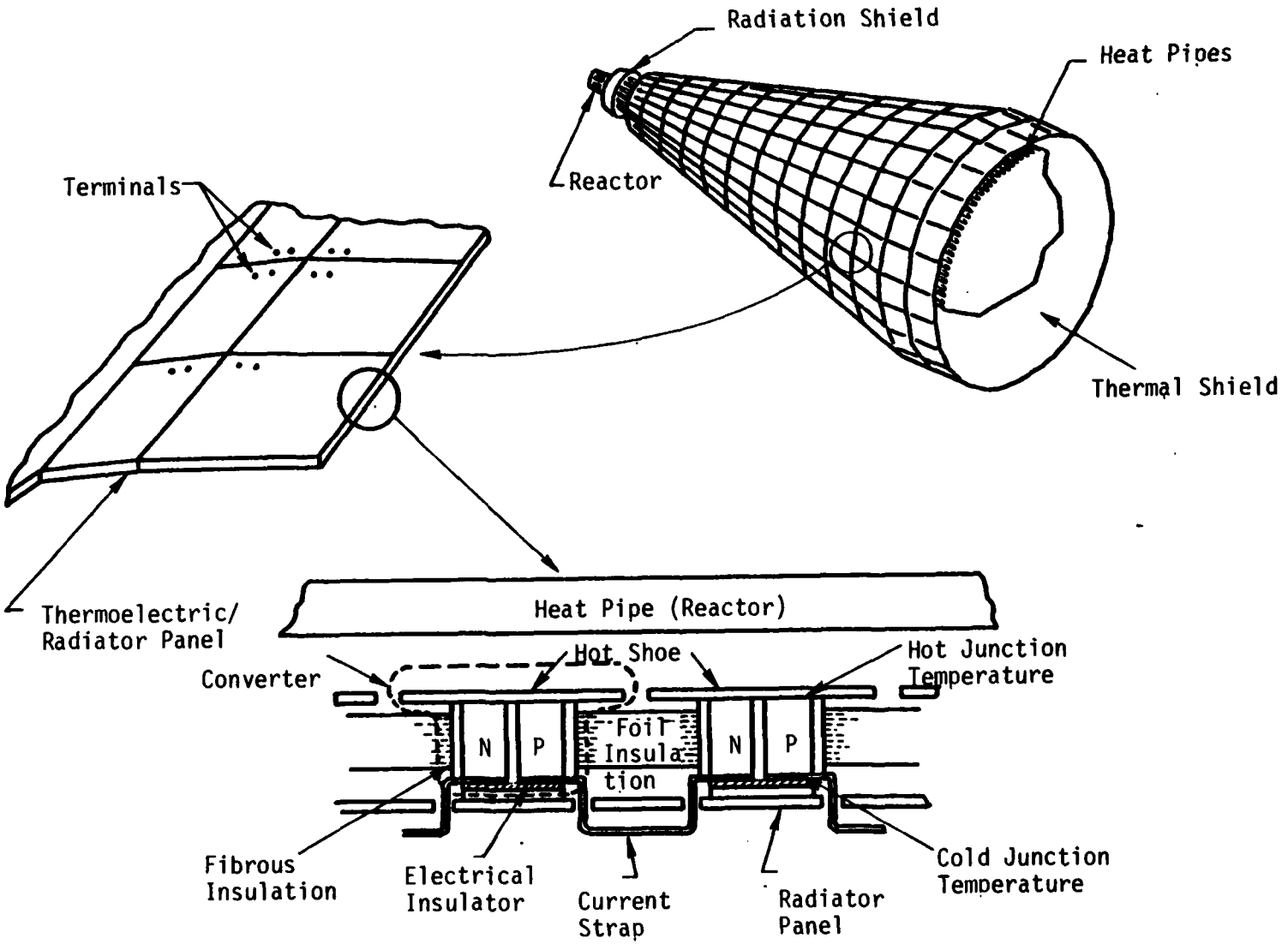

Figure 25. TE converters in the HPSNR.

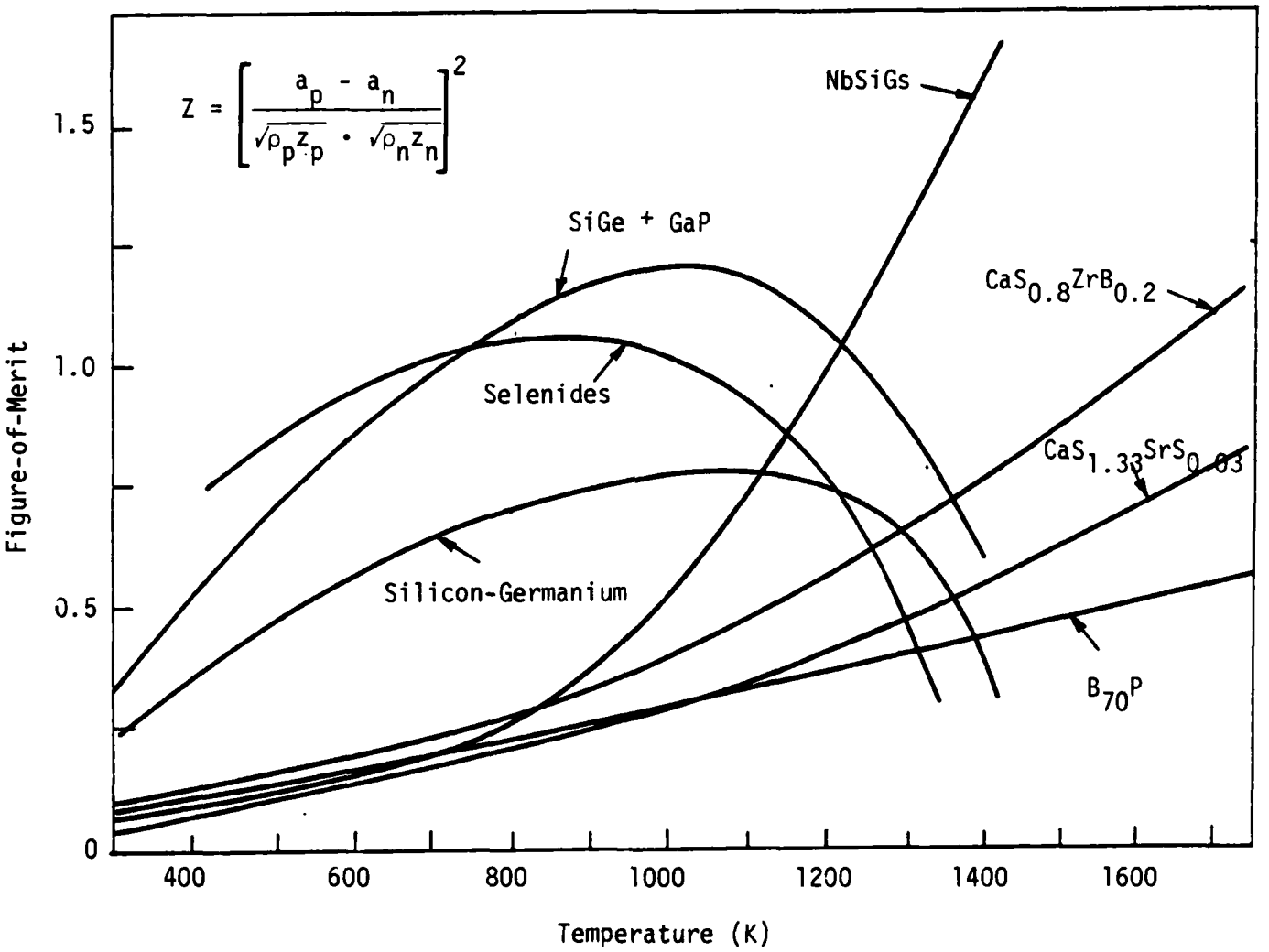

Figure 26. Figure of merit.

One major disadvantage of the TE system, however, is its low conversion efficiency (currently less than 7 percent). This means that large reactors would be needed for higher power levels (several hundred kilowatts to a few megawatts). Although the design and uniform fabrication of each TE module might be a problem, improved performance could be achieved by using semiconductor materials with higher figure-of-merit. By the 1990s, the objective is to obtain an improved efficiency of about 12 percent with a figure-of-merit of 2.0×10^{-3} for TE converters.

b. Thermionic conversion system--The thermionic conversion system is composed of an emitter or cathode, which surrounds the fuel column from which it receives heat and emits electrons, and a collector or anode which collects the electrons. The collector is cooled to limit the back emission of electrons. Additionally, most TI designs use a cesium plasma or vapor between the two plates in order to drop the barrier energies (or work function); cesium itself, has a low work function. However, the addition of cesium causes some electron losses due to arc dropping and electron scattering (Ref. 13). Figure 27 shows schematic of the in-core thermionic fuel element (TFE) and the TFE component functions (Ref. 16). The rate of electron emission from a hot metal surface is a function of both the metal temperature and the electrostatic energy barrier that the emitted electrons must overcome. The conversion efficiency can be calculated by:

$$\eta = \frac{0.9\ J\ V_o}{1.1\ P_{in}} \qquad (12)$$

where,

$0.9\ J$ = electric current flow attenuated by joule heating, A,

P_{in} = thermal power input , W,

V_o = output voltage, $V \sim (\psi - \phi_c - V_d)$,

ψ = effective barrier height, eV,

ϕ_c = collector work function, eV,

V_d = arc drop, eV.

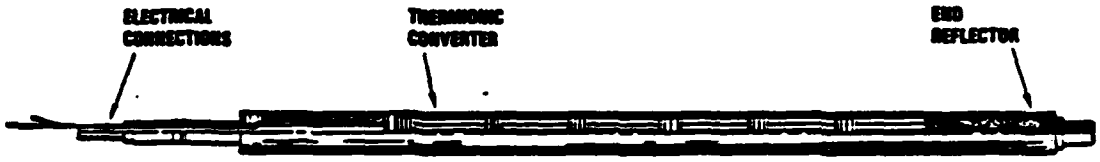

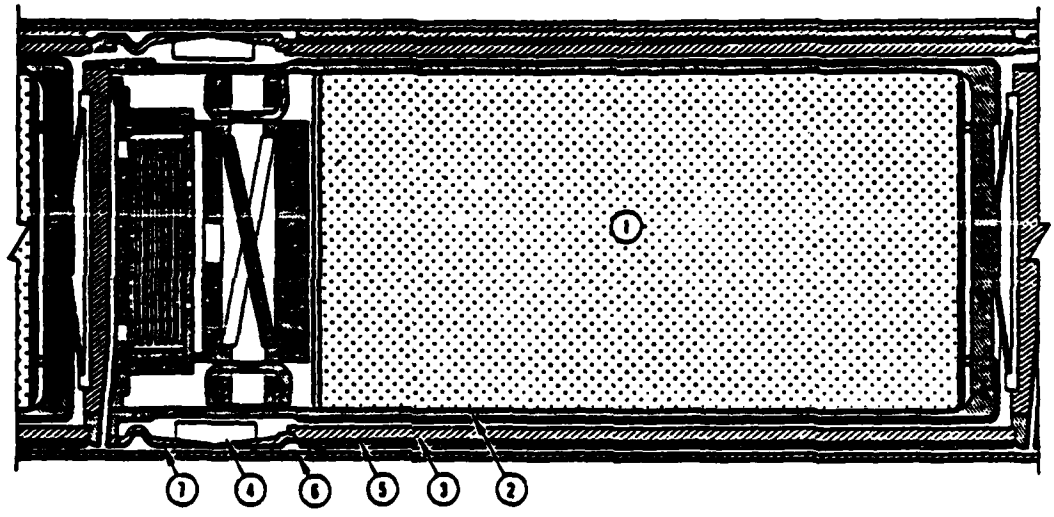

COMPONENT	PRIMARY FUNCTION	SECONDARY FUNCTION
(1) FUEL (URANIUM OXIDE)	FISSION	CONDUCT HEAT TO EMITTER/RELEASE FISSION GAS
(2) EMITTER (TUNGSTEN)	EMIT ELECTRONS	CONTAIN & RESTRAIN FUEL/CONDUCT HEAT & ELECTRICITY/SEPARATE CESIUM & FISSION GAS (F.G.)
(3) COLLECTOR (NIOBIUM)	COLLECT ELECTRONS	CONDUCT HEAT AND ELECTRICITY/SEPARATE Cs & F.G.
(4) INSULATOR SEAL (ALUMINA/NIOBIUM)	SEPARATE Cs & F.G.	ELECTRICALLY INSULATE EMITTER AND COLLECTOR
(5) SHEATH INSULATOR (ALUMINA/NIOBIUM)	ELECT. INSULATE CONVERTERS	CONDUCT HEAT
(6) SHEATH (NIOBIUM–1% ZIRCONIUM)	ISOLATE CONVERTERS & NaK (PHYSICALLY)	ALIGN EMITTERS & COLLECTORS
(7) INSULATION COATING (ALUMINA)	ISOLATE CONVERTERS FROM SHEATH FOLLOWING Cs ENVELOPE LEAK (ELECTRICALLY)	

Figure 27. In-core thermionic fuel element.

A TI system has many advantages. It has both a low specific area (0.86 m^2/kWe) and low specific weight (35 kg/kWe). The high emitter temperature results in conversion efficiencies of about 10-15 percent (Ref. 13). The TI system is also simple, is highly reliable, and has no moving parts. Additionally, redundancy is easily accomplished by incorporating extra TI modules. Current system designs have subsystems which are within existing material data bases.

Disadvantages of the TI conversion system are the relatively low conversion efficiency, the high operating temperature of the core (~2000 K), and material difficulties at such high operating temperatures. In-core thermionic fuel elements are continuously undergoing irradiation at high temperatures. Therefore, a key area for technological development is improving the converter lifetime of in-core thermionic. This will require more research in high temperature materials to ensure that they are compatible for along and reliable lifetime.

c. Alkali metal thermoelectric conversion system--The theory behind the AMTEC is to use the electrochemical permselective barrier material β"-alumina. This material has an electric conductivity that is much less than its ionic conductivity and acts as a straw sucking sodium ions (Na^+) from high temperature liquid sodium reservoir to a low pressure sodium vapor reservoir (Ref. 9). Electrodes are inserted into the low pressure reservoir and act as collectors of migration Na^+ ions. Electrons flow in the opposite direction of the Na^+ and as they meet the Na^+ ions, the latent heat of vaporization of the sodium is released and the Na vapor is condensed on a condenser plate. This condensed sodium is then pumped to the reactor core where it is heated and returned to the high temperature reservoir. Figure 28 shows a schematic of an AMTEC operation. The efficiency of AMTEC is calculated by:

$$\eta = \frac{IV}{IV + \frac{I}{F}(L + C\,\Delta T) + Q_{loss}} \qquad (13)$$

where,

I = total current flow, A

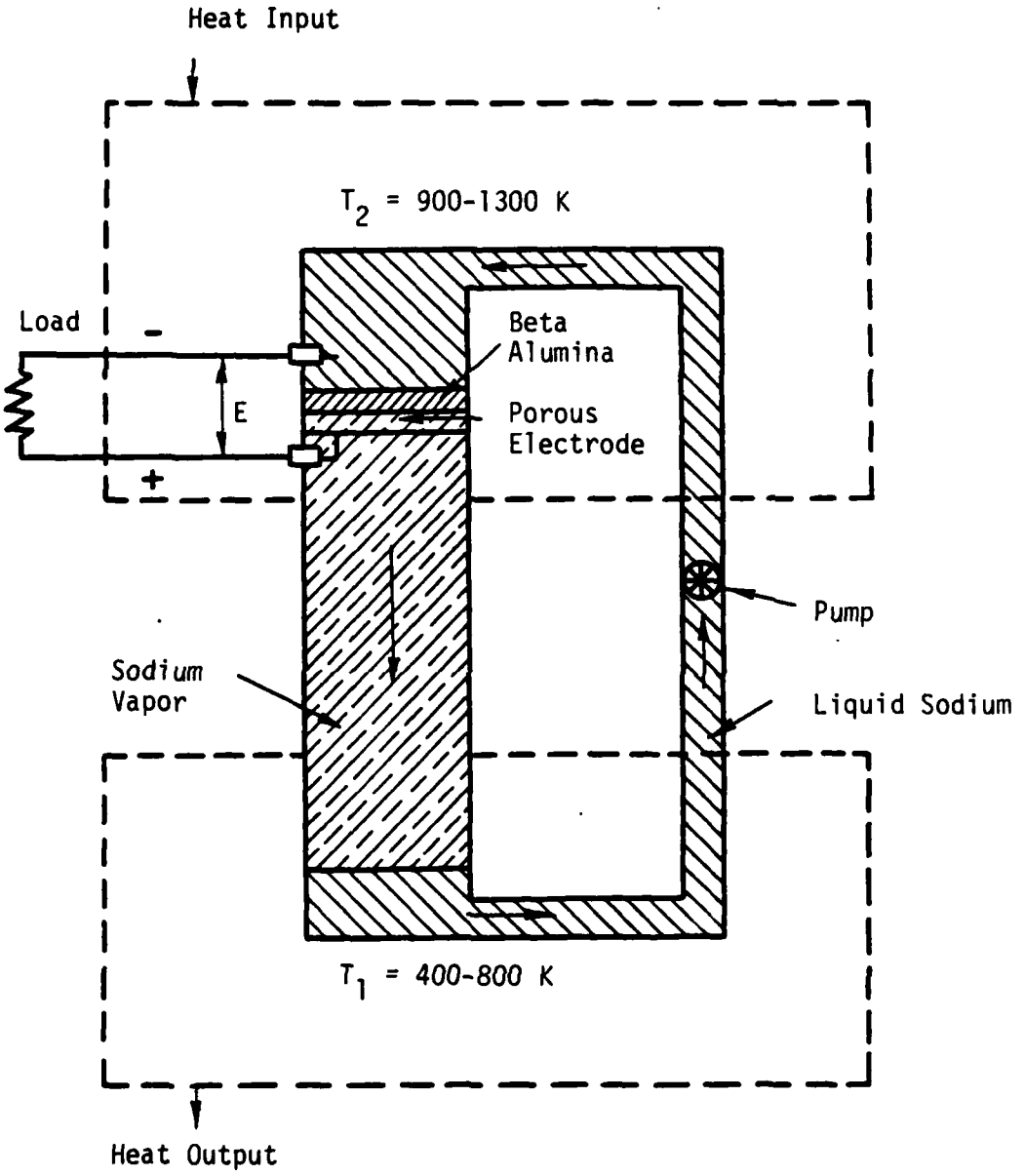

Figure 28. Schematic of an AMTEC operation.

V = total voltage

F = Faraday's constant

L = latent heat of vaporization

C = sodium liquid specific heat

ΔT = sodium temperature difference

Q_{loss} = all parasitic heat loss

Although the AMTEC is the least developed technology, it is very promising. It is simple, reliable and easily redundant. It has one of the lowest specific areas, (0.43 m^2/kWe) of any of the conversion systems (Ref. 10) and its efficiency is high, in the order of 14-23 percent (Ref. 9).

The major block to AMTEC's deployment is its relatively little experience outside the laboratory. Other disadvantages are that during continuous operation, the power level decreases because sintering decreases the porosity of the electrodes. Condensation in zero gravity must also be overcome. Fabrication technology also needs to be developed in order to assure module hermeticity (Ref. 9).

2. ACTIVE SYSTEMS

The active thermal-to-electric energy conversion systems are characterized by the use of working fluid which is vaporized or heated to a superheated stage and then used to turn a turbine and/or alternator. Therefore, these systems use dynamic components to convert thermal energy to electrical energy. The high efficiency and low specific mass (for large systems) are the common advantages of these active systems. In following subsections, the Rankine and Brayton cycles and the free piston stirling engine are discussed.

a. Rankine cycle--The Rankine cycle uses a nuclear reactor and/or heat exchanger to boil the working fluid. The working fluid is converted to a superheated vapor which expands through a turbine. The turbine is linked to an alternator which generates usable electric power. The expanded vapor is

then condensed by condensor, which is linked by another liquid metal loop to the radiator. Liquid metals (e.g., Na, NaK, Li, Hg, ..., etc.) used in the Rankine cycle have the advantage of operating at high temperatures because they have high boiling temperatures. They also have wide liquid phase ranges and high heat transfer capability at low pressures. Organic fluids could be used at low temperatures because they tend to thermally decompose at high temperatures; thereby requiring a large radiator. The organic cycle has a high reliability due to its low operating temperature, low operating pressure, and low turbine speed. If the working fluid is liquid metal, electromagnetic pumps can be used as circulators. If organic liquid is used, a conventional pumping system should be incorporated. Figure 29 shows the basic Rankine cycle and its T-S diagram. The efficiency of the system is calculated by:

$$\eta = \frac{\eta_{alt.}\eta_{turb.}\delta H_{turb.}(1 - f_{in})}{\Delta H_{total}} \qquad (14)$$

where,

η_{alt} = alternator efficiency (~0.95)

η_{turb} = turbine efficiency (~0.81)

f_{in} = fraction of internal power requirements (~0.125)

ΔH_{turb} = isentropic turbine work

ΔH_{total} = total heat input from reactor

In general, the Rankine cycle is characterized by a high heat rejection temperature (800-925 K); hence, it has a relatively smaller radiator size, high cycle efficiency (~30 percent), and demonstrated technology (Ref. 18). Additionally, there is considerable operational experience with Rankine cycles because they have been widely used commercially. Rankine cycles have also been designed, built and tested for space operation (Ref. 13). However, there are several critical technological areas that need further investigation. The technology must be developed to adequately demonstrate that the

Basic Rankine Cycle (Ideal)

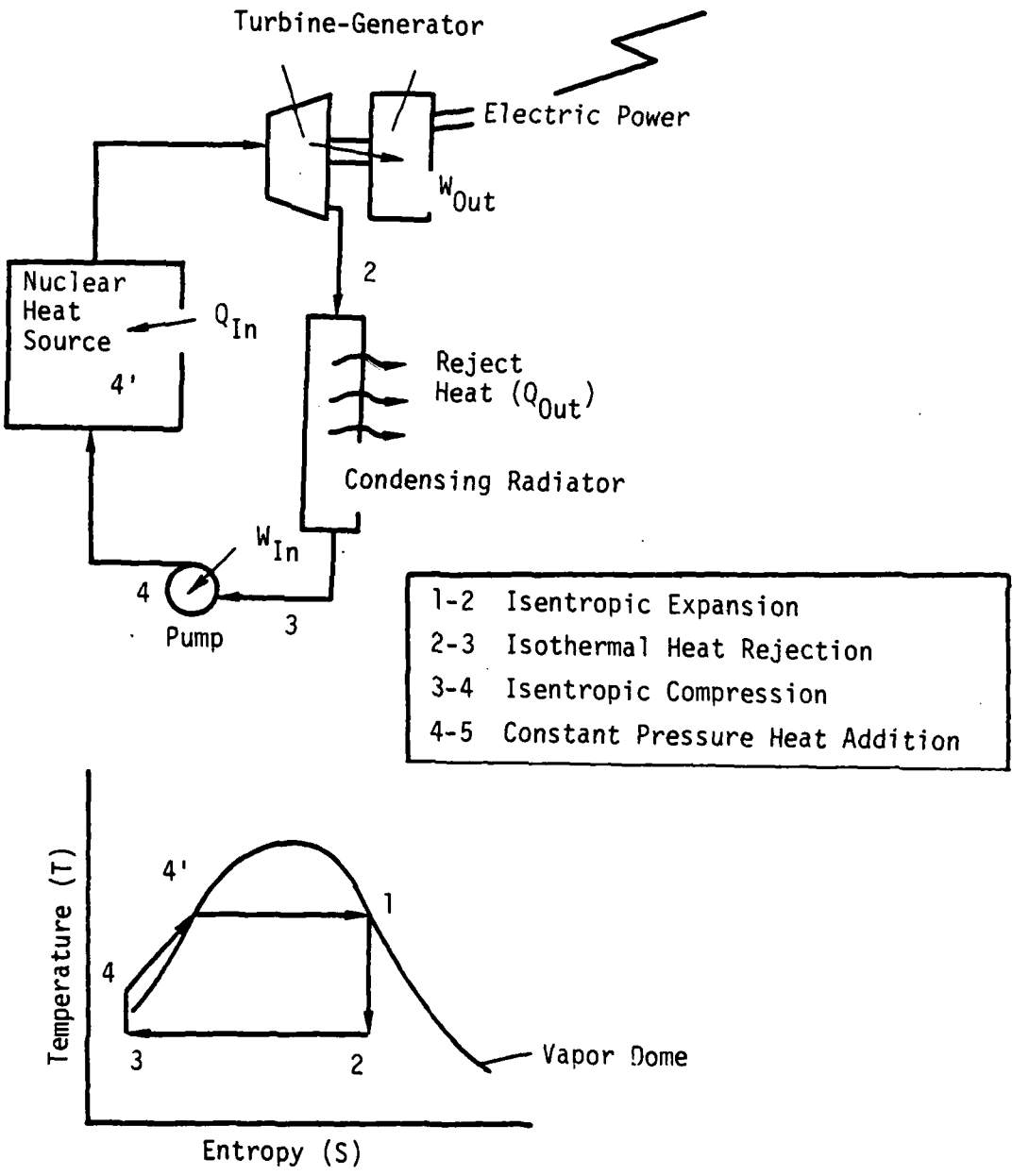

Figure 29. Rankine cycle and T-S diagram.

turbine-alternator unit can operate for a long lifetime (3-7 yr). Of particular importance, are the seals and bearings, which must operate reliably for up to 10 yr. A method of controlling the condensate near the turbine exit needs to be developed to minimize the turbine blade erosion. Certain problems need to be addressed, such as the zero gravity separation of the two phases in the condenser unit. The liquid metals become extremely corrosive in turbines if anything but pure vapor comes in contact with the blades. Another critical area needing development is the start-up and restart capabilities of liquid metal system.

b. Brayton cycle--The Brayton cycle is closed, inert gas cycle. The inert gas will probably be helium-xenon because it is noncorrosive and has an optimizable molecular weight (Ref. 13). The inert gas is heated by the nuclear heat source, either directly or through a heat exchanger. This high temperature, high pressure gas is then expanded in a turbine-alternator unit. The turbine rotating power turns a compressor which compresses the gas and an alternator to generate electricity. After the gas is cooled by a space radiator and compressed in the rotating compressor, it then enters the nuclear heat source to complete the cycle. Figure 30 shows an ideal Brayton cycle block diagram and its T-S diagram. The efficiency of the system can be calculated by:

$$\eta = \frac{(T_1 - T_2) - (T_4 - T_3)}{T_1 - T_5} \qquad (15)$$

where,

T_1 = turbine inlet temperature, K

T_2 = turbine outlet temperature, K

T_3 = compressor inlet temperature, K

T_4 = compressor outlet temperature, K

T_5 = recuperator outlet and cold pass temperature, K

Closed Brayton Cycle (Ideal)

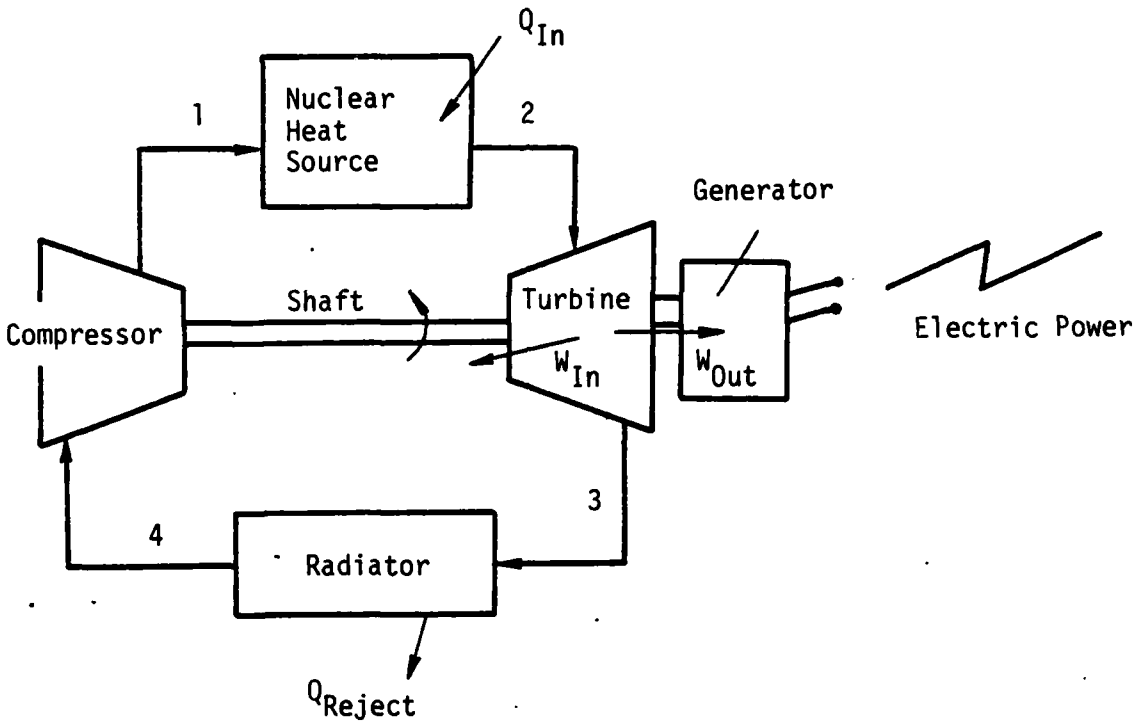

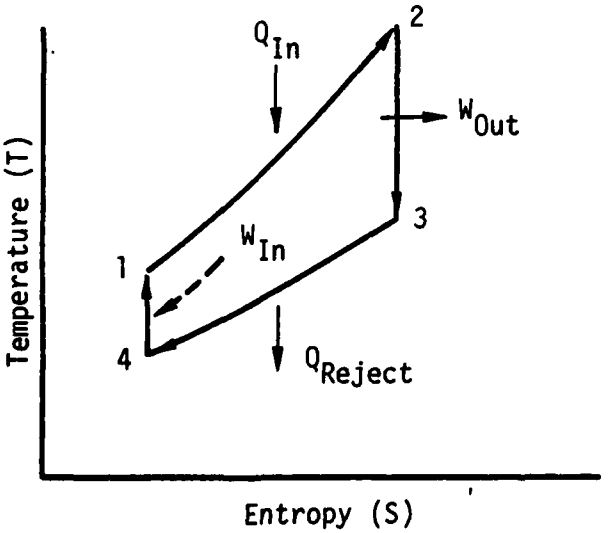

1-2 Constant Pressure Heat Addition

2-3 Isentropic Expansion

3-4 Constant Pressure Heat Rejection

4-1 Isentropic Compression

Figure 30. Brayton cycle and T-S diagram.

The Brayton cycle uses a high temperature working substance, which leads to a high energy conversion efficiency (34-37 percent). Another advantage is the extensive technology and experience available in this area. Much design and testing knowledge already exists in the electric power range of a few kilowatts to tens of megawatts (Ref. 19).

However, accompanying these advantages are the material problems associated with the limited creep allowed in the turbine blades. It is hoped that ceramic turbines capable of operating at 2000 K can be developed by 1990 (Ref. 13). Another area needing more research is determining whether a combined rotating unit with gas bearings can reliably operate for long periods of time with a turbine inlet temperature of 1500 K.

c. Free piston stirling engine--The FPSE is a thermal-to-mechanical-to-electrical energy conversion machine. The mechanical-to-electrical conversion is accomplished by a linear alternator. the thermal-to-mechanical portion of the engine is a bit more complicated but is accomplished by using the damped oscillation of two opposing pistons. One piston is the displacer piston and the other is a power piston. Both use an engine working fluid such as helium. This fluid is heated and cooled by a special heat exchanger, which is linked to the reactor coolant and radiator. The exchanger contains three sections linked together--a heater section, a storage section, and a cooler section. The gas travels from the heater through the storage section and on to the cooler and then in reverse. Figure 31 shows a diagram of FPSE and its operational principles. The efficiency of the FPSE is complicated and no single formula is available for its estimate; however, Ewell (Ref. 9) has estimated conversion efficiency on the order of 30 percent.

Although the FPSE is the least developed of the dynamic conversion systems, it promises high efficiency and low mass with a high heat rejection temperature, hence it will require a small radiator. The FPSE is also mechanically simple and has a high thermodynamic, electrical, and mechanical performance. This is because only two moving parts exist--the piston with its attached alternator component and the displacer. The FPSE has one of the smallest specific masses (29 kg/kWe) of any of the conversion systems. In addition, the specific radiator area (0.55 m^2 kWe) is thought to be only greater than those of the AMTEC and Rankine cycles. High performance, long life, and low vibration are expected for the FPSE.

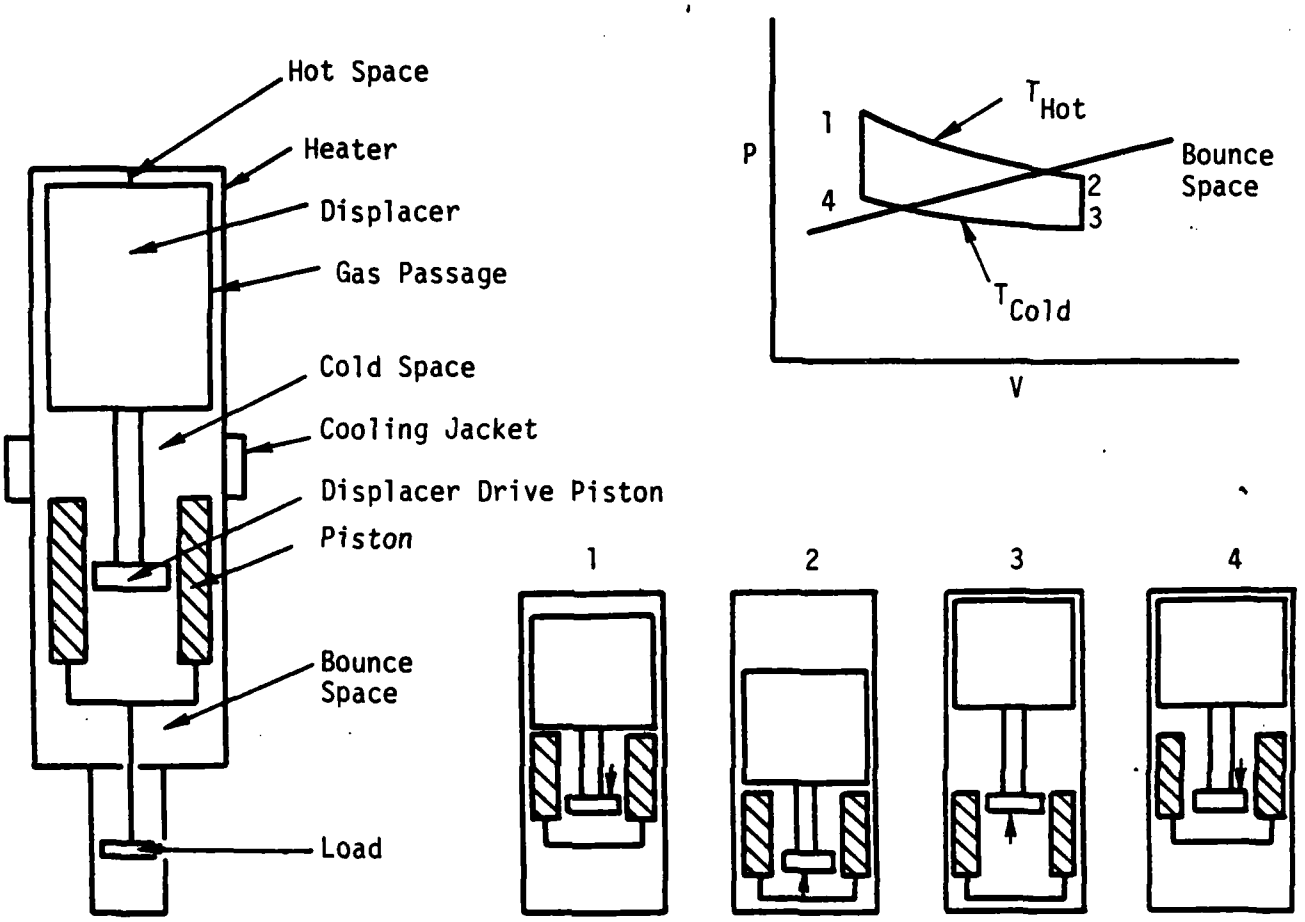

1-2 Piston expands working gas: displacer on piston.

2-3 Pressure in bounce space greater than pressure in working space. Forcing displacer toward hot space, working gas moved into cooled space, pressure drops.

3-4 Piston driven into working space by higher bounce space pressure.

4-1 Displacer driven toward cold space by working space pressure higher than bounce space pressure.

Figure 31. Schematic of a FPSE operation.

A disadvantage of the FPSE is the need for extended heat transfer surfaces to bring about isothermalization of the expansion and compression spaces. Regenerator problems also exist, as well as the availability of high temperature compatible materials. One serious question that must be addressed by research is whether the machine can be balanced in a zero gravity environment. Additionally, the alternator must be cooled below the heat sink temperature (Ref. 20). A liquid metal intermediate loop must be used instead of a large volume, direct gas cooled concept.

3. APPLICATION TO THE HPSNR SYSTEM POWER UPGRADE

The various thermal-to-electric energy conversion systems, discussed in the previous section, are summarized in Table 5. A wide range of technological readiness is found when the passive systems are compared. The TE conversion technology is attractive for immediate space applications because it is already developed and has been tested, while the AMTEC is essentially still in the laboratory stages. The AMTEC is also less attractive because its specific mass is too high to upgrade the HPSNR system's power. Consequently, only the TE and TI systems can be considered for the HPSNR system power upgrade. Both of these systems interface easily with the heat pipe reactor and both have similar specific masses and specific areas. As Table 5 indicates, the efficiency of the TI conversion system is 11-16 percent but only 7-12 percent for the TE converters. However, the TE conversion is still more attractive because of a more readily available technological base. For example, the high temperature of the in-core TI element will necessitate using advanced fuel materials as well as developing alternative nuclear fuel designs before an efficient, long-lived TI device can be built. It is anticipated that the development costs for such a device for near term use would be prohibitive (Ref. 13). Because of these factors, the TE conversion system appears to be the better conversion system for near space nuclear power production. However, by the late 1990s, the TI conversion system may be more attractive. The AMTEC conversion system may also be effective, provided it continues to be developed, because of its high efficiency and low specific area.

TABLE 5. THERMAL-TO-ELECTRIC CONVERSION SYSTEMS

System	Basic Process	Technology Readiness	Thermal Efficiency[a]	Temp. (K) Inlet	Temp. (K) Outlet	Specific Mass (kg/kW)	Specific Area (m^2/kW)
TE	Direct conversion	Best	7-12	1350	850	35	0.93
TI	Direct conversion	Good	11-16	2000	950	35	0.86
AMTEC	Direct conversion	Lab	14-23	1280	660	47	0.43
Rankine	2 phase lq-vp cyl.	O.K.	19-21	1400	900	34	0.42
Brayton	1 phase gas cycle	Good	34-37	1625	500	33	1.30
FPSE[b]	1 phase gas cycle	Lab	30	1325	700	29	0.55

[a]The efficiency range was calculated for both near term and advanced technology levels.

[b]FPSE was sized for only one system based on the preliminary data available.

The choice for an active conversion system is between the Rankine and Brayton cycles, and the FPSE. All three systems have high efficiencies and are suited for high power space nuclear systems (multimegawatts electric). Specific mass of the FPSE is the smallest while specific masses of the Rankine and Brayton cycle are comparable. The liquid metal Rankine cycle specific area is the smallest of the active systems with Brayton cycle being the largest. Additionally, all three systems can easily be linked to the heat pipe reactor. Although the FPSE is the simplest and most reliable, it also is the least developed. The Brayton cycle is well developed, but its moving parts require large amounts of proven redundancy. Rankine cycle has an additional problem of a two-phase flow separation in a zero gravity or subgravity environment. If the Rankine cycle were to be used, a liquid metal working fluid would be superior to an organic fluid. Based on these criteria, the Brayton cycle was chosen as the near future energy conversion system for high electric power systems (1-10 MWe). The FPSE was eliminated because it is not sufficiently developed and the Rankine cycle was rejected because it still requires more development for space application than the Brayton cycle. Additionally, the redundancy is also easier for a Brayton system. On the other hand, at such high power levels Rankine system could

still be an attractive alternative because it would require less radiator surface for rejecting the same amount of waste heat to space. The FPSE was the choice for the far future system because of its superior overall characteristics.

When the suitability of the thermoelectric converter and the Brayton cycle for possible utilization in upgrading the power of the HPSNR is compared, the basic question is what power level is desired. For up to 1 MWe, the TE conversion is probably a better choice. However, for a larger sized system, the Brayton cycle would be better. Since the TE system has more practical experience in space use, any near future upgrade of the heat pipe reactor system will best use a TE conversion system.

VI. FISSION GAS AND VOLATILE RELEASE-VENTING MODEL FOR SPACE NUCLEAR REACTORS

Another concern in the development of space nuclear reactors is venting the fission gases and volatile fission products from the reactor core while minimizing the mass and size of the system as much as is practically possible. The problems associated with the adequate venting of fission gases and volatiles are common to both low power (few kilowatts) and high power (several hundred kilowatts to multimegawatts) systems.

In general, there are three distinct processes for venting fission gases and volatiles from the reactor core. These are molecular flow at very low partial pressure of the gas in the core, transitional flow at intermediate pressure, and viscous flow at high partial pressure of the gas in the core. When fission products are vented directly into space, as the molecules of volatile fission products approach the exit of the venting passage, they are subjected to steep declines in temperature and pressure. Thus, it is possible that some of the volatiles may condense on the vent walls or may even solidify. Continuous deposition of volatiles on the walls of the venting passages may eventually plug the venting system (Fig. 32) and subsequently, because of the accumulation of gaseous fission products in the core, pressurization of the core containment could occur. Such pressure buildup, in turn, may either cause the core containment to fail, and/or partially damage the multifoil thermal insulation wrapped around the core containment walls.

A computer model has been developed to study the release of fission gases and volatiles from the fuel matrix into the core cavity and subsequent venting into space (Ref. 2). The model is generally applicable to space nuclear reactors that employ UO_2 fuel, regardless of the power output of the core, and can be used for designing the venting system for space nuclear reactors. The model consists of two coupled components: (1) an intragranular fission gas and a volatile release model that is based on an equivalent spherical grain concept, and (2) a venting model. In order to assess the effects of either partial or total plugging of the venting system on the core can pressurization, the model was applied to the present HPSNR design for 100 kWe and the results are summarized in the following subsections. (A

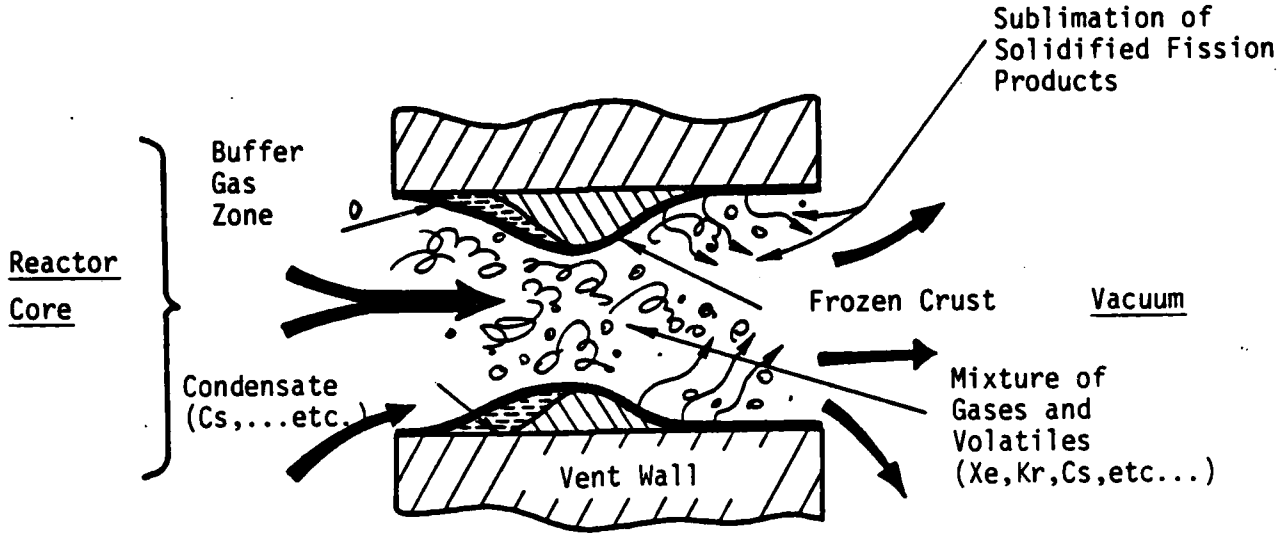

Figure 32. Venting of gaseous and volatile fission products.

detailed description of the model and the calculations are given in Refs. 2 and 3.)

1. FISSION GAS-VOLATILE RELEASE MODEL

An intragranular fission gas release model (Refs. 3 and 21) was developed and used to calculate the release fraction of noble gases (Xe and Kr) and volatile (Cs) fission product from the UO_2 fuel into the core cavity. The gas pressure within the core was calculated as a function of fuel burnup, fuel temperature, and the venting fraction of fission gases into space. The effect on the diffusion process of the resolution and on nucleation of gas bubbles within the grain was also considered in determining the effective gas diffusion coefficient (Ref. 3). The effects on the biased diffusion of gas atoms of temperature have been neglected in the present model because of the small spatial temperature variation in the HPSNR fuel wafers (~300°C).

The release fraction, RF, of a fission gas species is calculated using the following equation:

$$RF = 1 - \frac{\bar{C}(t)}{n\ t} \qquad (16)$$

where,

$\bar{C}(t)$ = average gas concentration in fuel grain

η = volumetric fission rate

t = time

For more details on the model description and governing equations, see References 2 and 3.

2. FISSION GAS VENTING MODEL

The gas flow in a vacuum can be classified either as molecular flow, transitional flow, or viscous flow. For viscous flow, the Knudsen number, Kn, is less than 0.01; for molecular flow, Kn is larger than 1; and for transitional flow, Kn is between 0.01 and 1. In the HPSNR, the fission gas temperature in the core is approximately the same as that of the fuel (~1700 K). Because the temperature in the space is about 250 K, the number density of the gas would change along the venting channel.

The governing equations for the vented rate of fission gas (Xe and Kr) from the core to the outer space are presented in References 2, 3, and 22.

3. CESIUM RELEASE MODEL

Unlike noble gases, volatile fission products exhibit strong chemical reaction with UO_2 fuel as well as with other fission products such as iodine. According to the cesium release computer model by Schumacher and Wright (Ref. 23), the cesium release fraction can be calculated in terms of the cesium's partial pressure in the fuel. The latter is calculated as a function of the oxygen-to-metal ratio (O/M) in the fuel and the fuel temperature. The model assumes that only the more stable of the two cesium uranate compounds, Cs_2UO_4 and $Cs_2UO_{3.56}$, and elemental cesium will contribute to the release of cesium. See References 2 and 3 for more details on the model description.

4. APPLICATION TO THE HEAT PIPE SPACE NUCLEAR REACTOR

To predict the effect of either partial or complete plugging of the core venting system on the potential failure of the core containment of the

HPSNR, calculations were conducted for the release fractions of noble gases (Xe and Kr) as well as of cesium. Both xenon and krypton possess the same release characteristics (Ref. 21). Figure 33 shows the predicted weighted release fractions of fission gases Xe, Kr, and Cs as a function of fuel burnup for a fuel temperature of 1700 K, the operating fuel temperature in the reference design of the HPSNR. In Figure 33, the weighted release fraction of cesium is the same as the cesium release fraction given by Equation 16. However, the weighted release fraction from Equation 16 can be multiplied by $[Y_{Xe}/(Y_{Xe} + Y_{Kr})]$ and $[Y_{Kr}/(Y_{Xe} + Y_{Kr})]$, respectively. As shown in Figure 33, the release fraction initially increases rapidly with fuel burnup up to 2.0 atom percent; then it increases slowly with fuel burnup. More than 90 percent of the Cs, approximately 80 percent of the Xe, but only 15 percent of Kr would be released into the core at the end of life (3 to 7 yr) or approximately 3 to 5 atom percent burnup.

To examine closely the effect of fractional venting of the reactor core on the core can pressurization, the maximum fuel burnup needed to avoid rupturing the HPSNR core can is plotted in Figure 34 as a function of venting fraction for varying fuel temperatures. As indicated in Figure 34, the maximum fuel burnup (atom percent) or the maximum operating lifetime in noble gases (Xe and Kr) as well as of Cs increases. When the fuel operating temperature is as low as 1400 K, a maximum fuel burnup of ~2.5 atom percent (or an operating lifetime of 5 yr) is attainable, even if the reactor core is completely plugged. As the fuel temperature increases from 1400 to 1700 K, more fission gases are released from the fuel matrix into the core cavity causing pressurization of the core can, and in turn, reducing the operational lifetime of the core. However, the HPSNR design requirement of 3 to 5 atom percent fuel burnup or 3 to 7 yr lifetime of the core can easily be attained with only 30 percent of the released gases vented into space.

As the previous discussion indicates, the complete plugging of the venting system in the reference design of HPSNR would not cause immediate failure of the core can. However, it would reduce the maximum fuel burnup and subsequently the core's lifetime. Operating the fuel at 1400 K, instead of at the 1700 K stipulated by the reference design, would not affect the operation of the core even if the core becomes completely plugged. Although operating at this low temperature would concomitantly increase the size and

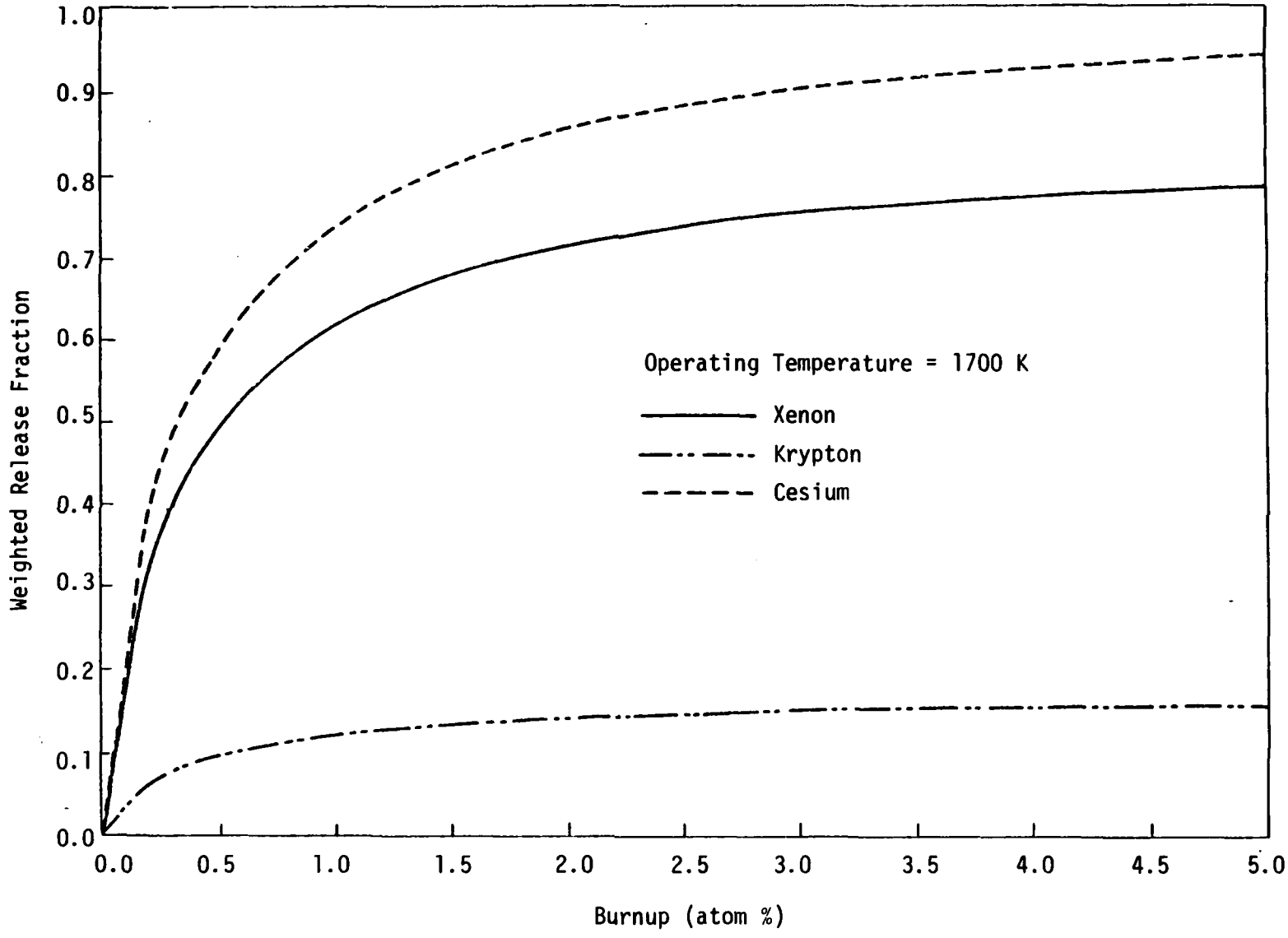

Figure 33. Weighted release fraction of gaseous and volatile fission products.

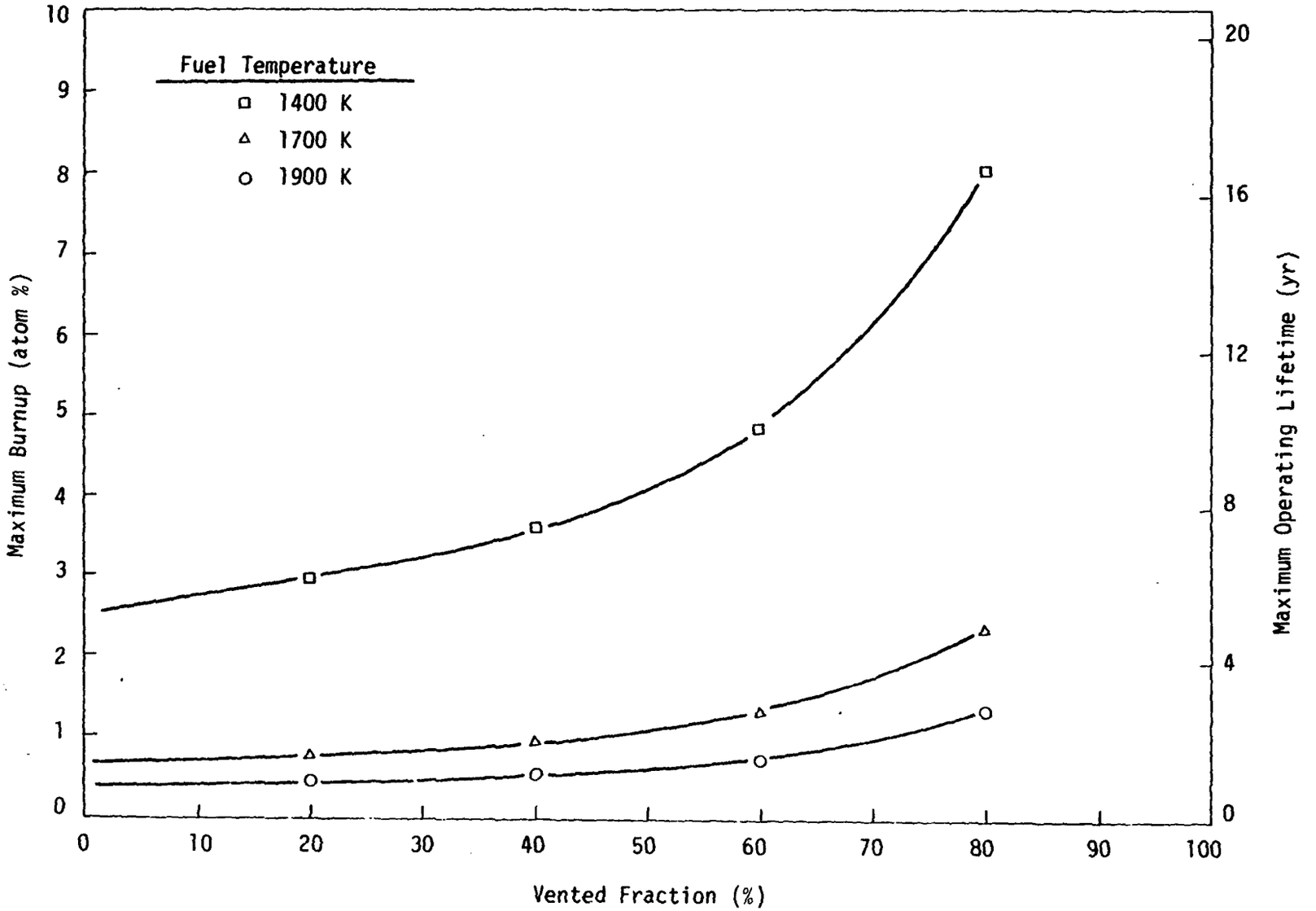

Figure 34. Maximum fuel burnup to avoid core can failure.

mass of the radiator, it would also reduce the conversion efficiency of the thermoelectric converters.

However, even well before the core can ruptures, applying an external pressure (in the order of a few kilopascals) on the multifoil insulation wrapped around the core can could cause overheating of the Be reflector. A major contributor to such a rupture is the thermal multifoil insulation wrapped around the core can because it does not insulate effectively. As shown in Figure 35, 100 foils would provide almost perfect insulation if all the released noble gases are readily vented to space. However, partial venting of these gases would reduce the insulating capability of the multifoils due to the pressure applied on the multifoils by the core can walls. For instance, at a fuel burnup of only 0.10 atom percent, the heat flux through a 100 foil insulation would increase from zero to 100 W/m^2, if only 80 percent of fission gas is vented out. With the venting system completely plugged, the losses from the core will almost double to about 260 W/m^2.

As delineated in Figure 36, applying a pressure on the multifoil insulation significantly reduces its insulation capability and subsequently overheats the Be reflector. The calculation on which Figure 36 was based assumed an adiabatic heating condition. The temperature of 900 K is an upper limit value for the proper operation of Be reflector (Ref. 6).

If the initial temperature of the Be reflector were 900 K and the applied pressure were 10 kPa, the temperature of Be and 25-foil insulation would reach its melting point after 39 days of continuous operation; the 100-foil insulation would take 10 days for Be reflector to reach its melting point. However, increasing the applied pressure to 40 kPa reduces the time for the reflector to reach its melting point; 19 days with the 100-foil insulation and 4 days with the 25-foil insulation, respectively. Figure 36 also shows that decreasing the initial temperature of the Be reflector from 900 to 600 K effectively increases the time for the Be reflector to reach its melting point. Similar arguments could also be made for the effect of overheating the control drums and radiation shield caused by the partial failure of the multifoil thermal insulation wrapped around the core can.

The fission gases in the HPSNR may be vented from the core through the structure clearance around the heat pipes that exit through the top BeO reflector. To prevent heat pipes from making contact with and in turn overheating the reflector, a multifoil thermal insulation is wrapped around a

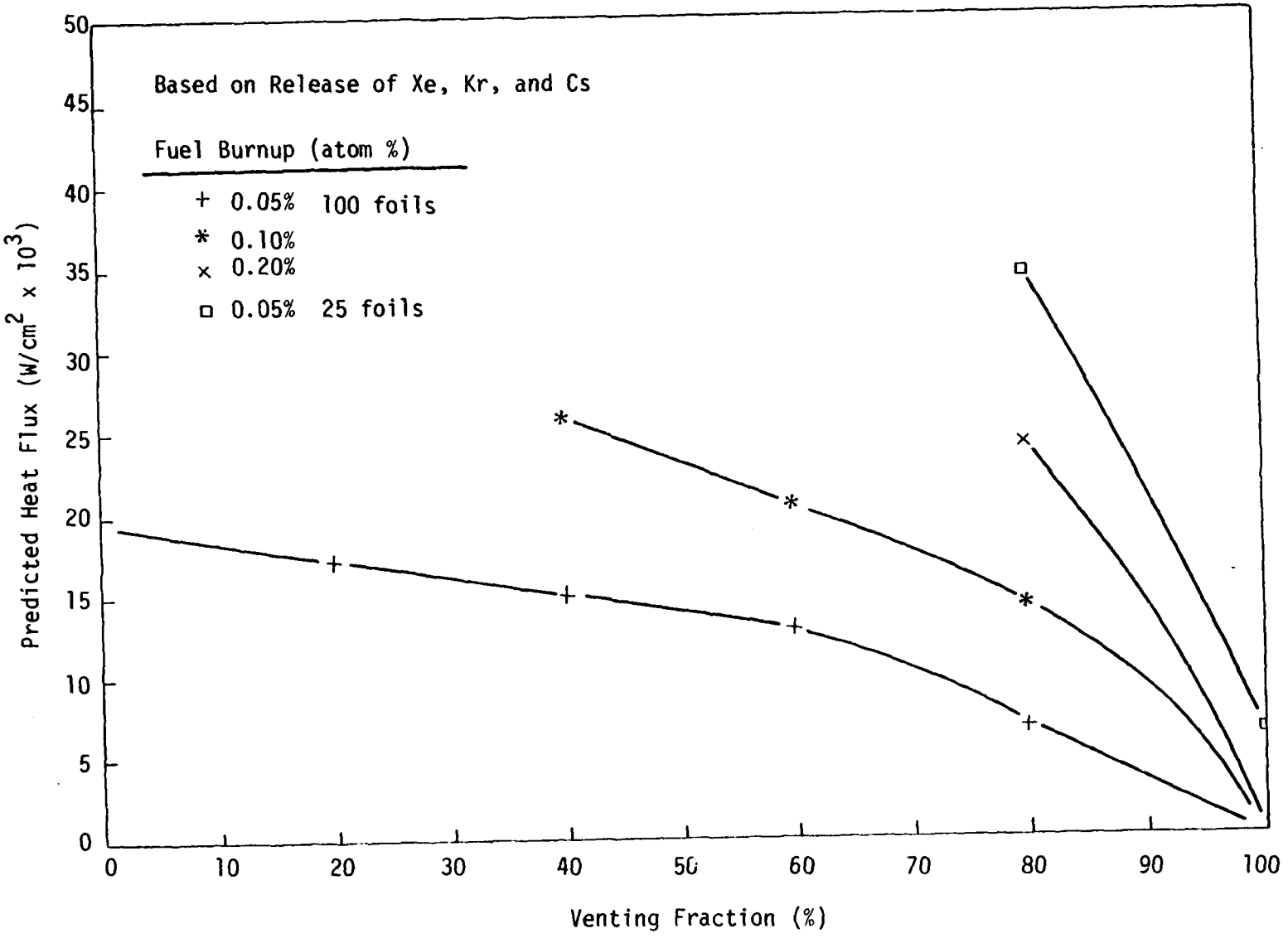

Figure 35. Predicted heat flux.

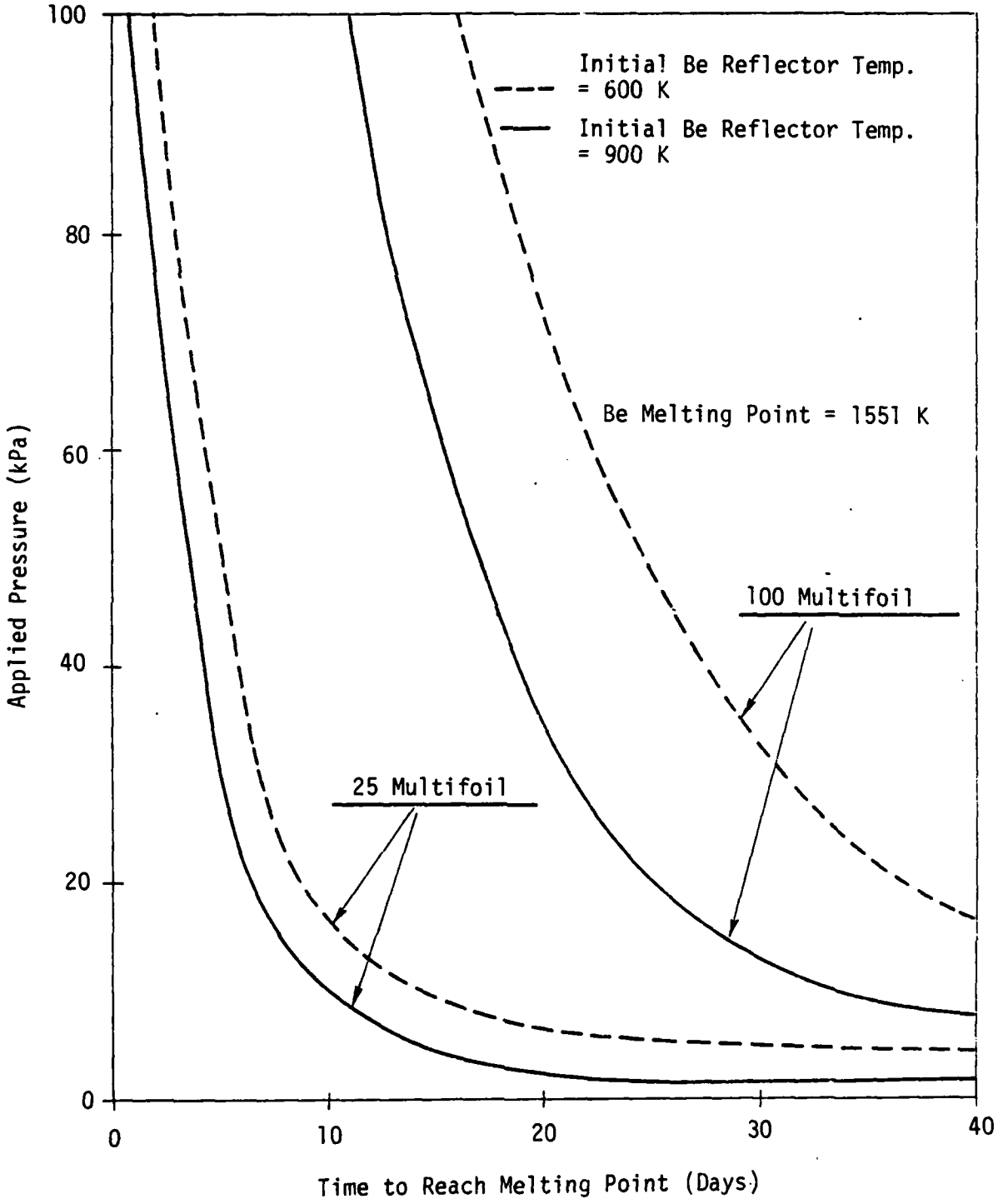

Figure 36. Applied pressure.

segment of the heat pipe. Between each heat pipe and the multifoil insulation, there is a narrow gap (few millimeters in size) which can be used to vent the fission products (both the noble gases and volatiles) into space (Fig. 37). The other possible location for venting the HPSNR core design is at the bottom reflector, as shown in Figure 37. Unlike exiting through the heat pipe and thermal insulation gap at the top reflector where the venting temperature is 1500 K, exiting at the bottom reflector would allow an average venting temperature of ~855 K.

Calculations were also conducted based on the assumption that only one venting gap at the heat pipe exit was open. The results delineated in Figure 38 show the partial pressure of the Xe, Kr, and Cs gases plotted as functions of fuel burnup. Initially the vented gases flow through the venting channel at a molecular flow ($Kn < 0.1$); subsequently, it becomes a transitional flow as the pressure in the core increases due to the partial accumulation of fission gases. For the gas exiting at the top reflector, as shown in Figure 38 and 39, the maximum pressure in the core is predicted to be only 23 Pa at 3 atom percent fuel burnup. On the other hand, for the gas exiting at the bottom reflector, as shown in Figure 39, the maximum pressure in the core is predicted to be 29 Pa at 3 atom percent fuel burnup. The higher pressure for the latter case is due to the lower venting temperature (855 K) which would decrease the flow through the channel. For both venting temperatures (1700 and 855 K), the pressure buildup in the core is well below the predicted rupture pressure of the HPSNR core can. (In Fig. 39, the critical pressure is the core pressure at which the flow in the venting channel changes from molecular flow to transitional flow.)

Although the computer models presented in this section were applied to a specific design (HPSNR), they could easily be applied to other space nuclear reactor designs. For example, these models could aid in designing a core's venting system as well as augmenting studies of the effects of fission gas and volatile venting on the performance of thermionic fuel designs.

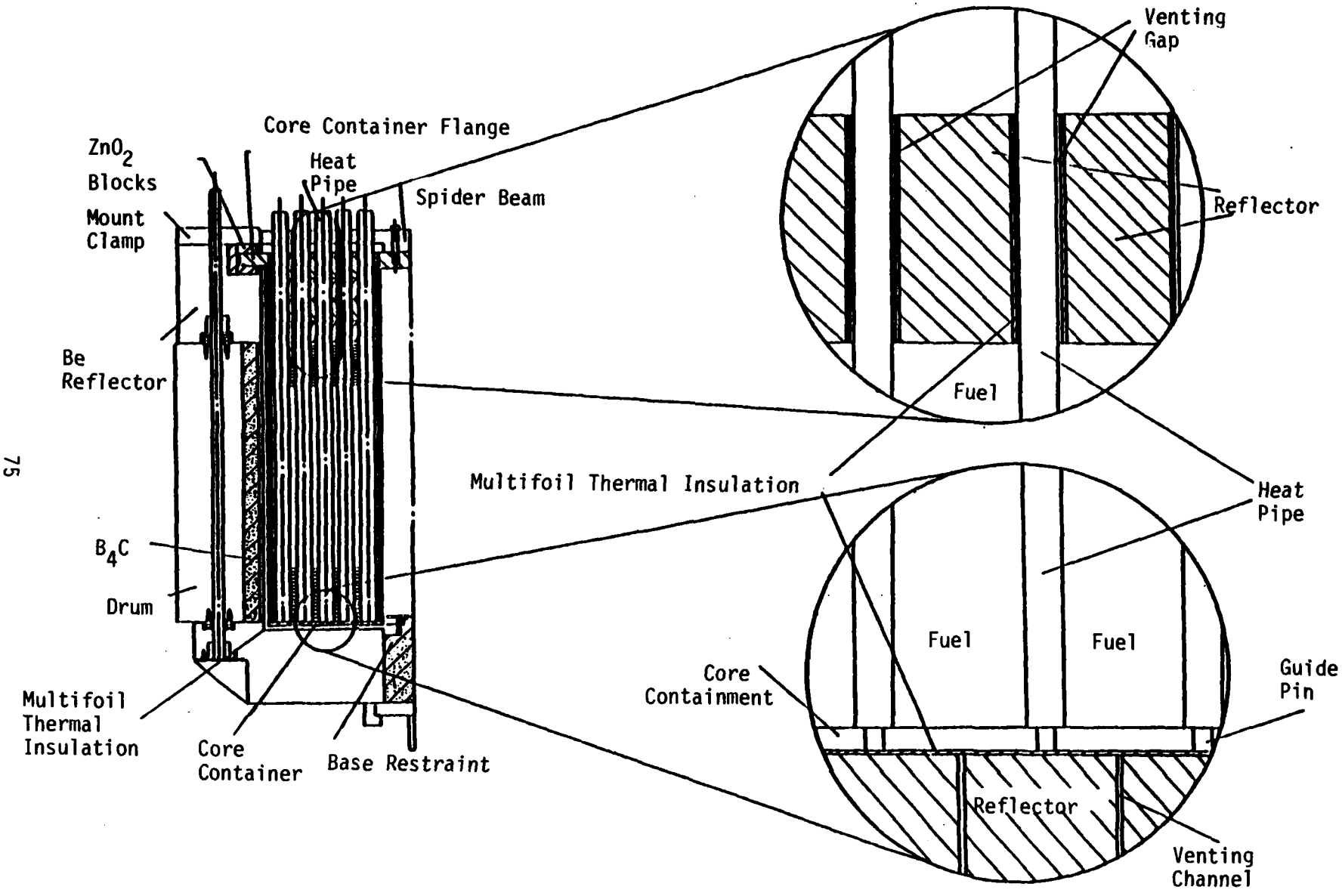

Figure 37. Possible location for venting in the HPSNR core.

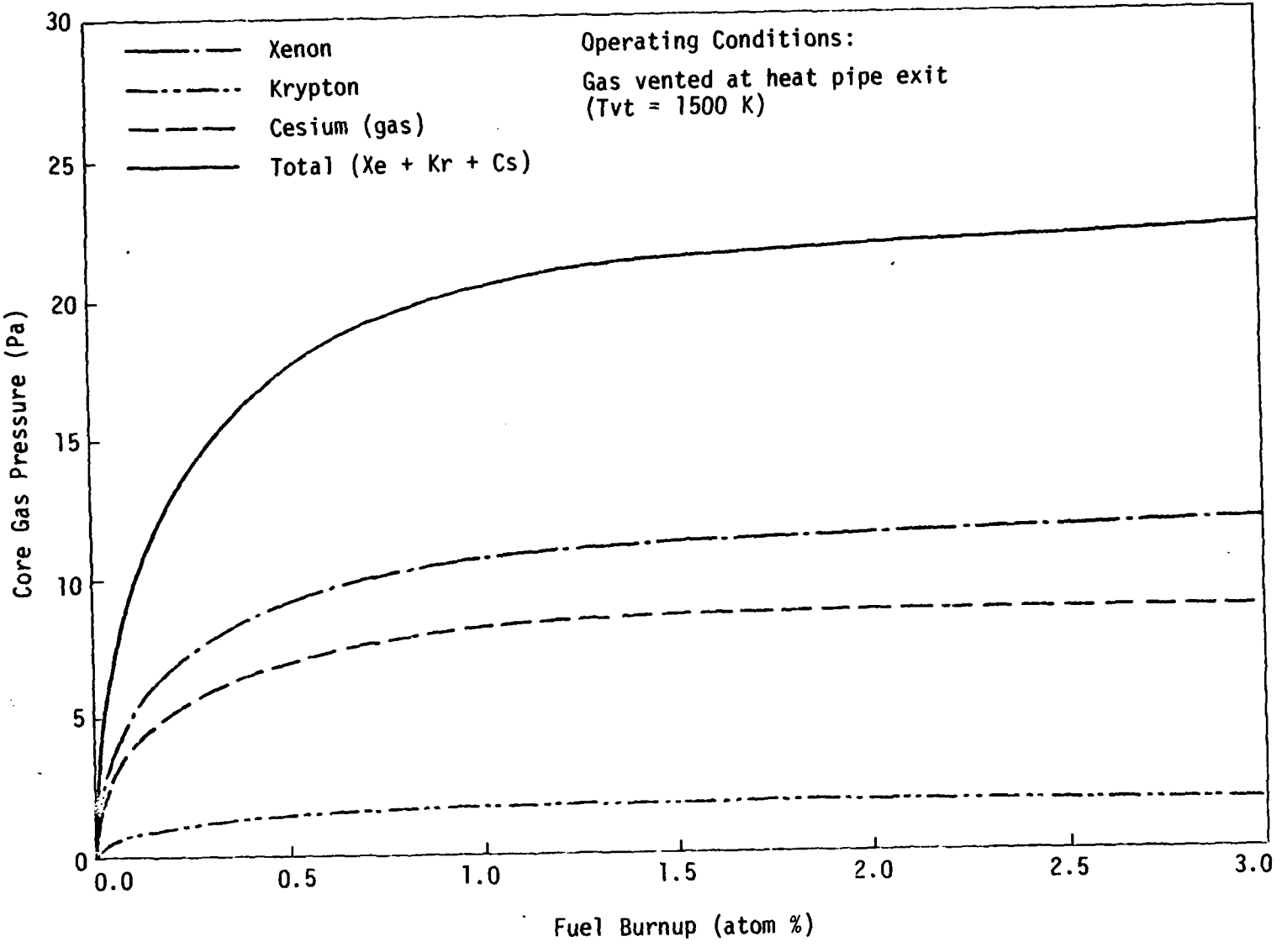

Figure 38. Core gas pressure for venting at bottom reflector.

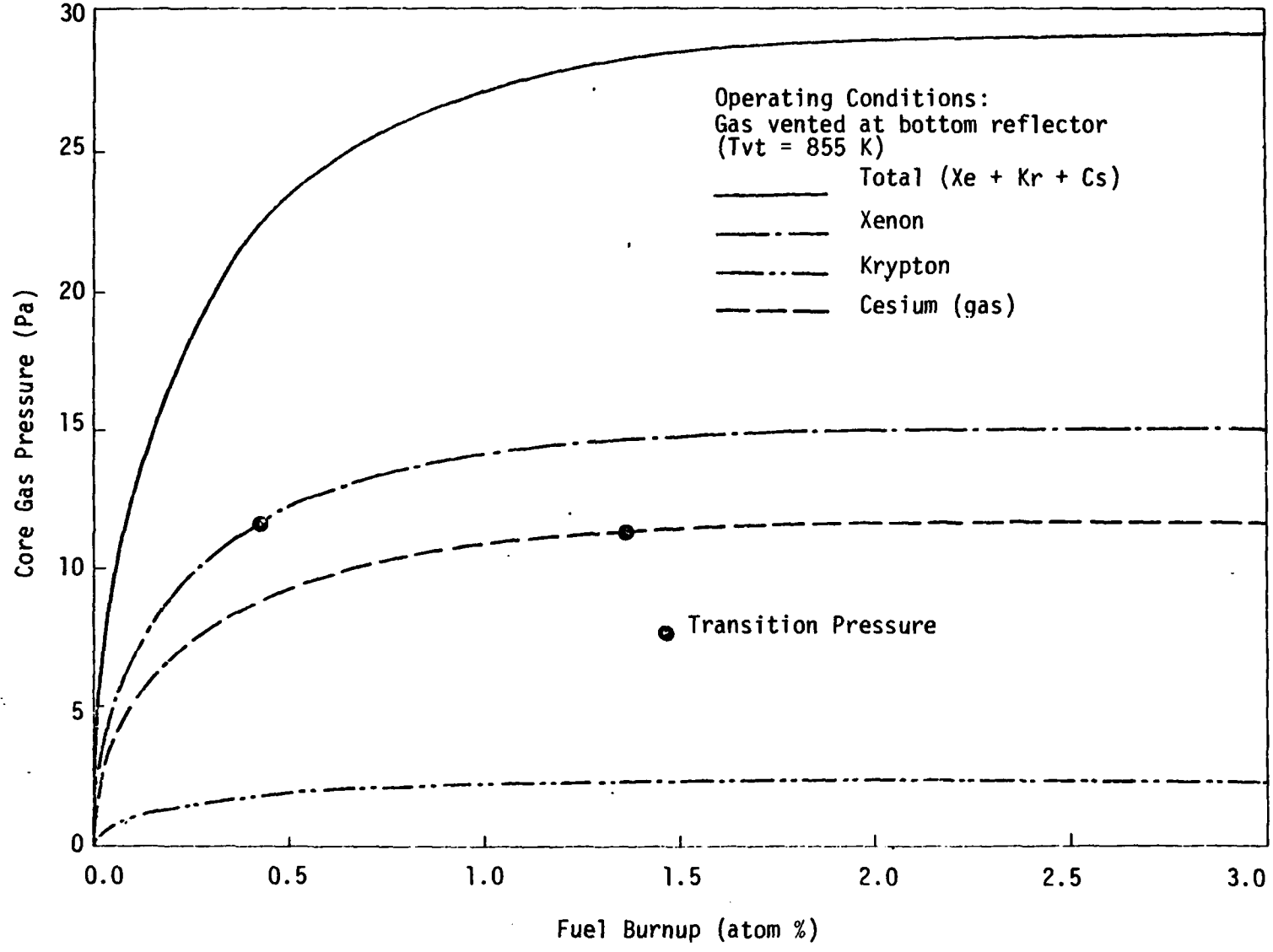

Figure 39. Core gas pressure for venting at heat pipe exit.

VII. SUMMARY AND CONCLUSIONS

This report investigated the feasibility of upgrading the power of the HPSNR system design and the effect of a partial or complete plugging of the venting system of the HPSNR on possible heating of the BeO reflector and on the core can pressurization. The report has also discussed the four primary methods for power upgrading; linear system size increase, pulse-mode operation, improved heat rejection, and improved thermal-to-electric energy conversion.

In the study of the power upgrade of the HPSNR by linear increase, the effects of increasing the core size on various subsystems as well as on the whole system were investigated as a function of electrical power output. Limitations imposed by the system; overall mass requirement, UO_2 fuel swelling, and the reactivity control were identified as the most limiting factors in upgrading the steady-state power of the HPSNR system. Possible methods for partially overcoming these limitations involve increasing the TE converter efficiency and using a more efficient radiator concept, UN fuel, a low temperature energy conversion system and a burnable poison or breeding concept. The maximum power achievable by linearly increasing the HPSNR system without violating any of these design limitations was found to be about 142 kWe with a system efficiency of 7.1 percent. If the system efficiency is increased to 12 percent, the maximum achievable power will be about 240 kWe. Although the pulse-mode operation could be an approach to upgrade the power of the HPSNR system, major design modifications would have to be introduced into the system design to allow it to operate in this mode.

Another approach for upgrading power involves enhancing the heat rejection system by using an improved radiator design. Two major radiator concepts were discussed for improving the performance of the radiator. These were the dust radiator and liquid droplet radiator concepts. These two concepts were compared with the panel type radiator used in the HPSNR baseline design. Although both the dust and the liquid droplet radiators offer significantly low specific masses, they still have many technical problems, such as, heat transfer to the metal spheres and long traveling distances for the dust radiator, and evaporation losses of the working liquid and freezing

of the liquid droplets for the liquid droplet radiator. Both radiator concepts, however, are attractive for high power rejection systems because each uses the large surface-area-to-mass ratio of small particles.

The last, and the most effective way of upgrading the electrical power output of the space nuclear power system, involves using an improved energy conversion system. A total of six different thermal-to-electric energy conversion systems were discussed and compared to determine their potential for upgrading the power of space nuclear power system. Among the passive systems (e.g., TE, TI, and AMTEC). The TE conversion system was chosen as a near future best conversion system for space nuclear power production with the TI conversion system as a possibility by the late 1990s. Among the active systems (e.g., Rankine cycle, Brayton cycle, and FPSE), the Brayton cycle was chosen as a near future energy conversion system for high electric power systems. The FPSE was chosen for far future use because of its overall superior characteristics. In conclusion, TE conversion was suggested for the near future for power levels up to 1 MWe. The Brayton cycle would be a better choice for large power levels. The best candidate for the far term space power reactor concepts appears to be an FPSE.

Finally, the consequences of either partial or complete plugging of the venting system in the HPSNR were studied by developing a coupled fission gas and volatile release-venting computer model. The calculation results showed that complete plugging of the venting system in the HPSNR would neither influence the core's performance nor its lifetime as long as the temperature of the fuel is kept at about 1400 K. However, operating the fuel of the HPSNR at the specific 1700 K operating temperature would encourage fission gas release from the fuel into the core cavity. Such a release could cause the core can to fail prematurely. In either case, moderate pressurization of the core without a core can failure could damage the multifoil insulation wrapped around the core can and cause overheating of the Be reflector, control drums, and radiation shield. However, it is highly unlikely that the HPSNR venting system would be completely plugged early in its life.

REFERENCES

1. Dean, V. F., El-Genk, M. S., Louie, D.L.Y., and Woodall, D. M., Design Status of the SP-100 Heat Pipe Space Nuclear Reactor System, Final Report, Vol. I, Report No. NE-101(85)AFWL-144-1 (February 1985).

2. Louie, D.L.Y., and M. S. El-Genk, "Effect of Venting System Failure on Operation of Heat Pipe Space Nuclear Reactor," Report No. NE-104(84) AFWL-144-1, Air Force Weapons Laboratory, Kirtland Air Force Base, New Mexico, July 1984, M.S. Thesis, University of New Mexico (1984).

3. Louie, D.L.Y., El-Genk, M. S., and Wright, S., "Fission Gas and Volatile Release-Venting Model for Space Nuclear Reactors," Space Nuclear Power Systems (Eds. M. S. El-Genk and M. D. Hoover), Robert E. Krieger Publishing Company, Inc., 1984.

4. Hedgepeth, J. M., "Ultralight Weight Structure for Space Power," Progress in Astronautics and Aeronautics, Vol. 61.

5. Mattick, A. T., and Hertzberg, A., "Liquid Droplet Radiator for Heat Rejection in Space," Journal of Energy, Vol. 5, No. 6, Nov.-Dec., 1981.

6. SP-100 Project Semi-Annual Technical Progress Review at Los Alamos National Laboratory, Los Alamos, New Mexico, October 1982.

7. Semi-Annual SP-100 Design Review at Los Alamos National Laboratory, Los Alamos, New Mexico, Aaril 1982.

8. El-Genk, M. S., et al., "Review of the Design Status of the SP-100 Space Nuclear Power System," Space Nuclear Power Systems, (Eds., M. S. El-Genk and M. D. Hoover), Robert E. Krieger Publishing Company, Inc., 1984.

9. Ewell, R., "Energy Conversion for Megawatt Space Power Systems," 18th Intersociety Energy Conversion Engineering Conference, Orlando, Fla., August 1983.

10. Katucki, R., et al., "Evolution of System Concepts for a 100 kWe Class Space Nuclear Power System," Space Nuclear Systems, (Eds. M. S. El-Genk and D. M. Hoover), Robert E. Krieger Publishing Company, Inc., 1984.

11. Ranken, W. A., et al., "Neutronic and Thermal Design for Heat Pipe Reactors," 18th Intersociety Energy Conversion Engineering Conference, Orlando, Fla., August 1983.

12. Cox, C. M., et al., "Fuel Systems for Compact Fast Space Reactors," Space Nuclear Power System, (Eds., M. S. El-Genk and M. D. Hoover), Robert E. Krieger Publishing Company, Inc., 1984.

13. Buden, D., et al., Selection of Power Plant Elements for Future Reactor Space Electric Power System, LA-7858, Los Alamos National Laboratory, Los Alamos, New Mexico, September 1979.

14. Buden, D., et al., "Space Nuclear Reactor," 18th Intersociety Energy Conversion Engineering Conference, Orlando, Fla., August 1983.

15. Barrattino, W. J., and El-Genk, M. S., "Thermal Analysis of Radiation Shield for Space Reactors Using Analytical and Finite Element Methods," Space Nuclear Power Systems, (Eds., M. S. El-Genk and M. D. Hoover), Robert E. Krieger Publishing Company, Inc., 1984.

16. Holland, M. H., et al., "Theremionic Fuel Element Technology Status," Space Nuclear Power Systems, (Eds. M. S. El-Genk and M. D. Hoover), Robert E. Krieger Publishing Company, Inc., 1984.

17. Bankston, C. P., "Alkaki Metal Thermoelectric Conversion for Space Nuclear Power Ssytems," Space Nuclear Power Systems, (Eds. M. S. El-Genk and M. D. Hoover), Robert E. Krieger Publishing Company, Inc., 1984.

18. Peterson, J., "Rankine Cycle Power Conversion Overview," Proceedings of the Air Force Office of Scientific Research Special Conference on Prime-Power for High Energy Space Systems, Norfolk, Va., February 1982.

19. Paeker, G. H., "Brayton Cycle Power Conversion for Space," Proceedings of the Air Force Office of Scientific Research Special Conference on Prime-Power for High Energy Space Systems, Norfolk, Va., February 1982.

20. Beale, W. T., "The Free Piston Stirling Engine--Its Promise as a Space Power Plant," Space Nuclear Power Systems, (Eds. M. S. El-Genk and M. D. Hoover), Robert E. Krieger Publishing Company, Inc., 1984.

21. Wood, M. H. and Matthews, J. R., "A Simple Operational Gas Release and Swelling Model," J. Nucl. Mater., 91, pp. 34-40, 1980.

22. Speight, M. V., "A Calculation on the Migration of Fission Gas in Material Exhibiting Precipitation and Resolution of Gas Atoms Under Irradiation," Nucl. Sci. Engr., 37, pp. 180-185, 1969.

23. Schumacher, G. and Wright, S. A., Advanced Reactor Safety Research Quarterly Report, Vol. 22, pp. 352-375, Sandia National Laboratory, Albuquerque, New Mexico, April-June 1982.

APPENDIX A
IMPROVED RADIATOR CONCEPTS

I. DUST RADIATOR CONCEPT

The dust radiator uses small solid particles first to carry the rejected heat from the energy conversion system (i.e., the cold leg of a thermoelectric converter) and then to radiate the heat into space. This approach is based on the fact that small particles have a higher surface-area-to-volume ratio than larger particles. Thus, the surface-area-to-mass ratio of the total system is large. (One useful quantity for comparing radiators is specific mass, defined as mass per radiating area. for a sphere the specific mass is

$$1/3 \cdot \rho \cdot a \qquad \text{(A-1)}$$

where ρ is the density of the particle and a is the radius of the particle.)

The basic principles of a dust radiator concept are simple. The dust particles (steel spheres) are heated in a container and are projected into a stream to be caught by another container. At this point, the dust particles can be recycled for reheating. The process is repeated to reject heat into space by the large surface area of the dust during its flight. Figure A-1 shows a conceptual design of a dust radiator for a space nuclear power system.

Following is a simplified analysis of the design concept by John M. Hedgepeth (Ref. A-1). In Hedgepeth's analysis:

(1) The kinetic energy carried by each dust particle is 0.5 percent of the amount of heat lost by the particle in its flight.

(2) The number of particles inside the chamber is about 20 percent of the particles in the stream.

(3) The number density of the particle in the stream is assumed to be such that approximately half of the solid angle seen by each particle is blocked by other particles.

Figure A-2 shows the radiated power versus the particle spacing and the particle diameter. Figure A-3 shows the radiated power versus stream length

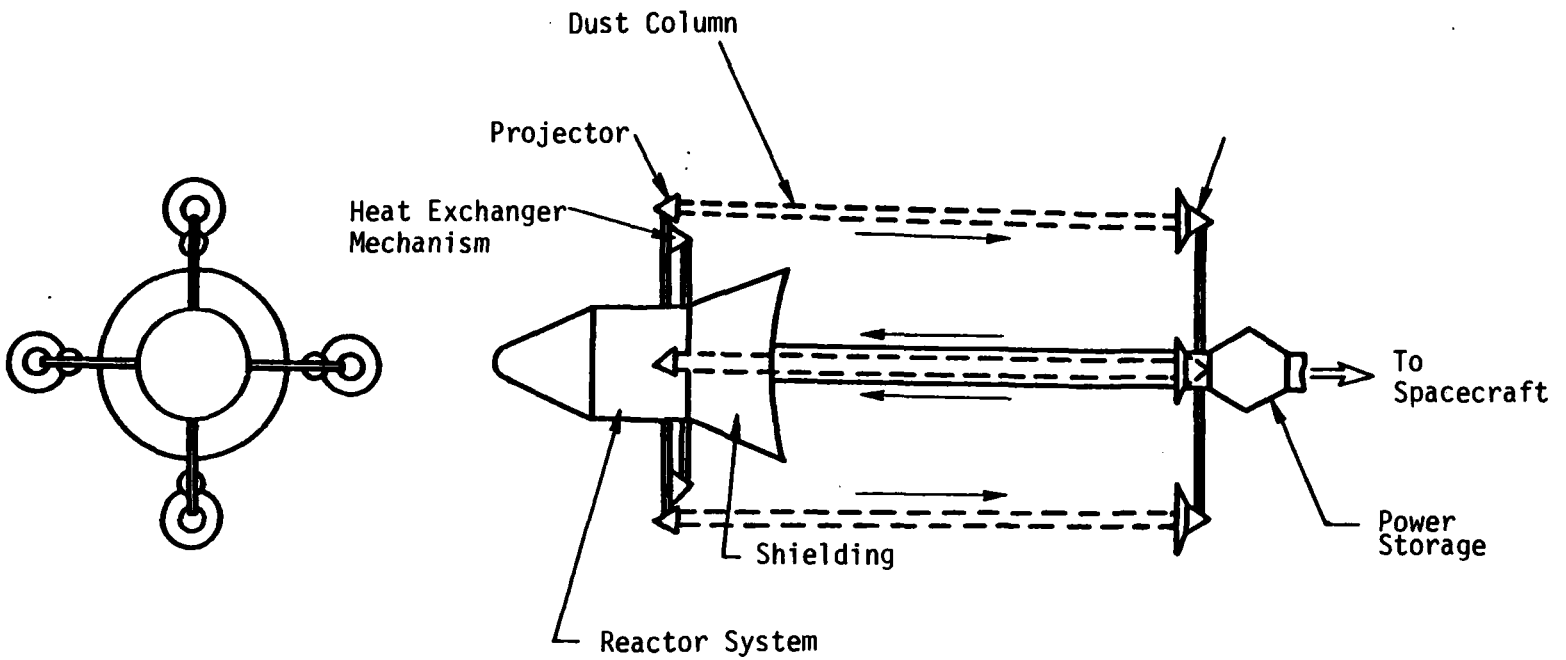

Figure A-1. Schematic of a typical dust radiator for a space nuclear reactor system.

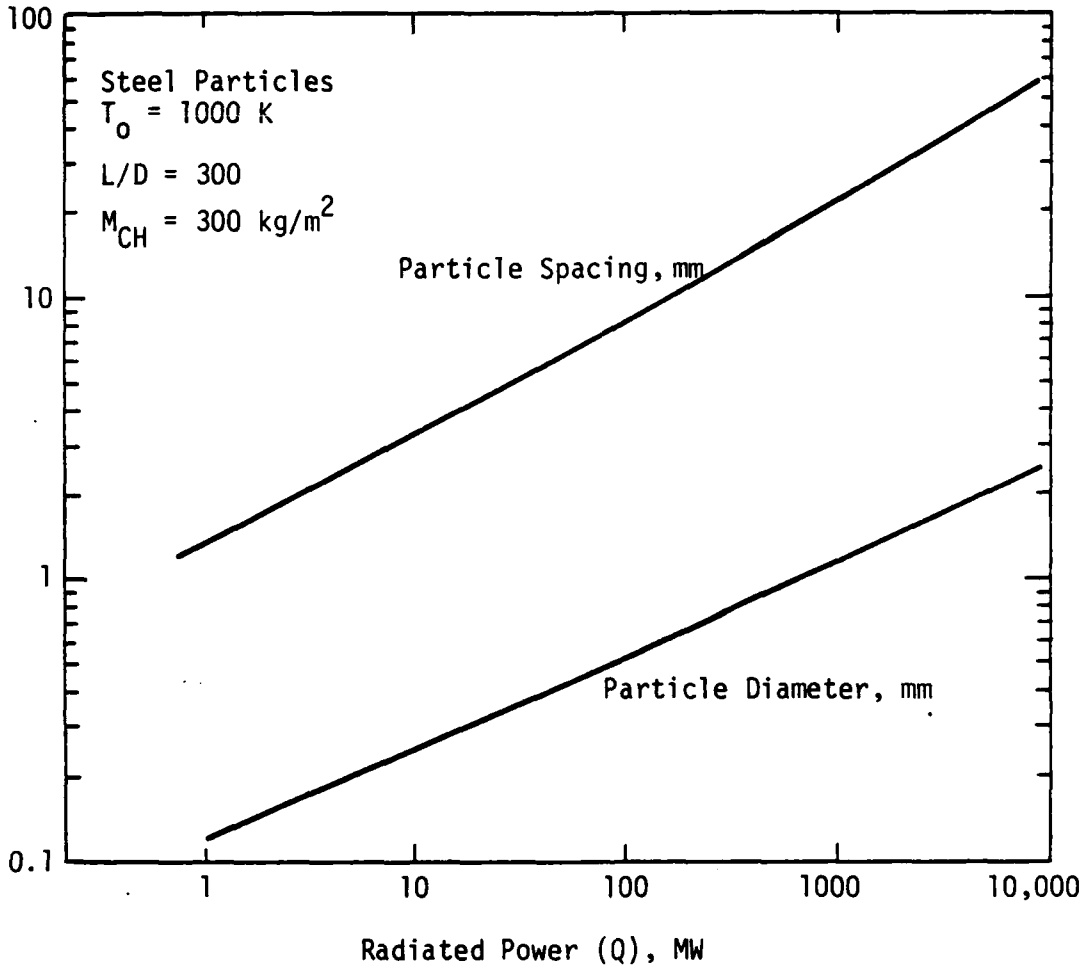

Figure A-2. Radiated power versus particle spacing and diameter.

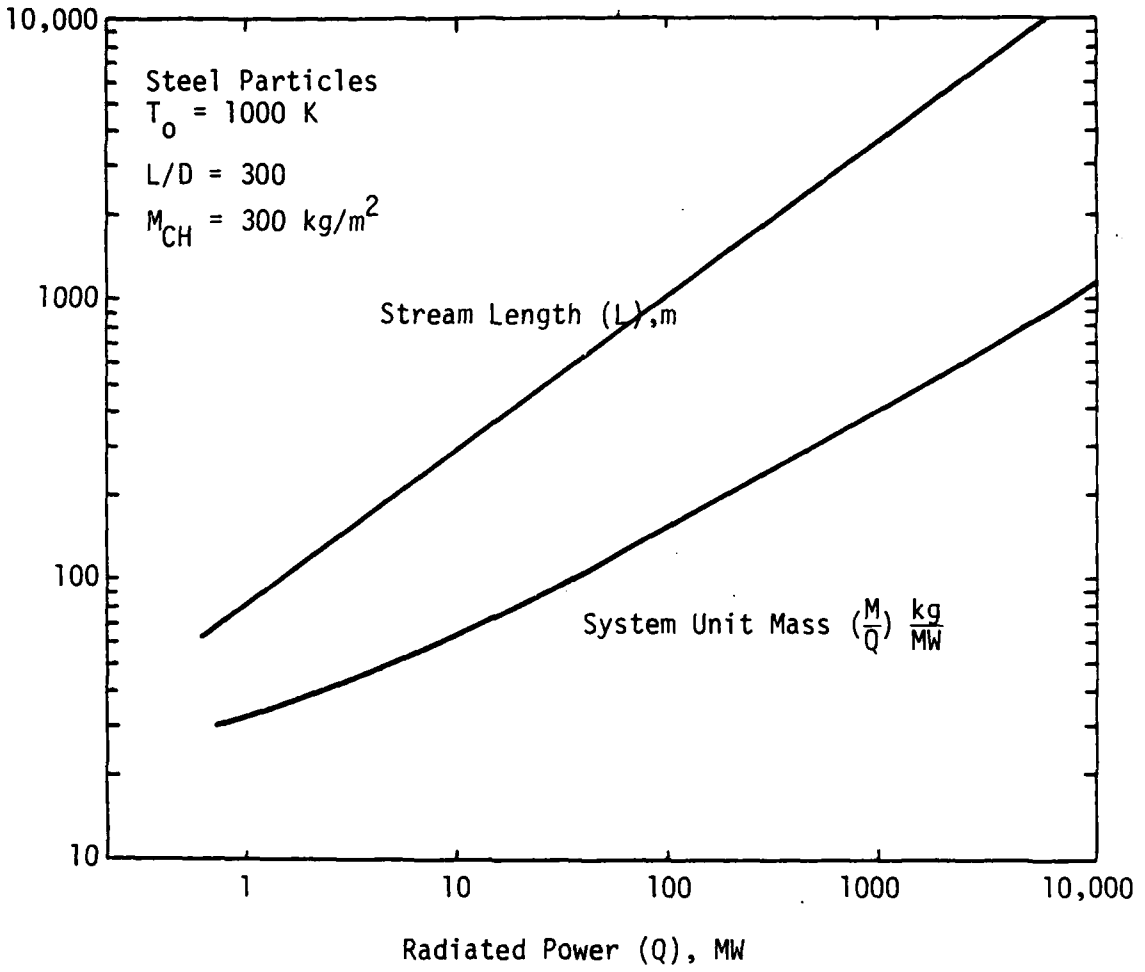

Figure A-3. Radiated power versus stream length and system unit mass.

required and system unit mass, defined as mass per radiated power. The exit temperature of the particles in the chamber is 1000 K and the particles are steel spheres. Table A-1 illustrates a simple analysis of a 10-MW radiated power dust radiator based on these two figures and their assumptions. The result shows that the required stream is 270 m long, that the particle spacing is 3.2 mm, that the particle diameter is 2.5 mm, and that the system unit mass is 64 kg/MW. Although this seems to be technologically possible, many heat transfer and engineering problems remain, such as, how to reheat the particles in the container, how to keep particles from dispersing in the stream, and how to capture the stream in the next chamber. These problems must be solved before this concept can be utilized successfully for the nuclear space power era. The required traveling distance of the particles in space must be short in order to minimize the materials used. (It should be noted that this dust radiator concept was being reviewed by the Air Force in the early 1960s.)

TABLE A-1. TYPICAL DUST RADIATOR SPECIFICATIONS FOR A SPACE NUCLEAR POWER SYSTEM

Radiated power	10 MW(th)
Dust particles	Steel
Particle diameter	0.24 mm
Particle spacing	3.2 mm
Required diameter of stream	0.9 m
Required stream length	270 m
System unit mass	64 kg/MW
Total system mass	640 kg

Emissivity of steel particle of 0.9, blockage of 0.5 or solid angle, kinetic energy of particle is 0.005 of radiated power

Note: All of these are based on the analysis done by Hedgepeth

AD-A160 280 HEAT PIPE SPACE NUCLEAR REACTOR DESIGN ASSESSMENT 2/2
VOLUME 2 FEASIBILITY ST..(U) NEW MEXICO UNIV
ALBUQUERQUE DEPT OF CHEMICAL AND NUCLEAR ENGI..
UNCLASSIFIED M S EL-GENK ET AL. AUG 85 F/G 18/9 NL

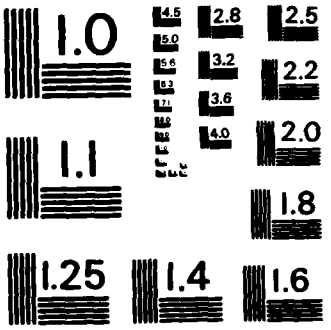

MICROCOPY RESOLUTION TEST CHART

NATIONAL BUREAU OF STANDARDS - 1963 - A

II. LIQUID DROPLET RADIATOR CONCEPT

The dust radiator discussed in Section I appears as a revolutionary lightweight design. However, this concept has significant problems, such as the inefficiency of heating the dust, the difficulties of controlling a stream of dust particles, and the collector efficiency of receiving the dust. The liquid droplet radiator, on the other hand, has the advantages of allowing heat transfer by conduction and of ease of manipulation. Compared with tube-fin and heat pipe systems, on the basis of surface area-to-mass ratio, the liquid droplet radiator is superior to these systems. For the best tube and fin system, the specific mass is 5-10 kg/m^2 (mass per radiating area). On the other hand, the specific mass of the droplet system is 0.11 kg/m^2 for a medium as heavy as liquid tin (ρ = 6.8 g/cm^3 and a = 100 mm). Thus, it is an improvement by a factor of 50 to 100 over the tube-fin radiator. The operating temperature range of the liquid droplet radiator is suitable for a high temperature rejection system (550-1000 K). Tin appears to be the best candidate at this operating range.

The droplet radiator concept can be visualized this way. The liquid absorbs heat rejected by the electrical energy conversion system and is projected into space in such a way that a thin converging sheet of small droplets are flying toward the collector module. A sheet configuration is better than a conical configuration for the droplet stream because the sheet configuration can minimize the solar radiation absorbed by the stream by correct orientation (Ref. A-2). The droplet generator is a pressurized plenum with an array of nozzles to form liquid jets, which break into droplets due to surface tension instability. This technique allows one to control the desired drop size and spacing. According to Mattick and Hertzberg (Ref. A-2), it is possible to generate up to 100,000 drops/s of droplets that have diameters below 50 μm and still have aiming accuracy better than 10 mrad.

The droplet collector is a rotating drum which forms a droplet stream into a continuous liquid by centrifugal acceleration. Pumps spaced symmetrically around the periphery of the drum then pressurize the liquid to overcome the centrifugal force and to provide the back pressure for the main heat exchanger pump. A typical diameter of the rotating drum is about 1 m.

Figure A-4 shows a liquid generator and collector. Figure A-5 shows a conceptual design of a liquid droplet radiator for a space nuclear reactor system.

There is an interesting note about allowing the droplets to freeze in flight. For a given droplet initial temperature (insertion temperature) and heat rejection, the mean radiation temperature would be lower for nonfreezing than freezing droplets (due to the heat released at constant temperature upon freezing) (Ref. A-2). Thus, a shorter flight-path would be required for freezing droplets. However, there are difficulties in immediately melting the frozen droplets upon collection. A large inventory of liquid may be needed to remelt these frozen droplets. Thus, it would increase the radiator system mass in comparison with the nonfreezing case.

Considering again a sheet configuration of droplets, if the droplets are spaced widely enough so that the light radiated by a droplet is not occluded by neighboring droplets (i.e., view factor ≈ 1), the radiator size becomes very large. However, liquid metals have low intrinsic emissivities ($\varepsilon \leq 0.1$), so that with closely-spaced droplets most of the radiation is reflected rather than absorbed. The net result is that the emissivity of a droplet sheet is larger than the intrinsic emissivity of the liquid metal droplet.

Plots of sheet emissivity versus optical depth for various intrinsic emissivities are given in Figure A-6. Optical depth is defined as the product of the number of droplets per unit volume, the cross sectional area of a droplet, and the sheet thickness. As can be seen in the figure, sheet emissivity increases with optical depth. However, the figure-of-merit for waste heat radiators in space is radiated power per mass. So increasing the optical depth of a sheet will be a compromise between the desire to reduce radiator size to keep the system manageable and the desire to reduce system mass. A comparison made by Mattick and Hertzberg (Ref. A-2) of this system and the heat pipe system concluded that for a typical heat pipe radiator with $\varepsilon = 0.8$, the mass of the system is still 5-10 times heavier at a given radiator temperature than a sheet of 100 μm in diameter tin droplets (with $\varepsilon = 0.1$, optical depth = 1).

One possibility for increasing the emissivity of a droplet sheet is to add a high emissivity powder to the surface of the droplet to increase the overall emissivity. The problem associated with this technique is to make

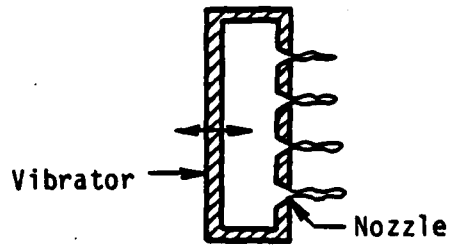

(a). Droplet generator.

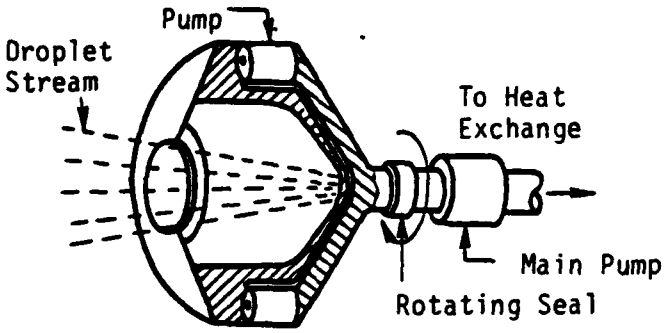

(b). Droplet collector.

Figure A-4. Liquid droplet generator collector for a droplet radiator.

sure the powder would stay on the periphery of the droplet and that it would be able to separate out upon collection.

One problem existing in this concept is evaporation loss while projecting the droplets into space. Therefore, extra liquid must be included to replace the liquid lost through evaporation. A radiating medium that has a low vapor pressure should be used to minimize the loss. More specifically, the medium should have a low vapor pressure and remain a liquid over a range of temperatures that is broad enough to allow reasonable operational tolerances. For instance, droplet freezing during the cooling process should not result if the droplets remain in space somewhat longer than planned. Also, slight overheating should not result in a catastrophic loss of fluid due to evaporation.

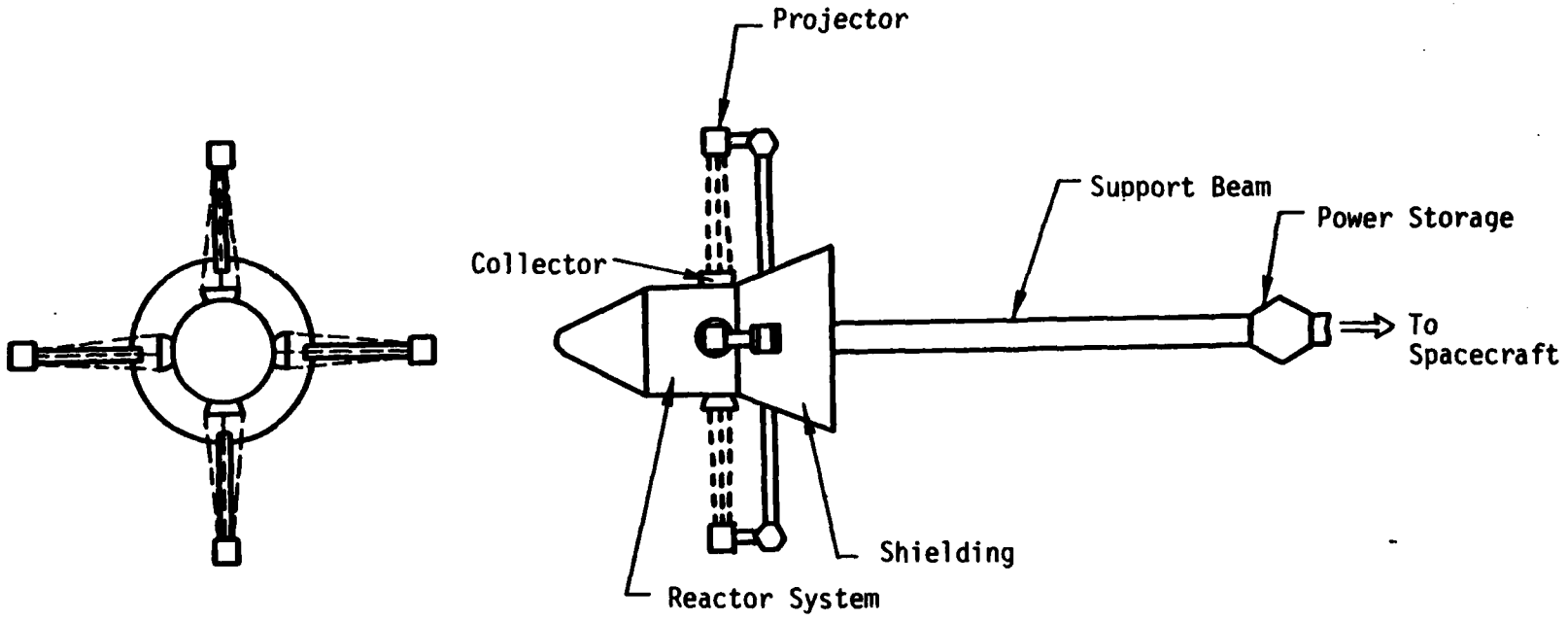

Figure A-5. Schematic of a typical liquid droplet radiator for a space nuclear reactor system.

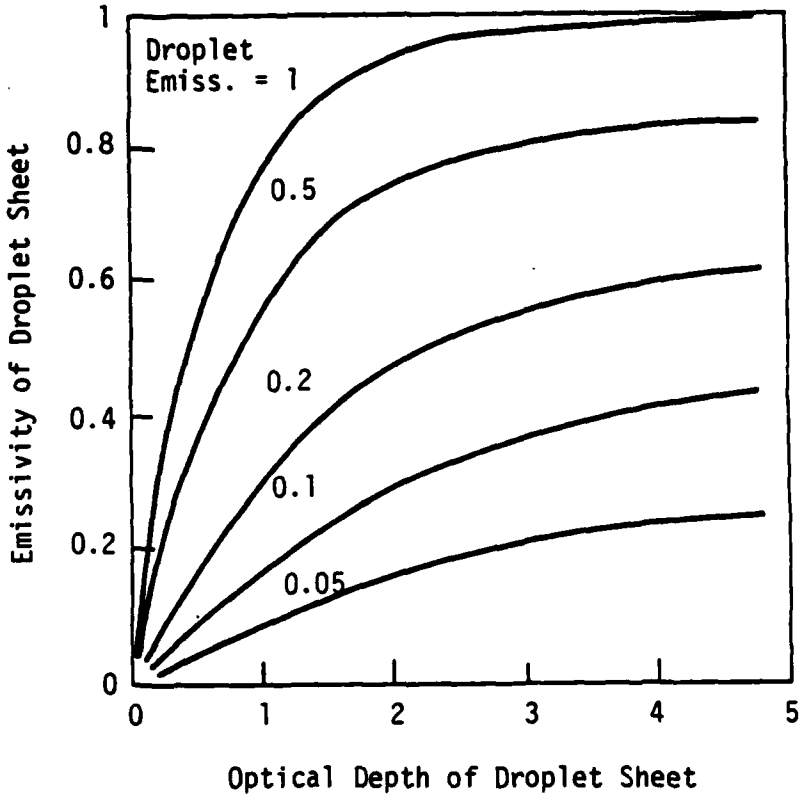

Figure A-6. Sheet emissivity versus optical depth of sheet by Mattick and Hertzberg (Ref. A-2).

In conclusion, the liquid droplet radiator seems possible conceptually. It has a low specific mass, possible high operating temperature range, and is compact. However, there are many technological problems that must be solved. For example, the problems with freezing during cooling and the problems of evaporation losses. In any case, for a space nuclear power system of high generating capacity, the liquid droplet radiator should be considered.

III. CONCLUSION

Both the dust and the liquid droplet radiators are good in their low specific masses, but they have many technological problems, such as the heat transfer, engineering, and material losses. Technological problems for the dust radiator are how to transfer heat from the source to the dust and how to shorten the traveling distance to reduce the need for excess dust particles. One suggestion is to use a reverse concept of the Cyclone nuclear reactor for transferring heat from the primary fluid to the particle in a centrifugal force generator. Figure A-7 shows the schematic of this idea. Another suggestion is to use particles that can be magnetized, so that when the particles are directed into space, after some distance, they will be attracted by a magnet on the spacecraft so that a loop traveling configuration would result. Figure A-8 shows the schematic of this idea. Both the dust and the liquid droplet radiator concepts are good for a high power rejection system because both can utilize the large surface-area-to-mass ratio of small particles to reject waste heat. Thus, the system may well be small and light.

REFERENCES

A-1. Hedgepeth, John M., "Ultralightweight Structures for Space Power, Progress in Astronautics and Aeronautics, Vol. 61.

A-2. Mattick, A. T., and Hertzberg, A., "Liquid Droplet Radiators for Heat Rejection in Space," J. Energy, Vol. 5, No. 6, Nov.-Dec. 1981.

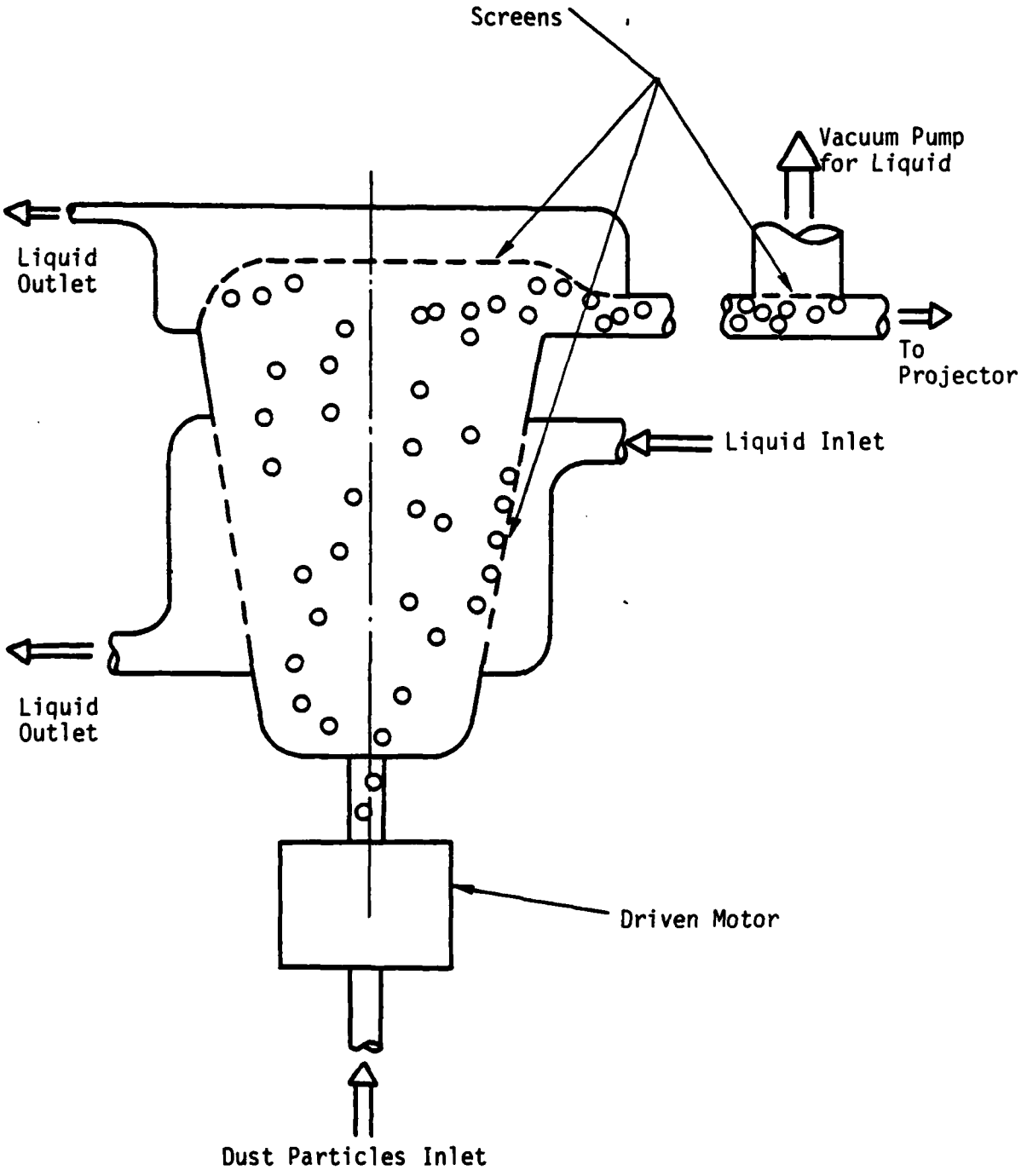

Figure A-7. Schematic of a centrifugal heat exchanger concept for a dust radiator.

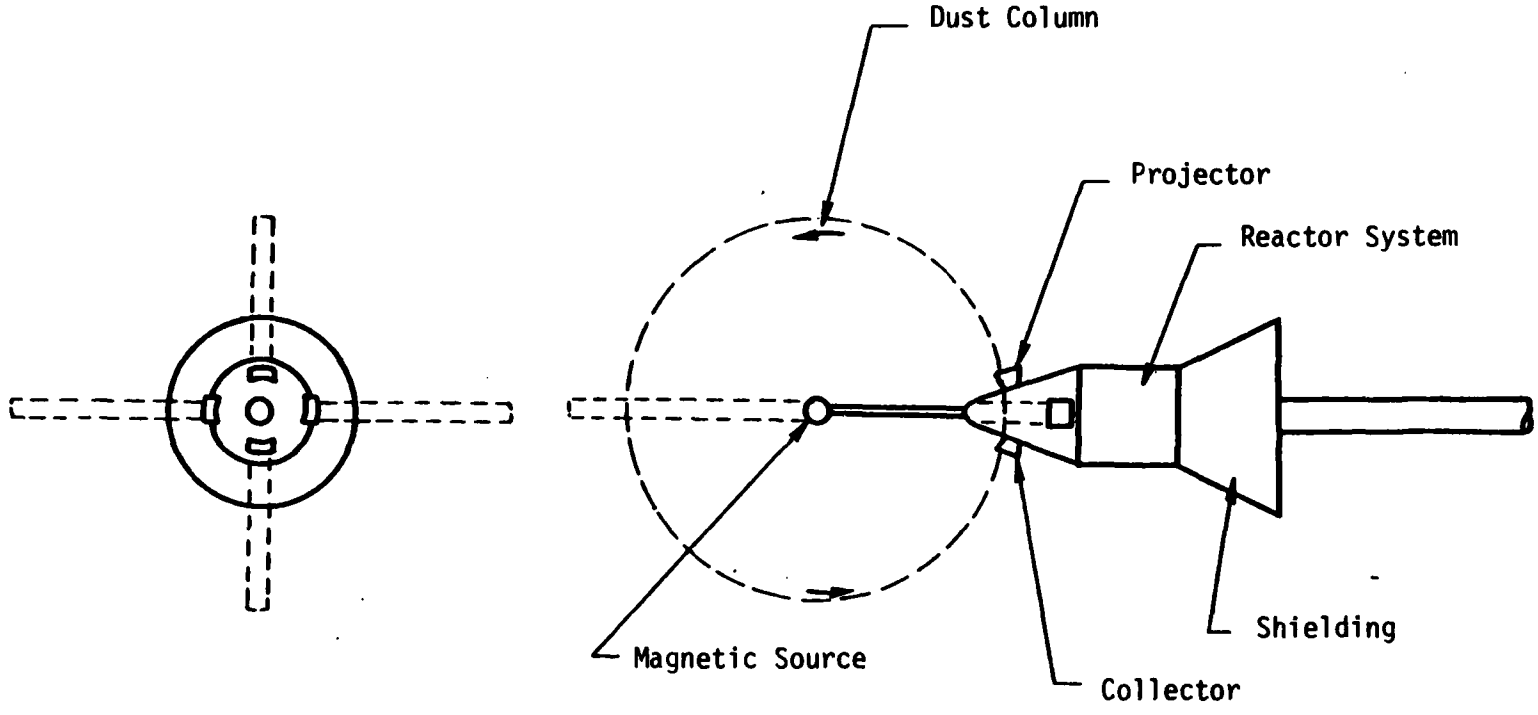

Figure A-8. Schematic of an advanced dust radiator concept for a space nuclear power system.

APPENDIX B

SPACE NUCLEAR POWER CONVERSION SYSTEMS

I. INTRODUCTION

The advantages of using a nuclear reactor as a prime energy source in space are well established. The limitation of advanced conventional systems to powers of less than 100 kWe is the main reason a nuclear source for future space use is desired (Ref. B-1). Surveillance, communications, propulsion, and weapons systems as well as commercial applications dictate the use of electric power systems capable of outputs of hundreds to thousands of kilowatts (Refs. B-1 and B-2). However, the final decision to choose either a single nuclear reactor or a multiunit conventional system lies in the size, cost, mass, and economics of each system. This is where the choice of an appropriate power conversion system for the nuclear core is of greatest importance. Since the majority of a power system's mass and size are in the power conversion system, an optimal conversion choice will minimize these determining factors.

Any conversion system which is considered must fall within mission and design limits. Mission requirements include automation, maintenance free operation, reliability, ruggedness, long lived, safe, small, lightweight, economic and have a minimum of moving parts (Ref. B-3). In addition to these requirements, the reactor must operate in zero gravity, be radiation and penetration resistant, be launch survivable, be able to withstand high shut down via an earth bound command (Ref. B-3). Most, if not all of these mission requirements can be met if the conversion system is designed with several factors taken into account. Some of these key design factors are:

(1) Efficiency
(2) Mass
(3) Reliability
(4) Size
(5) Peak operating temperature
(6) Heat rejection temperature
(7) Working fluid properties (dynamic)
(8) Lifetime
(9) Vibration and torque

(10) Power range

(11) Modularity

(12) Start-up and shutdown

(13) Power processing

(14) Radiation hardening

All energy conversion systems can be classified as either active (turbine and working fluid) or passive (submacroscale energy conversion techniques). Dynamic systems include the Rankine and Brayton and the free piston stirling engine cycles. Passive systems include thermoelectric, thermionic, magnetohydrodynamic (MHD), and alkali thermoelectric converter conversion techniques. Several hybrid active/passive designs also exist such as a TI/MHD system. This appendix describes each system in some detail. An analysis is then made of each system, which includes descriptions of any mode of each system, which includes descriptions of any current designs using the system as well as the advantages and disadvantages of each, with some emphasis on its compatibility with the heat pipe reactor. The analysis compares the alternative systems and selects the best active, passive, hybrid (if appropriate), and overall systems. "Best" here is defined as the most suitable in the near future for use in a heat-pipe reactor. The choice is based on current literature and research conclusions regarding the requirements and design factors stated earlier.

II. SYSTEM DESCRIPTIONS

1. ACTIVE SYSTEMS

The first power conversion systems discussed are the active systems; Rankine and Brayton cycles, and the free piston stirling engine. These all use a fluid which is superheated to a vapor that turns a turbine and/or alternator.

a. Rankine cycle--The Rankine cycle is a closed liquid cycle that uses a nuclear reactor to boil the working fluid [probably be an alkali liquid metal (such as mercury or potassium), or an organic fluid (Ref. B-4)]. The fluid is boiled to a superheated vapor and expanded through a turbine. The turbine is linked to an alternator which generates usable electric power. The expanded vapor is then condensed by a condensor, which is linked by another liquid metal loop to the space radiator. Electromagnetic pumps can be used as circulators if the working fluid is a liquid metal. A conventional pumping system must be incorporated if an organic liquid is used. The working fluid may be either directly heated in the reactor core or it can be coupled to a heat-pipe reactor. Figure B-1 shows a simplified schematic of a Rankine cycle. The ideal Rankine cycle is composed of:

1-2: Reversible adiabatic pumping

2-3: Constant-pressure heat transfer in the nuclear core

3-4: Reversible adiabatic expansion in the turbine

4-1: Constant-pressure heat transfer in the condensor

These steps are shown on the T-S diagram of Figure B-1. The efficiency, η, of the Rankine cycle is (Ref. B-4) determined by

$$\eta = \frac{\eta_{alt}\,\eta_{turb}\,\Delta H_{turb}(1 - f_{in})}{\Delta H_{total}} \qquad \text{(B-1)}$$

where

η_{alt} = alternator efficiency (~0.95)

η_{turb} = turbine efficiency (~0.81)

F_{in} = fraction of internal power requirements (~0.125)

ΔH_{turb} = isentropic turbine work

ΔH_{total} = total heat input from reactor

Power conditioning and thermal losses must also be considered.

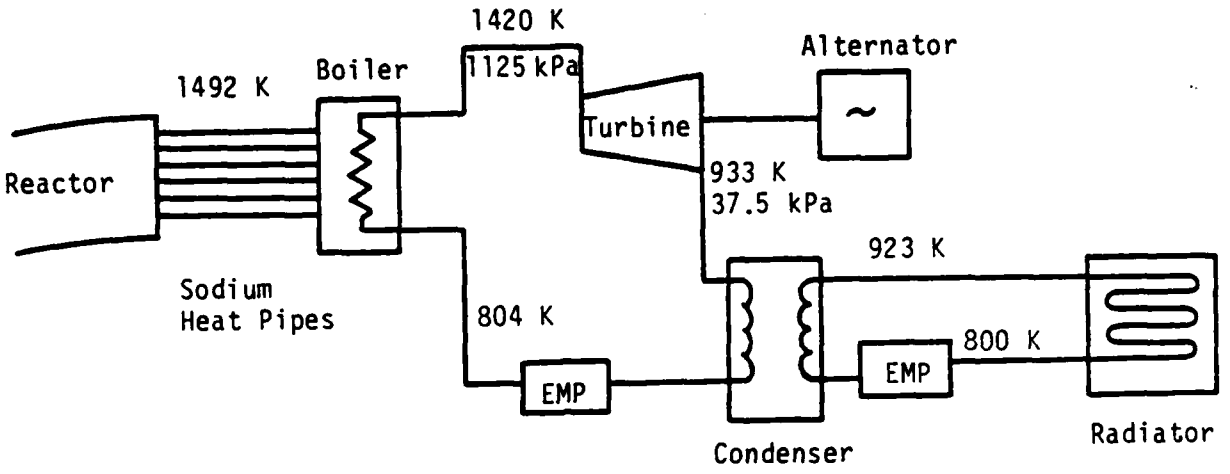

Figure B-1. Schematic of a potassium Rankine cycle (Ref. 1).

b. Brayton cycle--The Brayton cycle is a closed, inert gas cycle. The inert gas will probably be helium-xenon because it is noncorrosive and has an optimizable molecular weight (Ref. B-5). The cycle works by expanding the gas after it has been heated in the nuclear core. Expansion takes place in a turbine-alternator unit which produces a current. The gas leaves the turbine, passes through a reheater, and is condensed. The condensed gas is then reheated by the reheater. Before returning to the core, the gas is cooled in the space radiator. The entire gas cycle can be directly coupled to the core, to an intermediate liquid metal-to-gas heat exchanger, or to a heat-pipe-to-gas heat exchanger. An intermediate working fluid could also be used between the working fluid and radiator. Figure B-2 shows a simplified Brayton cycle along with its associated T-S diagram. The ideal Brayton cycle is composed of:

(1) Constant pressure heat transfer in core

(2) Adiabatic expansion in the turbine

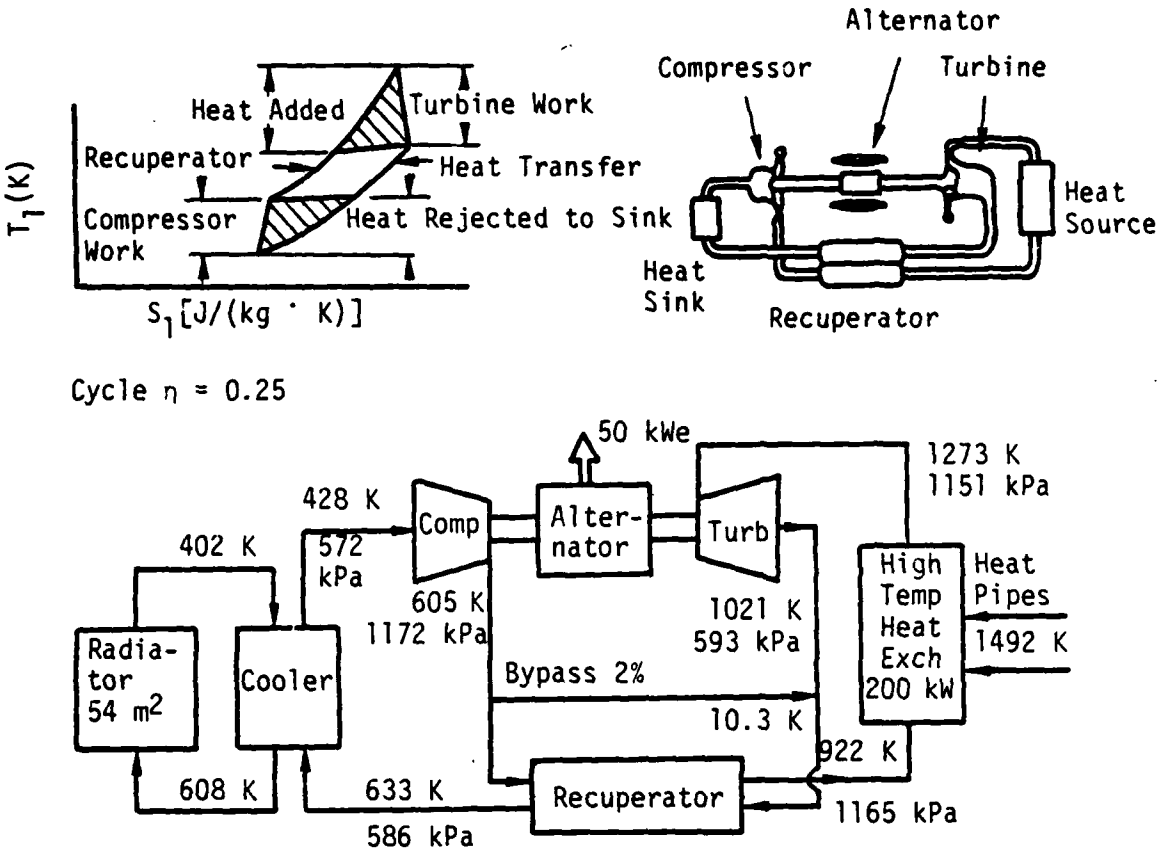

Figure B-2. Brayton cycle schematic (Ref. 1).

(3) Heat rejection to radiator

(4) Compression

These steps are shown in the T-S diagram. The efficiency (η) of the Brayton cycle is (Ref. B-4):

$$\eta = \frac{(T_1 - T_2) - (T_4 - T_3)}{T_1 - T_5} \qquad \text{(B-2)}$$

where

T_1 = turbine inlet temperature, K

T_2 = turbine outlet temperature, K

T_3 = compressor inlet temperature, K

T_4 = compressor outlet temperature, K

T_5 = recuperator outlet, cold pass temperature, K

The mass of the Brayton cycle conversion system is thought to be around 400 kg plus 800 kg/MW including redundancy features (Ref. B-4).

c. Free-piston Stirling engine--The FPSE is the newest member of the active space nuclear conversion system club but has the potential of being the most efficient as well as having a low specific mass and a high heat rejection temperature. The FPSE is a thermal-to-mechanical-to-electrical machine. The mechanical-to-electrical conversion is accomplished by a linear alternator. The thermal-to-mechanical portion of the engine is a bit more complicated but is accomplished by using the damped oscillation of two opposing pistons. One piston is the displacer piston and the other a power piston. Both use an engine working fluid such as helium. This fluid is heated and cooled by a special heat exchanger, which is linked to the reactor coolant and radiator. The exchanger contains three sections linked together: a heater section, a storage section, and a cooler section. The gas moves in a cycle traveling from the heater through the storage section and on to the cooler and then in reverse. The action of both pistons, which are 90 deg out of phase, are characterized by

(1) Constant-volume heating compression
(2) Constant-temperature, nonadiabatic expansion
(3) Constant-volume cooling expansion
(4) Constant-temperature compression

The T-S diagram of the ideal FPSE cycle is shown in Figures B-3 and B-4. Figure B-3 also shows a simplified schematic of a Stirling cycle power conversion free-piston linear alternator.

The efficiency of the FPSE is complicated and no single formula is available for its estimate. However, Figure B-5 shows a plot of efficiency versus cooler temperature for differing heater temperatures. Reference B-6 estimates an efficiency of about 30 percent, neglecting power conditioning and thermal losses.

2. PASSIVE SYSTEMS

The passive energy conversion systems create electricity through atomic processes (such as the Seebeck or MHD effects) rather than by a turbine generator. This section describes the thermoelectric, thermionic, magneto-

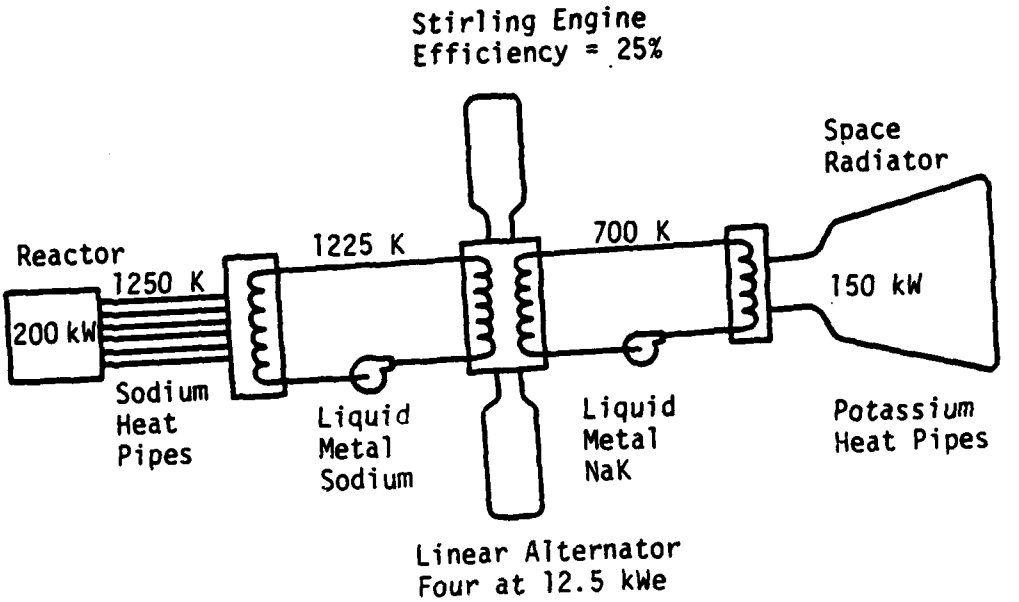

Figure B-3. Stirling cycle power-conversion free-piston linear alternator.

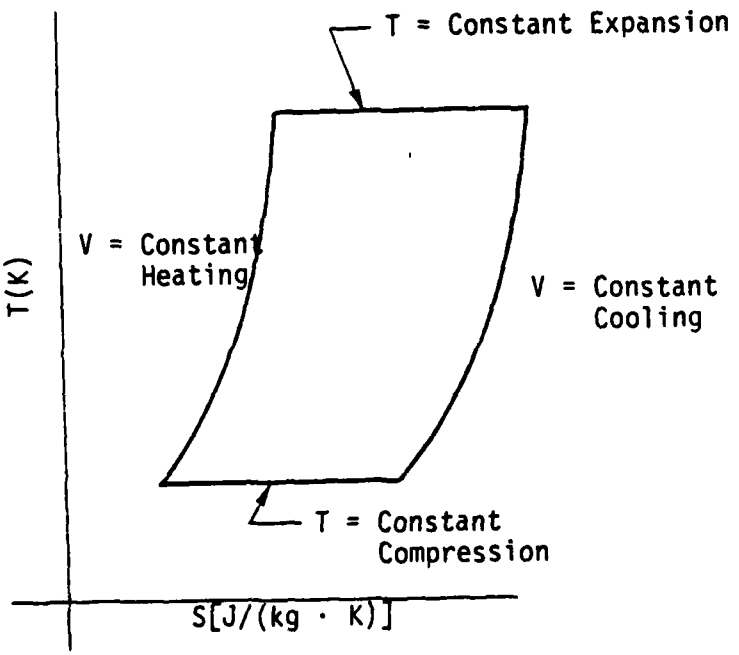

Figure B-4. Ideal Stirling cycle (Ref. 1).

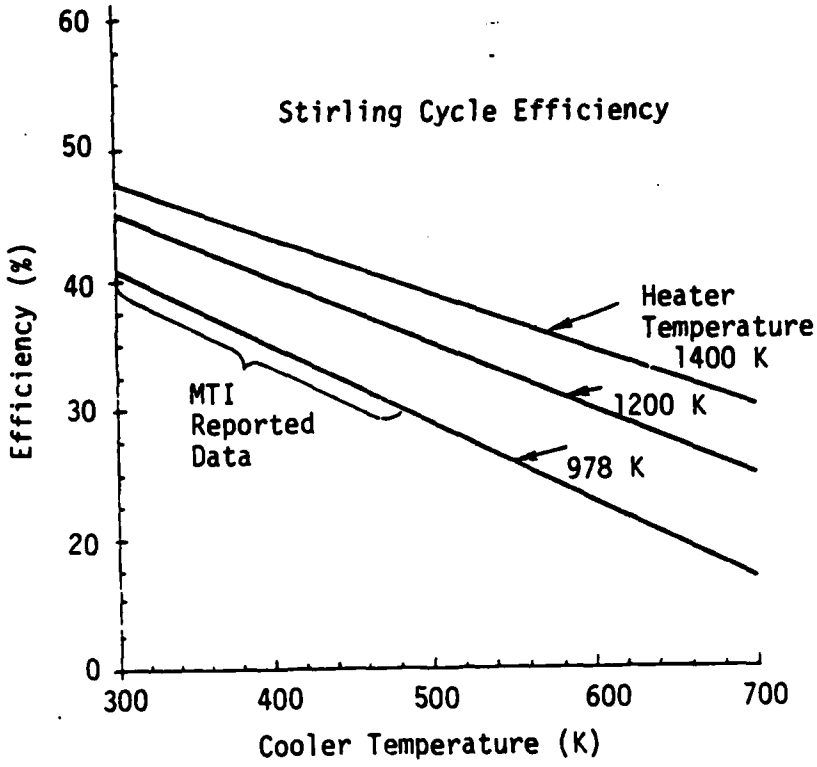

Figure B-5. Stirling cycle efficiency (Ref. 1).

hydrodynamic, and alkali metal thermoelectric converter passive energy conversion systems.

a. Thermoelectric converter systems--The thermoelectric converter operation depends mainly on the Seebeck effect, i.e., a potential is produced in a circuit of two dissimilar materials if the two junctions are maintained at different temperatures. The Seebeck coefficient, S, is a function of the material being considered and mathematically is

$$S = \frac{dE_s}{dT} \tag{B-3}$$

where

S = Seebeck coefficient

E_s = Thermoelectric potential

T = Temperature (K)

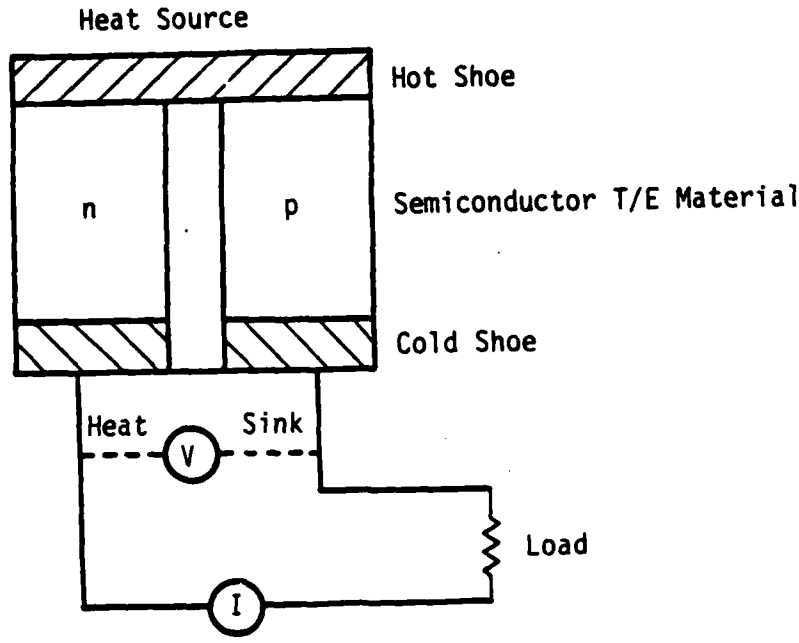

Figure B-6. Schematic of thermoelectric cell (Ref. 1).

Equation B-3 can be integrated for two materials (a and b) and temperatures T_H and T_L and to give

$$E_s = \int_{T_L}^{T_H} S_{ab}\, dT \qquad \text{(B-4)}$$

Experimentally determining S for different materials showed that n-p semiconductors have high Seebeck coefficients and, hence, are used widely in TE converters.

A typical n-p TE generator is shown in Figure B-6. The efficiency of the generator is (Ref. B-6)

$$\eta_{TH} = \frac{M\,\Delta T}{(1 + M)\,T_H + (1 + M)^2/Z - \Delta T/2} \qquad \text{(B-5)}$$

where

M = ratio of external load resistance to generator resistance

T_H = hot leg temperature

ΔT = temperature drop across generator

Z = figure-of-merit of the generator

and $$Z = \frac{m^2 \bar{S}_{pn}^2}{K_g R_g} \tag{B-6}$$

where

m = number of p-n legs

$$\bar{S}_{pn} = \int_{T_L}^{T_H} \frac{(S_p - S_n)\, dT}{T_H - T_L} \tag{B-7}$$

$$R_g = m(R_p + R_n) \tag{B-8}$$

$$R_p = \rho_p L_p / A_p \tag{B-9}$$

$$R_n = \rho_n L_n / A_n \tag{B-10}$$

ρ = electrical resistivity

L = semiconductor leg length

A = leg cross-sectional area

$$K_g = m(K_p + K_n) \tag{B-11}$$

$$K_p = K_p A_p / L_p \tag{B-12}$$

$$K_n = K_n A_n / L_n \tag{B-13}$$

K = semiconductor thermal conductivity

It can be seen that the figure-of-merit is an important determinant of the TE converter's efficiency. Note that Z is a function of the dimensions of the generator legs (A,L) and the semiconductor physical properties (S,K,ρ).

References B-3 and B-5 contain the physical properties of various semiconductors under consideration for space power use as a function of temperature. The figure-of-merit for various materials is shown in Figure B-7. Figure B-8 shows the effect doping has on a p-type material's figure-of-merit. Silicon-germanium semiconductor material is the choice TE material to date. Recently, doping Si-Ge with gallium phosphate resulted in a 30 percent improvement over the figure-of-merit of plain SiGe (Ref. B-5). Telluride TE material was used with success in many RTG missions such as Pioneer, Viking, and SNAP-27. Si-Ge was used in the Mariner and SNAP-19 missions.

An approximate relationship for conversion efficiency is (Ref. B-5):

$$\eta = 1/4\ Z\ \Delta T \qquad (B-14)$$

An alternate form of Equation B-14 is given in Reference B-4 as

$$\eta = \left[\frac{T_H - T_C}{T_H}\right]\left[\frac{\sqrt{1 + Z\,T} - 1}{\sqrt{1 + Z\,T} + T_C/T_H}\right] \qquad (B-15)$$

where

T_C = cold side temperature

T = average temperature C

The TE conversion system is extremely simple. The reactor is cooled either by heat pipes or a liquid metal coolant system. The heat is transferred to the radiator where it is rejected to space. The TE modules are situated between the hot side of the radiator (from the reactor) and the cold side (space side) of the radiator. The temperature gradient across the TE module is (neglecting thermal losses in the heat pipe) essentially the core temperature minus the rejection temperature of the radiator. Figure B-9 shows a typical TE module for use in a heat-pipe reactor.

b. Thermionic generator--The second passive method of converting thermal energy into electric energy is by a thermionic generator. Basically, this device works by using the heat produced by the reactor to boil off electrons from an emitter surface and condensing them on a collector surface. The emitter and collector surfaces are separated by a small gap,

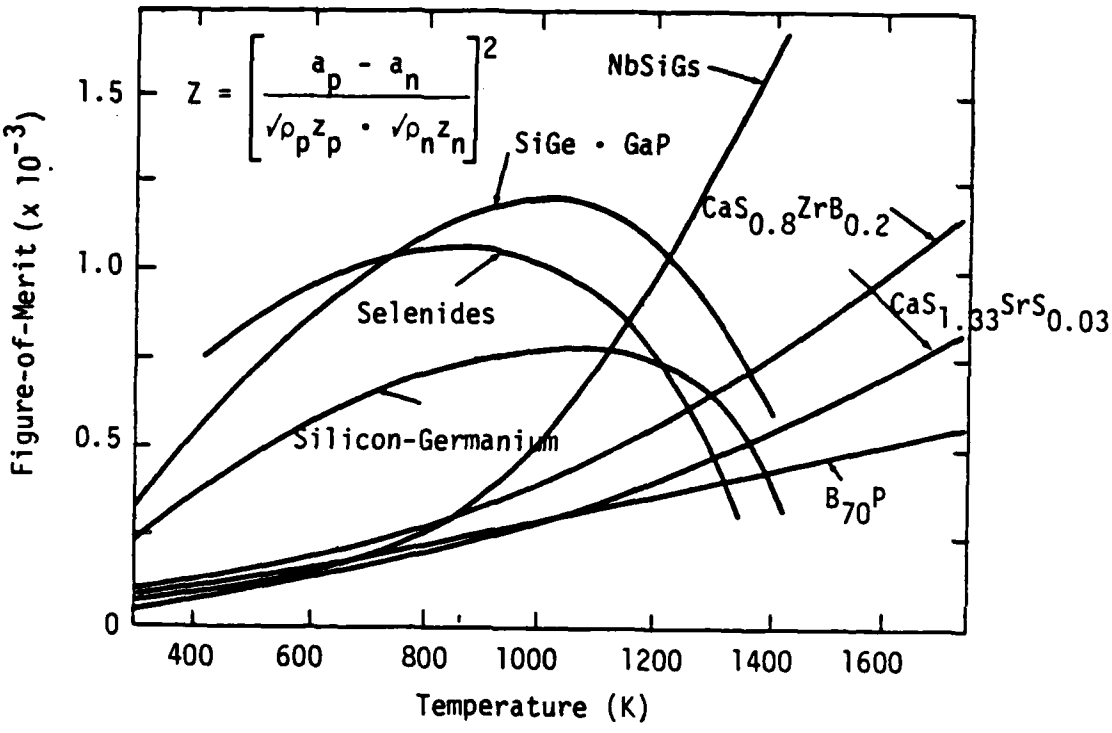

Figure B-7. Figure-of-merit for thermoelectric materials (Ref. 1).

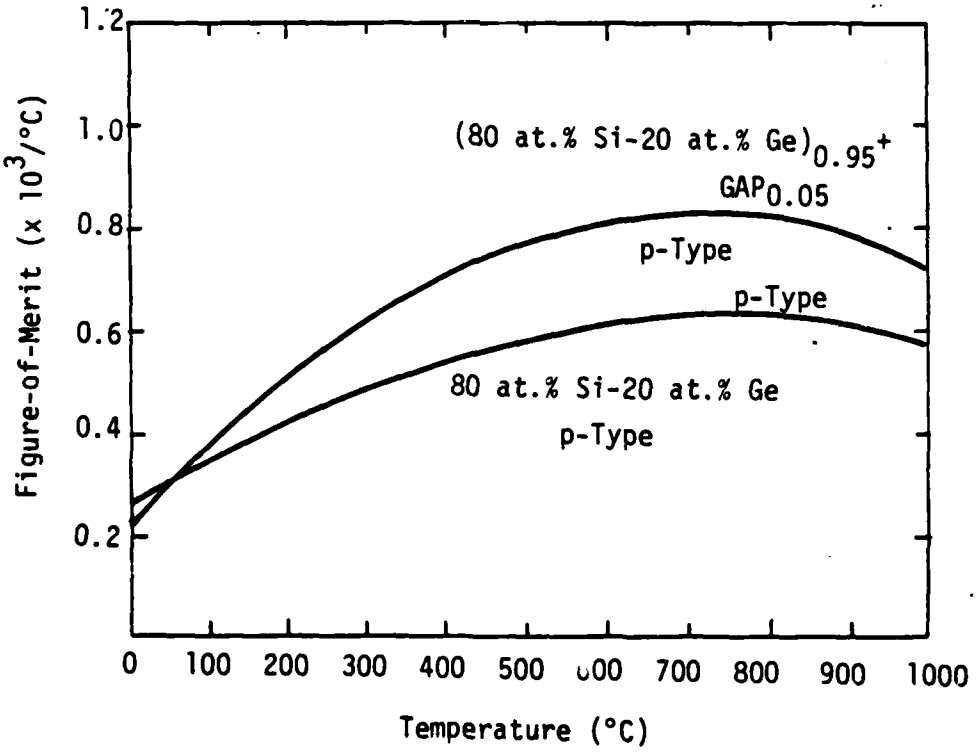

Figure B-8. Figure-of-merit as a function of temperature, p-type material (Ref. 1).

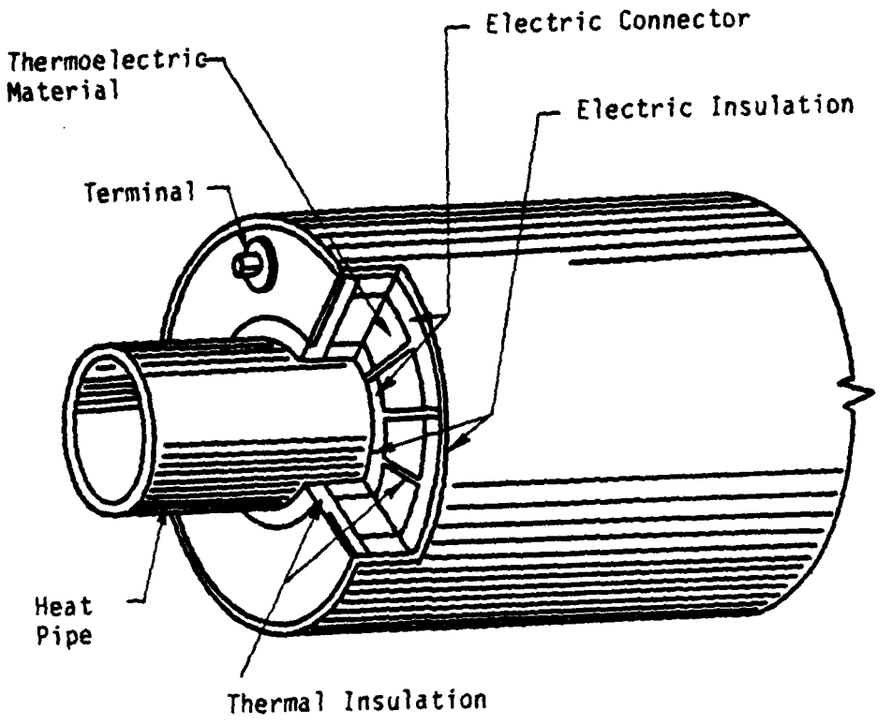

Figure B-9. Thermoelectric module (Ref. 1).

through which these electrons must cross. This electron flow is the current which is used. Figure B-10 shows a simple schematic of this process.

The method by which the TI module works is well known (Refs. B-3, B-5 and B-6). Potential barriers of the emitter (ϕ_E) and collector (ϕ_C) must be overcome in order for the electrons to cross the gap. The Richardson-Dushman equation (Eq. B-16) states the relationship between current density and temperature (Ref. B-6).

$$J_0 = M\,T^2 \exp(-e\phi_E/KT) \qquad (B\text{-}16)$$

where

J_0 = current density, m^2

M = material constant, $A/m^2\ K^2$

T = emitter temperature, K

ϕ_E = emitter work function, eV

e = electron charge

K = boltzmann constant

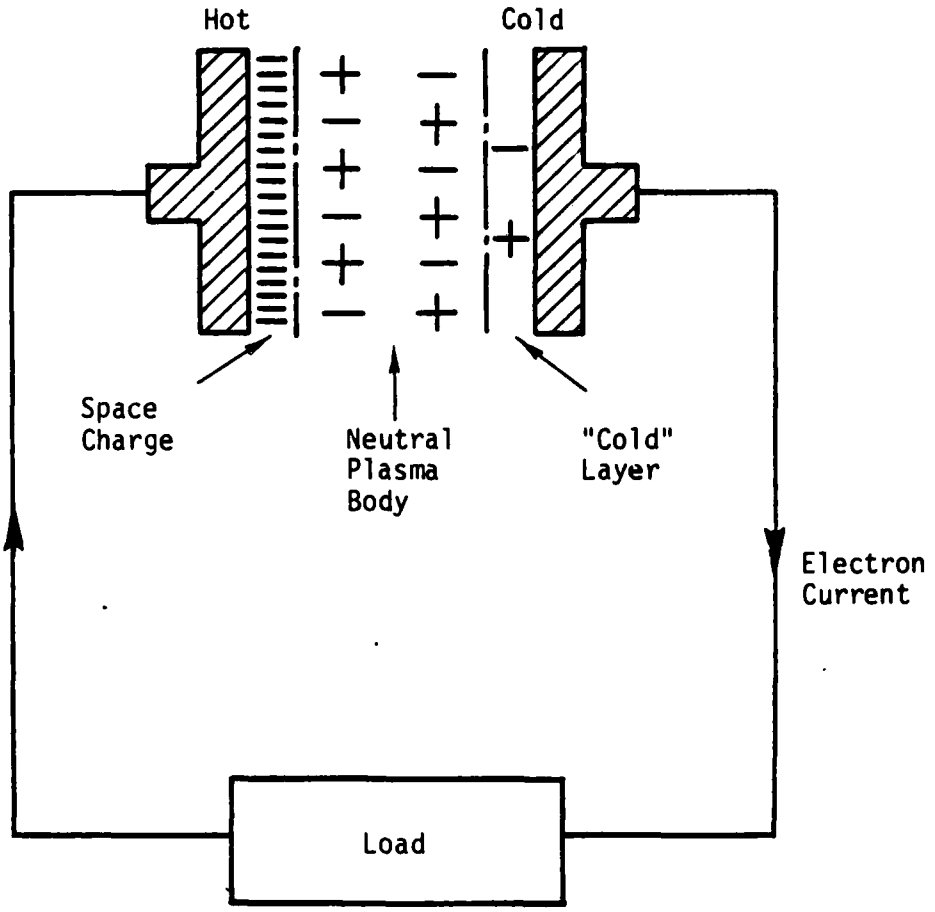

Figure B-10. Schematic of basic thermionic converter (Ref. 1).

Most TI designs use a cesium plasma or vapor between the two plates to drop the barrier energies (or work functions) substantially because cesium has a low work function itself. However, the addition of cesium causes losses due to arc dropping and electron scattering (Ref. B-5), so that the usable power is not simply the current density times the emitter area times the voltage drop across the external load resistance, but instead is

$$P_L = 0.9\ J[kT_E\ \ln(AT_E^2/J) - V_B] \tag{B-17}$$

where V_B is the Barrier index and is the sum of the losses due to the addition of a cesium vapor. The heat input required to the emitter is (Ref. B-5)

$$Q_{IN} = 1.8 \times 10^{-3}\ J\ T_E + 1.2 \times 10^{-12}\ (T_E^4 - T_C^4) \tag{B-18}$$

which directly leads to a TI conversion efficiency of (Ref. B-3)

$$\eta = \frac{P_L}{Q_{IN}} = \frac{0.9\ J[kT_E\ \ln(AT_E^2/J) - V_B]}{1.8 \times 10^{-3}\ J\ T_E + 1.2 \times 10^{-12}\ (T_E^4 - T_C^4)} \tag{B-19}$$

A more recent publication states the efficiency as (Ref. B-4)

$$\eta = 0.9\ J\ V_0/(1.1\ P_{in}) \tag{B-20}$$

where

$0.9\ J$ = current flow attenuated by joule heating, A

P_{in} = power input plus lead heat bypass, W

V_0 = output voltage, volt, $\simeq (\psi - \phi_c - V_d)$

ψ = effective barrier height, eV

ϕ_c = collector work function, eV

V_d = arc drop, eV

Currently there are two options by which TI conversion technology can be used in a space reactor. Out-of-core operation involves using heat pipes

to transfer the heat away from the core to a set of TI converters. The advantage of this system is the minimization of radiation exposure to the converters. The in-core concept places the modules directly in the core. Here, the temperature is higher but radiation damage becomes significant. Figure B-11 shows an in-core converter, heat pipe assembly, and reactor. Efficiencies on the order of 15 percent can be expected with power densities near 6 W/cm (Ref. B-5). The major blocks to development of this conversion technique are problems with the materials used and the need for demonstrating the technique.

c. Magnetohydrodynamic conversion--Magnetohydrodynamic conversion involves, just as its name implies, the creation of electric power by flowing a river of high velocity ionized particles through a magnetic field. This is possible because, as Faraday showed in the 19th century, an electromotive force (EMF) is created when a charged particle passes perpendicular to a magnetic field. Mathematically, this is

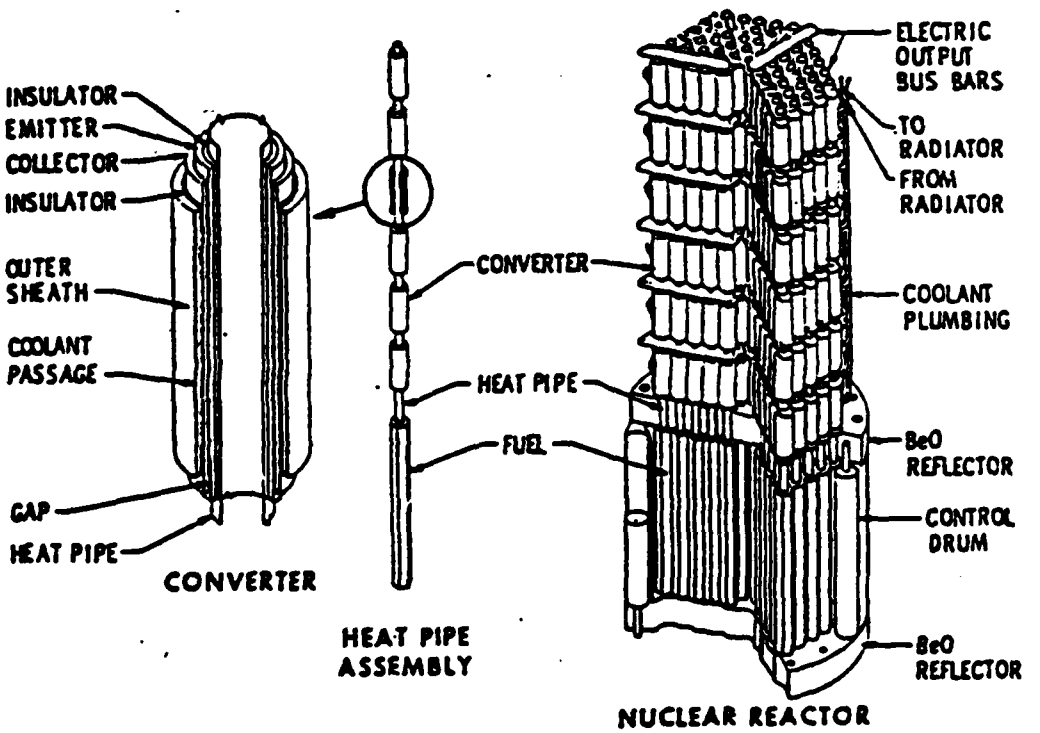

Figure B-11. NEP system with thermionic power conversion on reactor side of the neutron shield (Ref. 1).

$$\varepsilon = \bar{L} \cdot (\bar{V} \times \bar{B}) \qquad (B\text{-}21)$$

where

ε = emf (V)

$\bar{L}$ = length (m)

$\bar{V}$ = velocity (m/sec)

$\bar{B}$ = magnetic field strength (W/m^2)

This is a simplified equation but it shows the overall relationship between the usable current produced by an MHD device and the particle's velocity, the device's dimensions, and the magnetic field strength.

Figure B-12 is a simplified schematic of an MHD nuclear conversion system. It contains all of the necessary components; such as the reactor, the space radiator, and the MHD conversion unit. The working fluid, which probably will be argon, is ionized in the high temperature region of the reactor. It is then expanded in an MHD channel such as in Figure B-13, which is connected to an outside resistive load. The hot gas is cooled in the radiator and then compressed and stored for further use. An open cycle design calls for the expulsion of the fluid after it traverses the MHD channel. A thermodynamic T-S diagram of the closed cycle is shown in Figure B-14. An open cycle differs in that it does not contain steps 3-4 and 4-1.

A working fluid such as argon cannot be ionized enough at the maximum operating temperature of the reactor, so a seeding of the working fluid is required in most designs. This seeding involves adding a small fraction (~0.5 percent) of an element that has a low ionization potential. This element will be a liquid metal such as cesium (which is favored) or potassium. The easily ionizable seed allows a greater ionization of the working fluid and, hence, a greater amount of current is produced. This is possible since a greater ionization means a larger electrical conductivity. An alternative method calls for the use of a liquid metal working fluid that is injected with some gas as opposed to straight seeded gas. This foamed fluid would be separated into its constituent parts upon channel exit. This

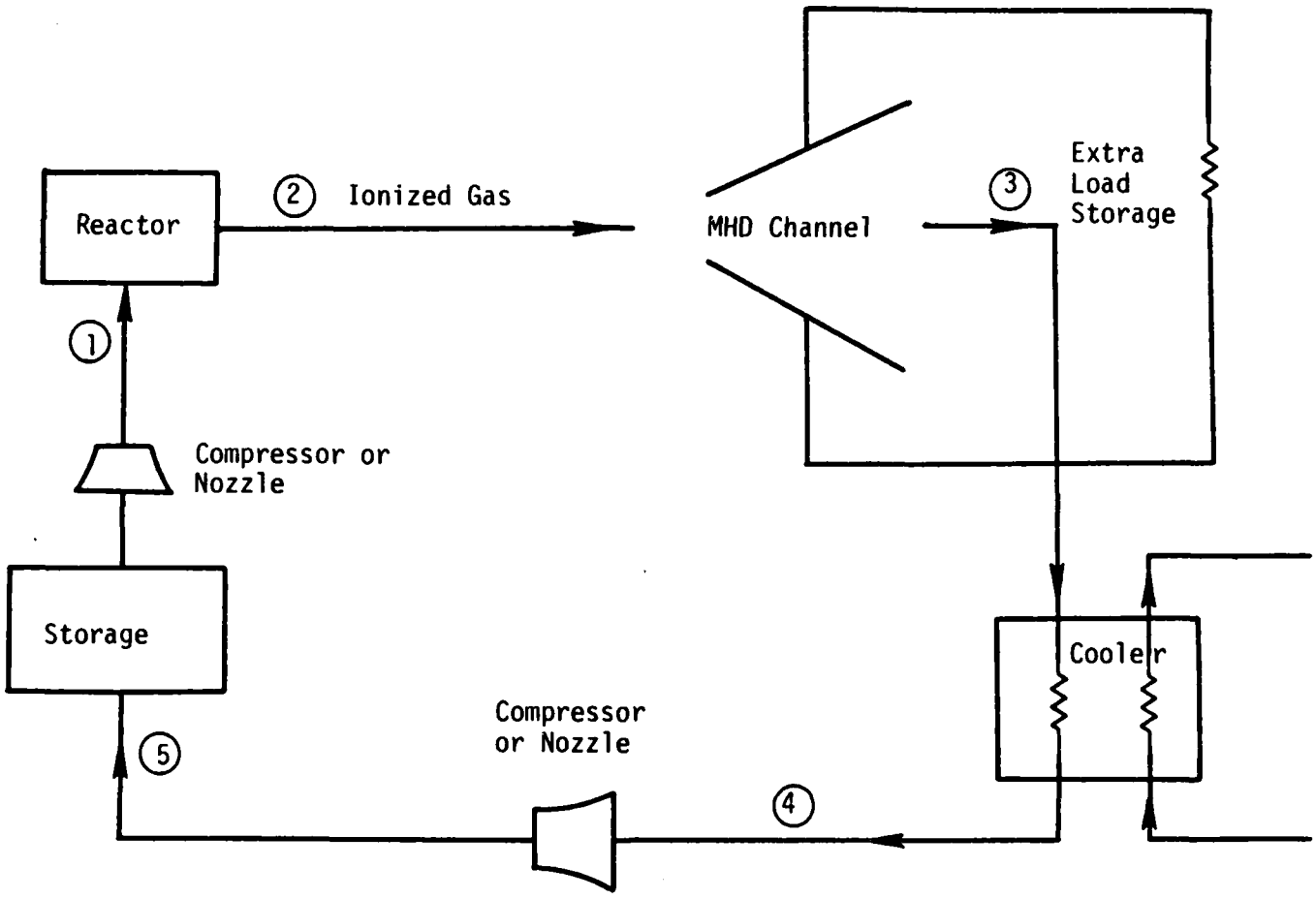

Figure B-12. Schematic of a MHD power cycle for a nuclear space reactor system (Ref. 9).

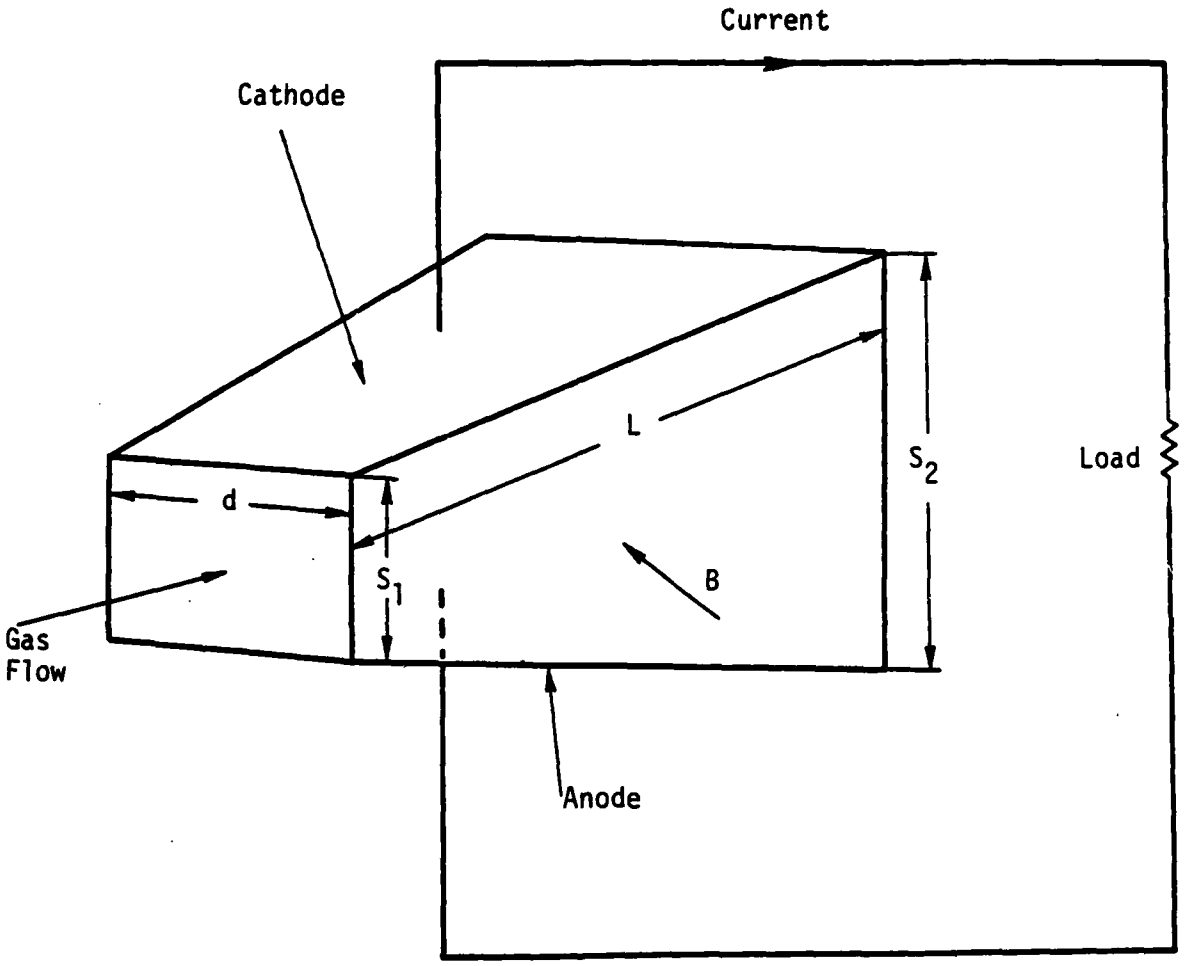

Figure B-13. Components of an MHD channel (Ref. 9).

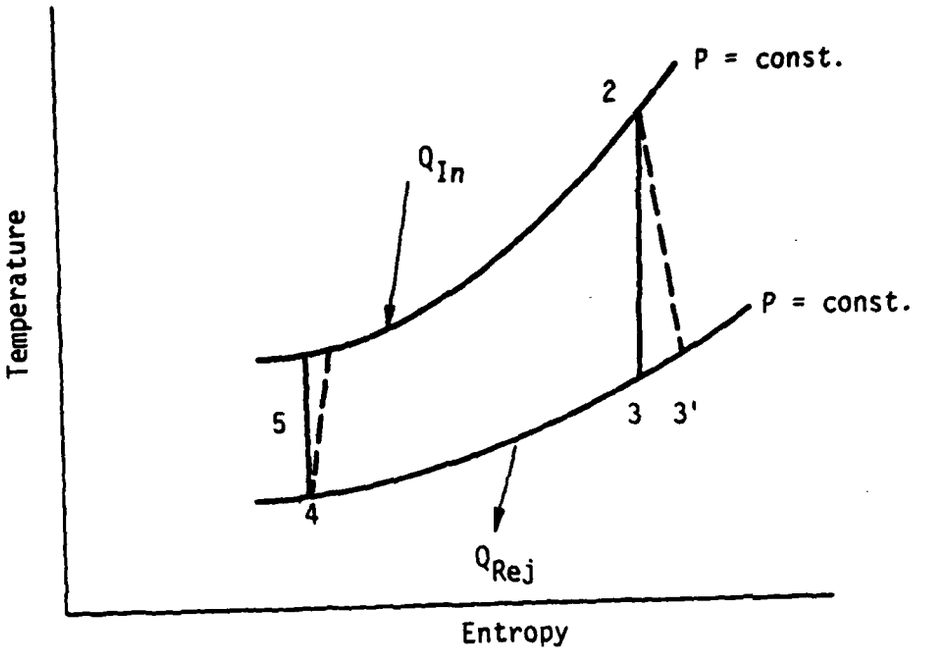

Figure B-14. Temperature-entropy diagram for the MHD cycle (Ref. 9).

mostly liquid metal working fluid has a large electrical conductivity and hence a larger specific power.

The useful power output of the MHD channel can be calculated by using the following equation (Ref. B-7):

$$P_{out} = \sigma V^2 B^2 (1 - K) K \left(\frac{S_1 - S_2}{2} \right) L d \qquad \text{(B-22)}$$

where

P_{out} = power output, W

σ = electrical conductivity, $\Omega^{-1} \cdot m^{-1}$

V = fluid velocity, m/s

B = magnetic field strength, G

K = electric conversion efficiency

S_1 = distance between electrodes at channel entrance, m

S_2 = distance between electrodes at channel exit, m

L = channel length, m

d = channel width, m

Figure B-13 shows the corresponding device dimensions.

The power output (P_{out}) (as shown in Equation B-22) depends on the channel dimensions, the magnetic field strength, and the fluid velocity. However, the electrical conductivity of the fluid now enters the scene. Higher working fluid conductivities lead to larger power outputs. The T-S diagram of Figure B-14 shows that the overall efficiency is similar to a Brayton cycle (Ref. B-7) with a possibility of exceeding 50 percent or more (Ref. B-3).

d. Alkali metal thermoelectric converter--The final passive conversion system discussed here is the alkali metal thermoelectric convertor device. The AMTEC concept is an old one which only recently has received attention as a possible space nuclear energy conversion system concept. The theory behind AMTEC is the use of the electrochemical permselective barrier material β"-alumina. This material has an electronic conductivity much less than its ionic conductivity and acts as a "straw," sucking Na^+ ions from a high temperature liquid sodium reservoir to a low pressure sodium vapor reservoir (Ref. B-4). Electrodes are inserted into the low pressure reservoir and act as collectors of migrating Na^+ ions. An external load can then be connected across the electrodes and the high temperature reservoir to complete a circuit. A simple diagram of the device is shown in Figure B-15. The desired current is an electron flow that goes in the opposite direction of the Na^+ flow. As the electrons meet the Na^+ ions, the latent heat of vaporization of the sodium is released and the Na vapor is condensed on a condensor plate. This condensed sodium is pumped to the core where it is heated and returned to the high temperature reservoir. One large AMTEC device or several smaller ones may be used with the final number being an optimum balance between redundancy and weight.

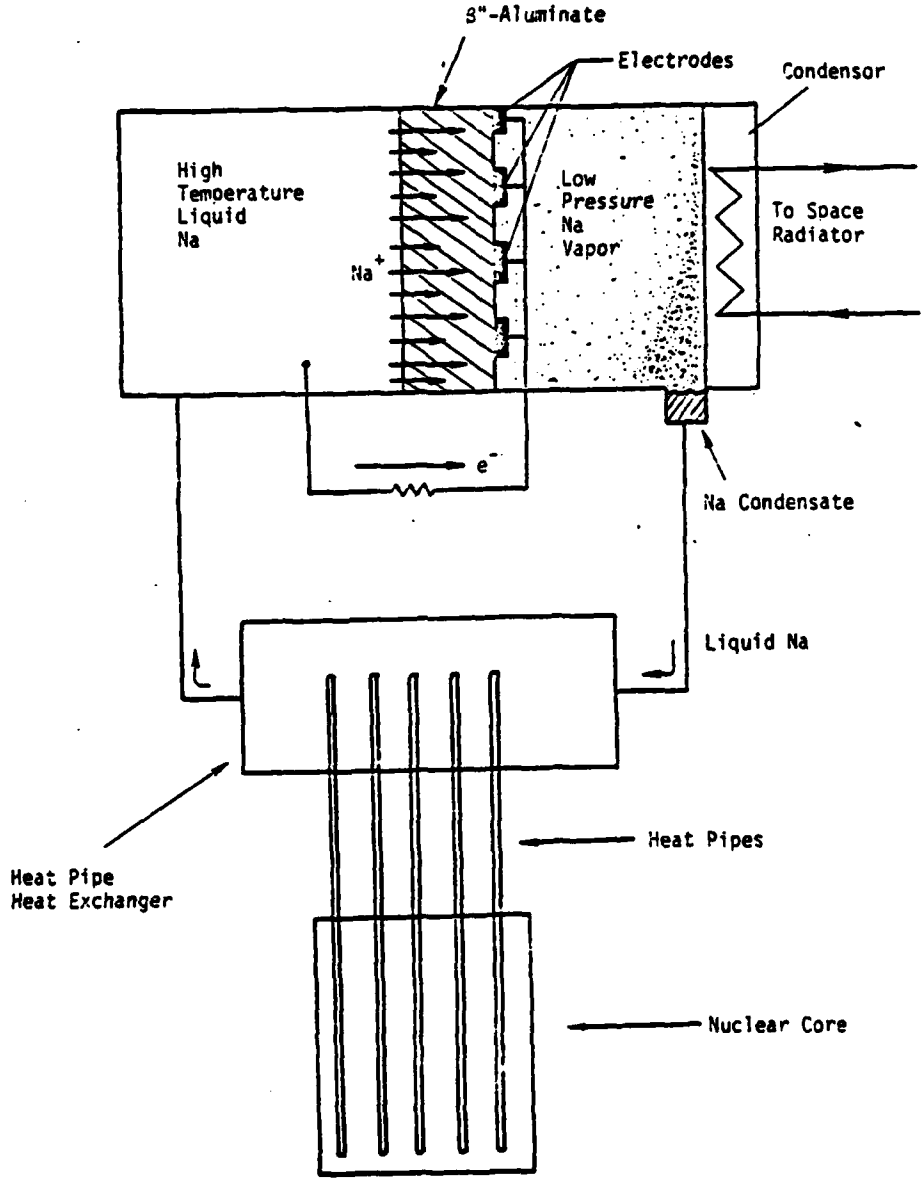

Figure B-15. AMTEC device with reactor configuration.

Efficiency of the AMTEC device is found using Equation B-23 (Ref. B-4):

$$\eta = \frac{IV}{IV + I/F(L + C\Delta T) + Q_{loss}} \qquad \text{(B-23)}$$

where

I = total current flow, A

V = total voltage, V

F = faraday's constant

L = latent heat of vaporization

C = sodium liquid specific heat

ΔT = sodium temperature difference, K

Q_{loss} = all parasitic heat losses, W

Losses will also occur in the electrical power conditioning equipment. Efficiencies are estimated to be somewhere between 14 and 23 percent. Conversion subsystem mass is approximately 400 kg/MW (Ref. B-4).

III. ANALYSIS

The analysis of the space power conversion systems is a complex and detailed subject and in the future, if not presently, a comprehensive book can be written on the subject. However, the analyses of the systems discussed in this appendix are abbreviated since the scope of this report is limited. Current and past designs are reviewed where appropriate with emphasis on the most recent investigations. The advantages and disadvantages of each system are presented, with an application to the heat-pipe reactor being a primary consideration.

1. RANKINE CYCLE

The Rankine cycle, as mentioned previously, is a closed system utilizing either a liquid metal or organic fluid to generate electric power. In general, the Rankine cycle is characterized by a high heat rejection temperature (800-925 K) hence a small radiator size, high cycle efficiency (19 percent), and demonstrated technology (Ref. B-8).

In fact, the radiator of a Rankine cycle is thought to be the smallest of any of the conversion systems (Ref. B-4). One reason behind this small radiator size is the operating temperature of the working fluid. Alkali liquid metals used in the Rankine cycle take advantage of the reactor's high temperature, wide liquid ranges, and high heat transfer capabilities at low pressures (Ref. B-9). If the corrosive natures of liquid metals are considered, two generic types of conversion links to the core can be considered. The first involves a turbo-alternator directly coupled to the liquid metal vaporized in the core. The other option involves using an intermediate heat exchanger. The direct couple works best utilizing potassium as the working fluid. Either potassium or cesium can be used if the intermediate exchanger is desired (Ref. B-9).

If an organic fluid is used as the working fluid, the advantage of a small radiator is lost because the organic fluids must operate at low temperatures. By themselves organic Rankine cycles are inefficient, but when combined with thermoelectric devices they can have efficiencies approaching those of liquid metal Rankine cycles (Ref. B-10).

Certain important points arise when organic and liquid metal systems are compared. Organic fluids must be used at low temperatures because they

tend to thermally decompose at high temperatures. Maximum temperatures of about 600-650 K are foreseen (Ref. B-5). Organic fluids are considered to be near term technology because no new materials need to be developed for their use as do liquid metal cycles. The organic cycle has a higher reliability because of lower operating temperature and pressure, lower turbine speed, and less required redundancy (Ref. B-10). The interface heat exchanger between the heat-pipe reactor and the organic cycle would also be simpler because of low corrosiveness of organic fluids.

The higher temperatures of the liquid metal cycles would lead to high efficiencies and small radiator and heat exchanger sizes. Liquid metal cycles are therefore attractive at power levels between 1 and 50 MW electric. There has also been extensive ground operational experience with liquid metals as well as proven technology using the Rankine cycle. Certain problems need to be addressed, such as, the zero gravity separation of two-phase flow in the system. Liquid metals are extremely corrosive in turbines if anything but pure vapor phase comes in contact with the turbine's blades. Liquid metal also allows an electromagnetic pump to be used.

Only some work has been done to date in the area of organic Rankine cycle design. There have been 50,000 h of experience accumulated with the Dowtherm A and Toluene systems. This experience showed an AC conversion efficiency of 19 percent and a DC efficiency of 18 percent (Ref. B-10). The reliability is estimated at over 95 percent for a 7-yr life span. An organic cycle is currently under development by the Sundstrand Corporation for the kilowatt isotope power system (Ref. B-11). Obviously much work needs to be done in this area before further consideration for space use will occur.

On the other hand, much work has been accumulated in the use of liquid metal Rankine cycles. Nasa Lewis studied a 300 kW potassium cycle as well as the SNAP-8 mercury cycle, which used NaK to cool a U-ZrH reactor (Refs. B-4 and B-5). Both studies used a 1400 K inlet vapor to study component materials and compatibility but were ended before completion. This left the data base of the system questionable. The overall Rankine cycle has been studied extensively by NASA-Lewis (Ref. B-5).

The most recent design of a multimegawatt space nuclear reactor can be found in Reference B-11. Here, a cladded, ceramic fuel reactor cooled by

potassium utilizes a closed Rankine cycle. The potassium is boiled at 1365 K and rejects 82 percent of its thermal power to space via a heat pipe radiator at 1020 K. This 5-MWe, 5-yr life concept uses a flywheel system to produce powers up to 100 MWe for 100 s or less. This 18 percent efficient device has an estimated radiator area of 660 m^2 and a total mass of 11,000 kg.

2. BRAYTON CYCLE

As mentioned earlier, the Brayton cycle can be either a closed or an open gas system. It utilizes a single-stage radial turbine, compressor, and alternator all on the same central shaft with foil-type gas bearings (Ref. B-4). Similar to the Rankine cycle, the Brayton cycle uses a high temperature working substance, probably helium-xenon. This high temperature leads to such benefits as high efficiency (25 percent) and a relatively small radiator size. The total system mass will also be small. Accompanying these advantages are the same material problems associated with the limited creep allowed in the turbine blades. Hopefully, ceramic turbines can be developed by 1990 that can operate at 2000 K. Larger sized components and lower pressure drops in the system will result in higher overall efficiencies (Ref. B-5). Two complete Brayton cycles will probably be needed for redundancy. Another disadvantage is the need to start the system up by external means. It may also be necessary to assemble the system in space because of its large size and mass. A major advantage is the extensive technology and experience available in this area. Much design and testing knowledge exists in the electric power range of a few kilowatts to tens of megawatts (Ref. B-12). Development and improvement in high temperature gas turbines is being undertaken currently as well as for use by the aircraft industry and for other ground uses (Ref. B-4).

Current designs include a 52-MWe unit the size of a VW van that has a specific weight of 1.8 lb/kW using 1700°F inlet turbine temperatures. Low power level turbine systems have been tested in the 2-15 kWe range. A space use designed Brayton cycle has been run for more than 30,000 h to demonstrate reliability and life of the components (Ref. B-5). The inlet turbine temperature was about 1150 K and an overall efficiency of 29 percent was observed with high reliability (Ref. B-4).

3. FREE-PISTON STIRLING ENGINE

The free-piston stirling engine is relatively new on the scene of space nuclear power applications. However, the FPSE is extremely promising. It is mechanically simple and has high thermodynamic, electrical, and mechanical performance. This is true because there are only two moving parts; the piston and its attached alternator component, and the displacer. The efficiency of the FPSE is thought to be high, approaching Carnot efficiency (Ref. B-13). In addition, the FPSE has the promise of a low system mass with a high heat rejection temperature and, hence, small radiator size. The FPSE has one of the smallest specific weights of any of the other conversion systems: on the order of 100 kWe and 300 kg mass. The specific area of the FPSE is thought to be only greater than those of the AMTEC or K-Rankine cycles. High performance, long life, and low vibration are expected.

A disadvantage of the FPSE is the need for extended heat transfer surfaces in order to bring about isothermalization of the expansion and compression spaces. Regenerator problems also exist as well as high temperature compatible materials (Ref. B-4). A serious question is whether the machine can be balanced in a zero gravity environment. The alternator must also be cooled below the heat sink temperature (Ref. B-13). A liquid metal intermediate loop must also be used instead of a large volume, direct gas cooled concept. Redundancy would require multiple piston-alternator units and since the major weight component of the system is the alternator, a larger system mass will occur (Ref. B-5).

The current status of development of the FPSE is in the infant stage. 1-, 3-, and 10-kWe output engines have been built, all with good but not outstanding results (Ref. B-13). Currently, a FPSE linear alternator convertor is being tested at Mechanical Technology Incorporated under the supervision of the Department of Energy (Ref. B-5). A FPSE conversion system design can be found in Reference B-5. Its system power is 50 kWe and has an overall net efficiency of 30 percent. A total mass of 400 kg is estimated. Transportation applications of the FPSE engine are being investigated by Phillips and the Ford Motor Company (Ref. B-5).

4. THERMOELECTRIC CONVERTER

The thermoelectric convertor, as described in Section II-2a, utilizes the electric potential formed across a circuit of two dissimilar materials

at different temperatures. The TE convertor is well developed and holds much promise as a near term candidate for space power conversion.

The prime attractiveness of the TE convertor is its lack of moving parts. In-flight experience with it has been extensive and has proven it to be reliable for continuous operation for up to 10 yr. This experience lies mainly in the area of radioisotope thermal generators, which use telluride as a base TE material. Silicon-germanium must be used for the high temperatures since it does not sublime at higher temperatures as does telluride. Compared to other devices, TE conversion has an average specific weight and an above average specific area (Ref. B-14).

One of the major disadvantages of TE conversion is its low efficiency, currently <10 percent. This means that large reactors are needed for the desired megawatt power levels. Design and uniform fabrication of each TE module might present a problem since construction of each module to exact specifications is difficult. Improved performance will come with the introduction of semiconductor materials with higher figures-of-merits. Efficiencies might surpass the 10 percent mark in the near future.

Experience in the area of actual performance comes from the many uses of TE conversion techniques in past space missions. Telluride semiconductor material was used in the SNAP-3A, Nimbus III, Pioneer, Viking, Transit and SNAP-27 missions. Si-Ge material was used in the MHW-LES 8/9, Mariner, and SNAP-10A missions (Ref. B-5).

Many designs utilizing a TE conversion system exist but the best design so far is the Los Alamos National Laboratory's heat-pipe reactor design which uses thermoelectric conversion modules.

5. THERMIONIC CONVERSION

The thermionic conversion module uses heat to produce a usable current and therefore becomes more efficient as the operating temperature increases. A TI system will have a low specific area and one of the lowest specific weights of any conversion system. High emitter temperatures (1650 K) lead to efficiencies of about 15 percent (Ref. B-5). Out-of-core designs allow optimization of both the reactor core and the TI modules. Since the TI system has no moving parts, high reliability and simplicity result. Redundancy is easily accomplished by incorporating excess TI modules. Current

system designs have subsystems which are within existing material data bases.

Disadvantages of thermionic conversion are the resulting low efficiencies and material difficulties. In-core TFE's are continuously undergoing irradiation as well as high temperatures. The integrity of the cesium vapor envelope is affected by these conditions and is a major block to long life. Electrode distortion can also cause failure.

Practical converters were demonstrated in the 1960s and results indicated a successful 5-yr life span of a 8-W/cm, 17-percent efficient TI element (Ref. B-4). A 1000-h test under electric load at 1675 K is currently in progress (Ref. B-5).

One of the most current designs is the SP-100 Thermionic System concept by GA Technologies and Martin Marietta (Ref. B-15). This design calls for 150 to 200 TFEs which are cooled by a NaK coolant. The dimensions of the system are well within the SP-100 guidelines. A present 3-yr life span is estimated with a near term 7-yr life span predicted. The Gulf General Atomic Corporation thermionic reactor is also a sturdy design and is presented in brief in Reference B-3.

6. MAGNETOHYDRODYNAMIC CONVERSION

The magnetohydrodynamic conversion system is suited only for high temperature reactor use and hence, not near term application. The general concept of an MHD conversion system has been studied thoroughly because of its applicability in terrestrial situations. Many types of MHD conversion systems exist including a self-excited system where some of the current produced by the channel is used to power the channel's magnets. Liquid metal as the working fluid is also possible since liquid metals have higher electrical conductivities, which would lead to a more efficient device. Additionally, a disk generator may be used to improve performance. The system can also operate on either an open or closed cycle. A turbogenerator might also be adapted in conjunction with an MHD channel to increase the overall efficiency. As can be seen, a virtual cornucopia of combinations are possible. Therefore, only a brief look is taken at some possibilities.

MHD power in general means higher efficiencies due to the high operating temperature. Some estimate efficiencies as high as 40 percent or more

(Ref. B-16). The MHD device, essentially, has no moving parts and is capable of start-up and shutdown virtually immediately by controlling the working fluid flow. Since the MHD system is a volume generating device, less surface to volume losses lead to higher powers, lower masses, smaller radiators, and higher efficiencies.

A major disadvantage of the MHD machine is the temperature bounded MHD channel and electrode materials and magnets, which the hot working fluid or gas must come in contact with. The effective seeding of the working gas is also a concern. This results from the need of higher fluid electrical conductivities at low system pressures (Ref. B-17). The desire to use superconducting magnets is also a potential engineering question.

The turbo-MHD concept allows the hot working gas coming from the reactor to pass through a turbine first before the MHD channel. Up to 20 percent more enthalpy extraction is possible along with a smaller radiator size. Overall efficiency is lower but the radiator and compressor temperatures are higher by about 200-400 K, which leads to a higher specific power. This concept has been demonstrated at 375 MWe and 7.5 percent enthalpy extraction from a 1900 K flow (Ref. B-16). Difficulties lie in the sensitivity of the system weight to component performances.

"In disk generators, a swirling flow is expanded radially against an axial field with power extraction from inner and outer radii" (Ref. B-16). The advantage of this disk generator over a conventional linear generator is that it may offer high performance with simpler magnets and require less power consolidation equipment. The disk generator creates no thrust and is a single output device. It can take higher electric fields than the electrode walls of the linear generator. Its configuration also eliminates end losses due to magnetic field fringing. The disk generator is also more reliable, compact and efficient (Ref. B-18). The major problem lies in the development of the appropriate technology for nuclear application in space.

The self-excited MHD is compact, has low specific weight and high power, is simple, has no moving parts, is storable, maintenance free, and can be started or stopped instantly at high repetition rates (Ref. B-19). Problems are in the high interaction magnetohydrodynamic flow behavior, power generation at moderate-to-high magnetic Reynolds number and controlled high-conductivity working fluid generation (Ref. B-19).

Not many designs exist for MHD application to space nuclear systems since it is by far the most far term concept under consideration to date. The problem with materials and temperatures are far from being solved and so comprehensive designs are not abundant. For a brief overview of this field, refer to Reference B-20.

7. ALKALI METAL THERMOELECTRIC CONVERSION SYSTEM

The alkali metal thermoelectric conversion system is the least developed technology yet holds many promises. It is simple and hence reliable and easily redundant. It has one of the lowest predicted specific areas of any of the conversion systems (Ref. B-14). Efficiencies are high and on the order of 14-23 percent (Ref. B-4). The AMTEC device is also fairly light. The major block to AMTEC's deployment is its relatively little experience outside the laboratory. During continuous operation, the power level decreases due to a decreasing porosity of the electrodes from sintering. The maximum high power life is only 1000 h currently (Ref. B-4). Condensation in zero gravity is also a technology problem to be overcome. Fabrication technology also needs to be developed in order to assure module hermeticity.

No AMTEC conversion system design was found however, a self contained device has been operated in the laboratory at a hot side temperature of 1073 K and an efficiency of 19 percent. These modules might easily replace current TE modules in the LANL heat pipe reactor once the technology is ready.

REFERENCES

B-1. Redd, F. J. and Fornoles, E. V., "Emerging Space Nuclear Power Needs," "Space Nuclear Power Systems," (Eds. M. S. El-Genk and M. D. Hoover), Robert E. Krieger Publishing Company, Inc., 1985.

B-2. Ambrus, J. H. and Beatty, R.G.G., "Mission Applications Overview for SP-100 Program," "Space Nuclear Power Systems," (Eds. M. S. El-Genk and M. D. Hoover), Robert E. Krieger Publishing Company, Inc., 1985.

B-3. Burkhart, C., Coffey, S. and Louie, D., Nuclear Reactors 1-10 MW(e) for Space Applications, Dept. of Chemical and Nuclear Engineering, University of New Mexico (1982).

B-4. Ewell, R., "Energy Conversion for Megawatt Space Power Systems," Proceedings of the 18th Intersociety Energy Conversion Engineering Conference, Orlando, Fla., Aug. 1983.

B-5. Buden, D., "Selection of Power Plant Elements for Future Reactor Space Electric Power Systems," Los Alamos Scientific Laboratory, Report LA-7858, Sept. 1979.

B-6. Culp, A. W., Jr., Principles of Energy Conversion, McGraw-Hill, 1979.

B-7. Barratino, W. J., "Considerations for Increasing the Power Output of a Space Reactor," Special Topic Paper for the Dept. of Chem. and Nuclear Engineering, University of New Mexico, Nov. 1982.

B-8. Buden, D., "Overview of Space Reactors," Proceedings of the Air Force Office of Scientific Research Special Conference on Prime-Power for High Energy Space Systems, Norfolk, Va., Feb. 1982.

B-9. Hoffman, H. W. and Yoder, G. L., "Liquid Metal Heat Transfer Issues," "Space Nuclear Power Systems," (Eds. M. S. El-Genk and M. D. Hoover), Robert E. Krieger Publishing Company,Inc., 1985.

B-10. Bland, T., "Nuclear Powered Organic Rankine Systems for Space Applications," Proceedings of the Air Force Office of Scientific Research Special Conference on Prime-Power for High Energy Space Systems, Norfolk, Va., Feb. 1982.

B-11. Jones, J. E., MacPherson, R. E. and Nichols, J. P., "Multimegawatt Space Nuclear Power Concept," "Space Nuclear Power Systems," (Eds. M. S. El-Genk and M. D. Hoover), Robert E. Krieger Publishing Company, Inc., 1985.

B-12. Parker, G. H., "Brayton Cycle Power Conversion for Space," Proceedings of the Air Force Office of Scientific Research Special Conference on Prime-Power for High Energy Space Systems, Norfolk, Va., Feb. 1982.

B-13. Beale, W. T., "The Free Piston Stirling Engine--Its Promise as a Space Power Plant," "Space Nuclear Power Systems," (Eds. M. S. El-Genk and M. D. Hoover), Robert E. Krieger Publishing Company, Inc., 1985.

B-14. Katucki, R., et al., "Evolution of Systems Concepts for a 100 kWe Class Space Nuclear Power System," "Space Nuclear Power Systems," (Eds. M. S. El-Genk and M. D. Hoover), Robert E. Krieger Publising Company, Inc., 1985.

B-15. Snyder, H. J., et al., "SP-100 Thermionic System Concept," "Space Nuclear Power System," (Eds. M. S. El-Genk and M. D. Hoover), Robert E. Krieger Publishing Company, Inc., 1985.

B-16. Seikel, G. R. and Zanderer, B., "Potential Role and Technology Status of Closed-Cycle MHD for Lightweight Nuclear Space Power Systems," Proceedings of the Air Force Office of Scientific Research Special Conference on Prime-Power for High Energy Space Systems, Norfolk, Va., Feb. 1982.

B-17. Smith, J. M., "NASA Lewis Research Center Combustion MHD Experiment," Proceedings of the Air Force Office of Scientific Research Special Conference on Prime-Power for High Energy Space Systems, Norfolk, Va., Feb. 1982.

B-18. Louis, J. F., "The MHD Disk Generator as a Multimegawatt Power Supply Operating with Chemical and Nuclear Sources," Proceedings of the Air Force Office of Scientific Research Special Conference on Prime-Power for High Energy Space Systems, Norfolk, Va., Feb. 1982.

B-19. Maxwell, C. D., et al., "Self-Excited MHD Power Source for Space Applications," Proceedings of the Air Force Office of Scientific Research Special Conference on Prime-Power for High Energy Space Systems, Norfolk, Va., Feb. 1982.

B-20. Dicks, J. B., "MHD Power: Overview," Proceedings of the Air Force Office of Scientific Research Special Conference on Prime-Power for High Energy Space Systems, Norfolk, Va., Feb. 1982.

END

FILMED

11-85

DTIC